



# Etude de la voie TGF $\beta$ dans le cholangiocarcinome intrahépatique : implication des ARN longs non-codants

Aude Merdrignac

## ► To cite this version:

Aude Merdrignac. Etude de la voie TGF $\beta$  dans le cholangiocarcinome intrahépatique : implication des ARN longs non-codants. Biochimie, Biologie Moléculaire. Université de Rennes, 2019. Français.  
NNT : 2019REN1B020 . tel-02421163

HAL Id: tel-02421163

<https://theses.hal.science/tel-02421163>

Submitted on 20 Dec 2019

**HAL** is a multi-disciplinary open access archive for the deposit and dissemination of scientific research documents, whether they are published or not. The documents may come from teaching and research institutions in France or abroad, or from public or private research centers.

L'archive ouverte pluridisciplinaire **HAL**, est destinée au dépôt et à la diffusion de documents scientifiques de niveau recherche, publiés ou non, émanant des établissements d'enseignement et de recherche français ou étrangers, des laboratoires publics ou privés.

# THESE DE DOCTORAT DE

L'UNIVERSITE DE RENNES 1  
COMUE UNIVERSITE BRETAGNE LOIRE

ECOLE DOCTORALE N° 605  
*Biologie Santé*  
Spécialité : Biochimie, Biologie moléculaire et cellulaire

Par **Aude MERDRIGNAC**

## **Etude de la voie TGF $\beta$ dans le cholangiocarcinome intrahépatique Implication des ARN longs non-codants**

Thèse présentée et soutenue à Rennes, le 14 juin 2019  
Unité de recherche : Inserm UMR 1241 - Nutrition, métabolisme et Cancer - NuMeCan

### **Rapporteurs avant soutenance :**

Pr Valérie PARADIS                    PU-PH, Hôpital Beaujon, APHP  
Pr Olivier SOUBRANE                 PU-PH, Hôpital Beaujon, APHP

### **Composition du Jury :**

Président : Pr Laurent SULPICE      PU-PH, CHU de Rennes

Examinateurs : Pr Thomas DECAENS    PU-PH, CHU de Grenoble  
                  Thomas DERRIEN          PU-PH – Université Rennes 1  
                  Laura FOUASSIER        Chargé de recherche, INSERM, Centre de Recherche Saint Antoine, Paris  
                  Pr Valérie PARADIS        PU-PH, Hôpital Beaujon, APHP

Dir. de thèse : Cédric COULOUARN    Chargé de recherche, INSERM, UMR NuMeCan, Rennes

### **Invité :**

Pr Karim BOUDJEMA                    PU-PH, CHU de Rennes

## **Remerciements**

Je remercie en premier lieu Cédric Coulouarn, mon directeur de thèse, qui m'encadre depuis le Master 2 et sans qui ce travail n'aurait pu aboutir. Tu as eu la patience de partager tes connaissances et ton expertise. Je te remercie particulièrement de ta rigueur et de ta compréhension sur mon emploi du temps.

Je remercie chaleureusement Gaëlle Angenard qui m'a accompagnée dans mes expérimentations et soutenue quand les résultats n'étaient pas ceux escomptés. Ce travail n'aurait pu se faire sans ton aide technique ni celle de l'équipe : Kilian, Coralie, Camille...

Je remercie le Professeur Sulpice qui a été le premier à me proposer ce projet et qui m'a encouragée dans la réalisation de ce travail. J'espère que notre collaboration se poursuivra dans la même confiance.

Je remercie le Professeur Boudjema de la formation qu'il m'a apportée par son expertise chirurgicale, son expérience et sa rigueur.

Je remercie Madame le Professeur Paradis et Monsieur le Professeur Soubrane qui me font l'honneur d'accepter d'être les rapporteurs de ce travail.

Je remercie Monsieur le Professeur Thomas Decaens, Monsieur Thomas Derrien et Madame Laura Fouassier et qui me font l'honneur d'accepter d'être les examinateurs de ce travail.

Je remercie le Docteur Damien Bergeat mon collègue et soutien au cours du Master et le Docteur Véronique Desfourneaux pour la formation précieuse à ses côtés.

Je remercie enfin et surtout Anaël et Lizenn.

## Table des matières

Table des matières .....	3
Liste des abréviations .....	4
Légendes des figures .....	6
I. Introduction .....	7
1. Cholangiocarcinome intrahépatique .....	7
<i>i. Epidémiologie et facteurs de risque</i> .....	7
<i>ii. Histologie et microenvironnement tumoral</i> .....	9
<i>iii. Cancérogénèse et altérations moléculaires</i> .....	11
<i>iv. Diagnostic</i> .....	13
<i>v. Traitement et pronostic</i> .....	14
2. Voie du « Transforming Growth Factor $\beta$ » (TGF $\beta$ ) .....	15
<i>i. Voie de signalisation / Mécanisme de transduction du signal</i> .....	15
<i>ii. Rôle du TGF<math>\beta</math> dans la cancérogénèse</i> .....	17
<i>iii. TGF<math>\beta</math> et cholangiocarcinome intrahépatique</i> .....	20
3. ARN longs non-codants (ARNlnc) .....	22
<i>i. Caractéristiques des ARNlnc</i> .....	22
<i>ii. ARNlnc et cholangiocarcinome</i> .....	28
<i>iii. ARNlnc et TGF<math>\beta</math> dans la cancérogénèse hépatique</i> .....	29
II. Objectifs .....	33
III. Résultats .....	34
1. Article n°1 .....	34
2. Article n°2 .....	63
3. Article n°3 .....	71
5. Publications de travaux cliniques .....	90
IV. Discussion .....	92
1. Signature TGF $\beta$ dans le CCI .....	92
2. ARNlnc et CCI .....	93
3. ARN non codants biomarqueurs .....	97
4. Applications thérapeutiques .....	99
V. Conclusion .....	102
VI. Références .....	103

## Liste des abréviations

ABCC1: ATP binding cassette subfamily C member 1  
ACE: antigène carcino-embryonnaire  
ANRIL: antisense noncoding RNA in the INK4 locus  
APC: adenomatous polyposis coli  
ARID1A: AT-rich interaction domain 1A  
a-SMA : actine-alpha de type musculaire lisse  
ATB: lncRNA-activated by TGFβ  
BAP1: BRCA1 associated protein-1  
CA19-9: carbohydrate antigen 19-9  
CASC15: cancer susceptibility candidate 15  
CBX7: chromobox 7  
CCI: cholangiocarcinome intrahépatique  
CD: cluster of differentiation  
CDKN: cyclin-dependent kinase Inhibitor  
CDKN2B-AS1: cyclin-dependent kinase inhibitor 2B - antisense RNA 1  
CDS: coding DNA sequence  
CHC: carcinome hépatocellulaire  
CK: cytokératine  
CPS1-IT1: carbamoyl-phosphate synthase - intronic transcript 1  
CRNDE: colorectal neoplasia differentially expressed  
CSP : cholangite sclérosante primitive  
CPS1-IT1: CPS1 intronic transcript 1  
CTGF: connective tissue growth factor  
CYFRA 21-1: cytokeratin-21-fragment  
EGF: epidermal growth factor  
EGFR: epidermal growth factor receptor  
EMT: epithelial-mesenchymal transition  
EPCAM: epithelial cell adhesion molecule  
EPIC1: epigenetically-induced lncRNA1  
EZH2: enhancer of zeste 2 polycomb repressive complex 2 subunit  
FGFR: fibroblast growth factor receptor  
FXR: farnesoid X receptor  
H3K27me3 : trimethylated lysine 27 of histone H3  
H3K4deme : demethylated lysine 4 of histone H3  
HGF/MET: hepatocyte growth factor  
HOAIR: HOX transcript antisense RNA  
HOTTIP: HOXA distal transcript antisense RNA  
HOXD10: homeobox D10  
IDH1/2: isocitrate dehydrogenase 1/2  
IL: interleukin  
JAG-1: jagged1  
JAK: janus kinase  
JAM2 : junctional adhesion molecule 2  
JNK: c-Jun NH<sub>2</sub>-terminal kinase  
KRT: keratin  
LGL : lethal giant larvae  
LOXL2: lysyl oxidase like 2  
LSD1: lysine-specific histone demethylase 1  
MALAT1: metastasis associated lung adenocarcinoma transcript 1  
MAPK: mitogen-activated protein kinase  
MEG3: maternally expressed gene 3  
MLL : mixed lineage leukemia

mPGES-1: microsomal prostaglandin E synthase-1  
mTOR: mechanistic target of rapamycin  
NBAT1: neuroblastoma associated transcript 1  
NEAT1: nuclear paraspeckle assembly transcript 1  
NF-Y: nuclear transcription factor Y  
PANDA: p21-associated ncRNA DNA damage-activated  
PATJ : PALS1-associated tight junction protein  
PCAT1: prostate cancer associated transcript 1  
PCDH10 : protocadherin 10  
PD1:programmed cell death 1  
PDGFR: platelet-derived growth factor receptor  
PD-L1:programmed cell death-ligand 1  
PGR : progesterone receptor  
PI3K: phosphatidylinositol 3-kinase  
PIP: prolactin-inducible protein  
PLK2: polo like kinase 2  
PPAR:peroxisome proliferator-activated receptor  
PTCH: patched  
PTEN : phosphatase and tensin homolog  
PTENP1: phosphatase and tensin homolog pseudogene 1  
PTHRP: parathyroid hormone-related protein  
PVT1: plasmacytoma variant translocation 1  
q-RT-PCR: quantitative-real-time polymerase chain reaction  
REST: RE1 silencing transcription factor  
RhoA: Ras homolog family member A  
ROR: regulator of reprogramming  
(S)HH: sonic hedgehog  
SMO: smoothened, frizzled class receptor  
SNHG1: small nucleolar RNA host gene 1  
SNO : ski-related novel gene  
SNP: single nucleotide polymorphism  
SOCS-3: suppressor of cytokine signaling 3  
SOX: Sry-related HMG box  
S1PR2: sphingosine-1-phosphate receptor 2  
SPP1: secreted phosphoprotein 1/osteopontin  
SPRY4-IT1: sprouty RTK signaling antagonist 4-intronic transcript 1  
STAT3: signal transducer and activator of transcription 3  
TAMs: tumour-associated macrophages  
TANs: tumour-associated neutrophils  
TCGA: the cancer genome atlas  
TEM: transition épithélio-mésenchymateuse  
TF: transcription factor  
TGF $\beta$  : transforming growth factor  $\beta$   
TH: transplantation hépatique  
TLINC: TGF $\beta$  induced long intergenic non coding RNA  
TRAIL: TNF-related apoptosis inducing ligand  
TP53: tumor protein 53  
TUG1: taurine upregulated gene 1  
VEGF: vascular endothelial growth factor  
VEGFR: vascular endothelial growth factor receptor  
VIM: vimentine  
ZEB: zinc finger E-box binding  
ZEB2-AS : ZEB2 antisense RNA

## Légendes des figures

Figure 1: Classification anatomique des cholangiocarcinomes .....	7
Figure 2: Incidence mondiale du cholangiocarcinome au cours de la période 1971-2009.....	8
Figure 3: Types de CCI selon l'aspect macroscopique .....	10
Figure 4: Voies de signalisation intracellulaires impliquées dans la prolifération et l'apoptose dans le cholangiocarcinome .....	12
Figure 5: Résumé des classes de CCI .....	13
Figure 6: Représentation schématique de la voie de signalisation canonique TGF $\beta$ dépendante des SMADs.....	16
Figure 7: Schéma de l'activité biphasique de la voie TGF $\beta$ pendant la cancérogénèse: de la suppression à la promotion de la tumeur.....	17
Figure 8: Schéma d'une transition épithélio-mésenchymateuse typique .....	19
Figure 9: Classification des ARNlnc selon leur organisation génomique.....	23
Figure 10: Associations moléculaires possibles des ARNlnc aboutissant à de multiples fonctions.....	23
Figure 11: Exemples de description de modes d'actions des ARNlnc selon leur localisation nucléaire ou cytoplasmique.....	24
Figure 12: Schéma du mode d'action de HOTTIP .....	25
Figure 13 : Schéma du mode d'action de HOTAIR sur les complexes d'histone PRC2 et LSD1/coREST/REST.....	25
Figure 14: Schéma du mode d'action de PANDA .....	26
Figure 15 : Représentation schématique de l'unité transcriptionnelle de H19 .....	27
Figure 16 : Représentation schématique de l'action de PTENP1 .....	27
Figure 17: Schéma du mode d'action de ZEB2-AS.....	29
Figure 18 : Schéma du mode d'action de l'ARNlnc ATB .....	30
Figure 19 : Schéma du mode d'action d'ANRIL .....	32
Figure 20 : Niveaux d'expression de LINC00312 et LINC00313 .....	96
Figure 21 : Schéma du déroulement de l'analyse intégrée du profil d'expression des ARNcirc régulés par le TGF $\beta$ , puis du profil d'expression des microARN prédis interagissant avec ces ARNcirc et du profil d'expression de leurs ARNm cibles prédis .....	99

## I. Introduction

### 1. Cholangiocarcinome intrahépatique

#### i. Épidémiologie et facteurs de risque

Le cholangiocarcinome est un cancer développé à partir des cellules de l'épithélium de l'arbre bilaire. Il est classé selon sa localisation anatomique par l'Organisation Mondiale de la Santé en intrahépatique (au-delà des divisions en canaux biliaires de 2<sup>nd</sup> ordre), périhilaire ou distal<sup>1</sup> (figure 1).

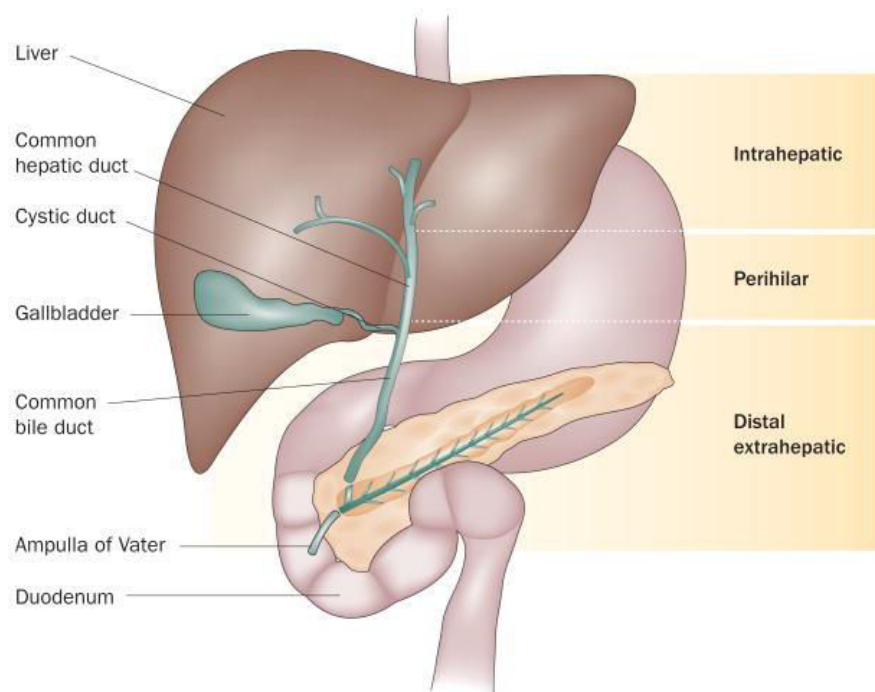
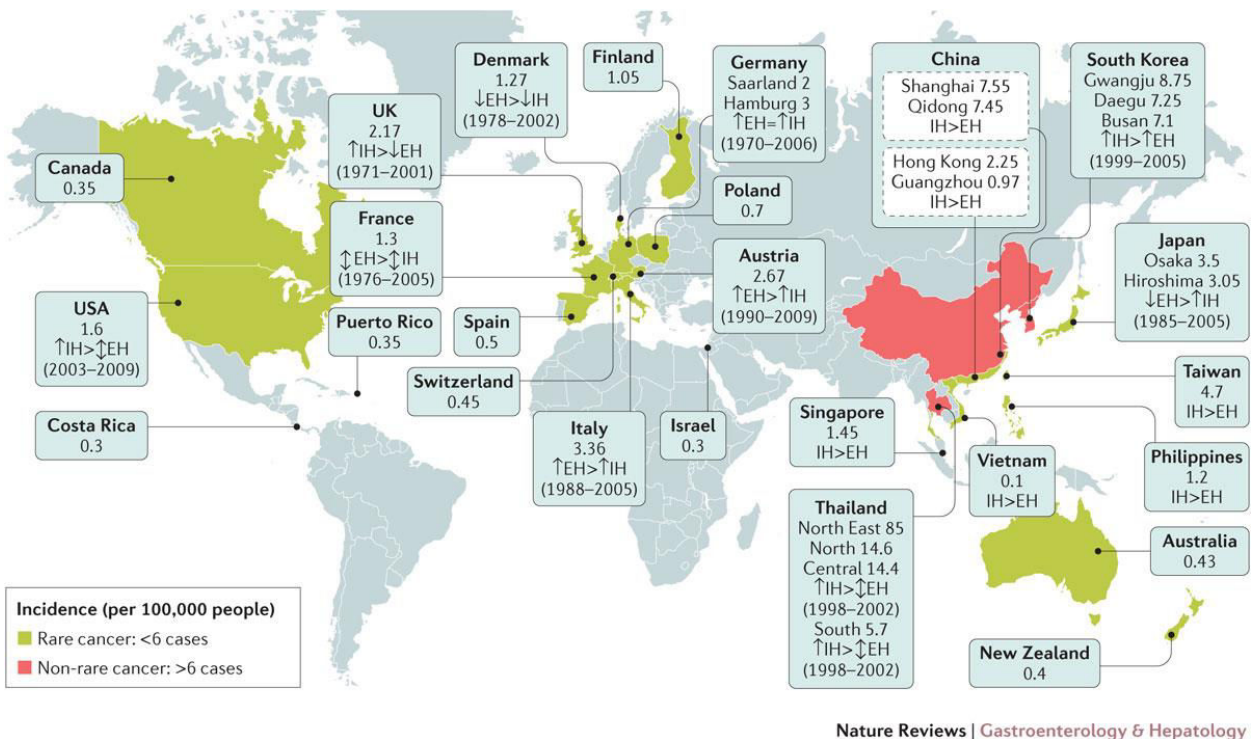


Figure 1: Classification anatomique des cholangiocarcinomes. Blehacz, *Nat Rev Gastroenterol Hepatol*, 2011<sup>2</sup>.

Nous n'aborderons dans ce travail que la localisation intrahépatique (CCI). Le CCI est classiquement la 2ème tumeur hépatique primitive après le carcinome hépatocellulaire (CHC) représentant 10 à 20% des tumeurs hépatiques primitives<sup>3</sup>. Cependant, son incidence est très variable dans le monde (figure 2). Elle est forte en Asie du Sud-Est (jusqu'à 85/100000 en Thaïlande) et à l'opposé faible dans certains pays d'Occident (0.3/100000 au Canada)<sup>4</sup>.



Nature Reviews | Gastroenterology & Hepatology

Figure 2: Incidence mondiale du cholangiocarcinome au cours de la période 1971-2009. Les pays avec la plus faible incidence sont en vert (<6/100000 cas, cancer rare), alors que les pays avec la plus forte incidence sont en rose (>6/100000 cas). La forme avec la plus forte incidence (intrahépatique (IH) versus extrahépatique (EH)) et la tendance de l'incidence (↑augmentation, ↑stabilité, ↓diminution) sont indiquées si les données sont disponibles. *Banales, Nat Rev Gastroenterol Hepatol, 2016*<sup>5</sup>.

L'incidence forte en Asie du Sud-Est est expliquée par des facteurs de risque spécifiques comme l'infection parasitaire par les douves *Opisthorchis viverrini* et *Clonorchis sinensis*. Les anomalies de l'arbre biliaire, comme les kystes du cholédoque, et les calculs biliaires intrahépatiques fréquents dans cette région sont également impliqués.

En Occident, dans la majorité des cas, le CCI survient sur un foie sain comme l'a montré la série récente de 522 patients de l'Association Française de Chirurgie<sup>6</sup>. Cependant, la cholangite sclérosante primitive (CSP) est un facteur de risque bien connu qui augmente la prévalence du cholangiocarcinome à 5 à 10% au cours de la vie<sup>7</sup>. Plus récemment, les facteurs de risque classiques du CHC ont également été reconnus comme impliqués dans le CCI (hépatites virales chroniques B et C, cirrhose, obésité, diabète et alcool) suggérant des voies de carcinogénèse communes aux deux tumeurs<sup>8</sup>. L'ensemble des facteurs de risque connus du cholangiocarcinome sont présentés dans la table 1.

**Table 1: Facteurs de risque du cholangiocarcinome**

**Généraux**

Age >65 ans

Obésité

Diabète

**Maladies inflammatoires**

Cholangite sclérosante primitive

Lithiasis hépatique (Cholangiohépatite orientale)

Calculs de l'arbre biliaire

Anastomose bilio-digestive

Cirrhose hépatique

**Maladies infectieuses**

*Opisthorchis viverrini* (douves hépatiques)

*Clonorchis sinensis* (douves hépatiques)

Hépatite C

Hépatite B

Infection VIH

**Drogues, toxines et produits chimiques**

Alcool

Tabac

Thorotraste

Dioxine

Vinyl chloride

Nitrosamines

Asbestose

Pilule contraceptive orale

Isoniazide

**Congénitaux**

Kystes du cholédoque (type I, solitaire, extrahépatique; type IV, extrahépatique et intrahépatique)

Maladie de Caroli

Fibrose hépatique congénitale

Table adaptée de Banales, *Nat Rev Gastroenterol Hepatol*, 2016<sup>5</sup>

Globalement, l'incidence du CCI est en augmentation même si l'évolution des classifications au cours du temps a pu modifier l'incidence des différentes localisations<sup>9,10</sup>. Une des causes de cette augmentation pourrait être le syndrome métabolique<sup>11</sup>.

*ii. Histologie et microenvironnement tumoral*

La forme basée sur l'aspect macroscopique de CCI la plus fréquente est la forme *mass-forming* trouvée chez 86 % des patients opérés. Le type *mass-forming* correspond à une masse infiltrant le parenchyme hépatique via le système porte et les vaisseaux lymphatiques

<sup>12,13</sup>

Les 2 autres formes sont le type *periductal infiltrating* et le type *intraductal growth* (figure 3).

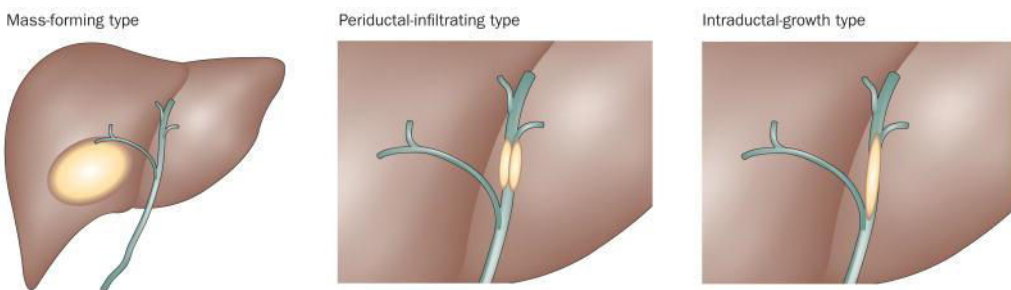


Figure 3: Types de CCI selon l'aspect macroscopique. Blechacz, Nat Rev Gastroenterol Hepatol, 2011<sup>2</sup>.

Histologiquement, le CCI peut être classé en 2 sous types selon son origine anatomique sur l'arbre bilaire intrahépatique : mixte issu des petits canaux biliaires et mucineux issu des larges canaux biliaires. Le type mixte, correspondant presque exclusivement au type *mass-forming*, est fréquemment associé aux hépatopathies chroniques (cirrhose ou hépatites virales) et n'est pas précédé de lésion prénéoplasique. Le type mucineux, qui peut avoir toutes les apparences macroscopiques, est plus fréquemment associé à la CSP. Il peut être précédé de lésions néoplasiques et partage des caractères avec les cholangiocarcinomes distaux et les cancers pancréatiques<sup>5</sup>. La différenciation du CCI avec des métastases hépatiques d'autres cancers du tractus digestif est aidée par des marqueurs immunohistochimiques de l'origine bilaire (e.g. positivité de la cytokératine 7, CK7)<sup>14,15</sup>.

Le CCI correspond à un adénocarcinome plus ou moins différencié avec un riche stroma fibreux desmoplastique<sup>5,16</sup>. Ce stroma contient principalement du collagène de type 1 et des myofibroblastes caractérisés par l'expression de novo d'actine-alpha de type musculaire lisse (a-SMA)<sup>17</sup>. De nombreuses cellules inflammatoires (macrophages) et vasculaires sont également présentes dans le microenvironnement du CCI. L'analyse moléculaire du stroma tumoral après microdissection laser réalisée dans notre équipe avait mis en évidence une surexpression du *Transforming Growth Factor β* (TGFβ)<sup>18</sup>. Ces résultats étaient concordants avec l'action profibrotique connue du TGFβ dans le foie. Les macrophages produisent des médiateurs profibrotiques dont le TGFβ qui est responsable de l'activation de cellules hépatiques étoilées quiescentes en myofibroblastes<sup>19</sup>. Les myofibroblastes jouent un rôle

majeur dans la progression du CCI. Ils agissent sur la prolifération, la migration, l'invasion, la résistance à l'apoptose et la TEM des cholangiocytes tumoraux par la régulation autocrine et paracrine de voies de signalisation (e.g. voie Hedgehog) <sup>17</sup>. Leur abondance comme celle de protéines de la matrice extra cellulaire (e.g. périostine), est corrélée à un mauvais pronostic chez les patients opérés <sup>16,17</sup>.

### *iii. Cancérogénèse et altérations moléculaires*

Le CCI résulte d'un processus complexe de cancérogénèse impliquant la transformation de cholangiocytes et dans certains cas de cellules souches. Des marqueurs de cellules souches cancéreuses (e.g. CD13, CD44) sont présents dans au moins 30% des cellules de cholangiocarcinome <sup>20</sup>. L'injection de cellules souches cancéreuses a permis de générer des CCI humains dans des foies cirrhotiques murins <sup>20</sup>. L'hypothèse de la transformation en CCI à partir d'hépatocytes a été également proposée. En effet, des modèles murins ont permis de convertir des hépatocytes en cholangiocytes via l'activation des voies de signalisation Notch et Akt <sup>21,22</sup>.

Parmi les altérations moléculaires rencontrées dans le CCI, les mutations génétiques les plus fréquemment mises en évidence sont *KRAS* (19%), *TP53* (16%) et *IDH1/2* (15%) <sup>23</sup>. Les mutations *KRAS* ont été associées à un phénotype plus agressif <sup>24</sup>. D'autres mutations sont moins fréquentes : *ARID1A*, *BAP1*, *BRAF* et *EGFR* <sup>23</sup>. Des fusions de gènes codant pour des protéines tyrosine kinase, comme FGFR2 qui agit comme récepteur membranaire aux facteurs de croissance des fibroblastes, sont décrites dans 20% des cas <sup>23</sup>. Elles aboutissent à la formation de protéines de fusion qui ont une action oncogénique en activant des voies de signalisation e.g. la voie MAPK <sup>25</sup>. De rares altérations chromosomiques correspondant à des gains ou des pertes sur l'un des bras chromosomiques ont été décrites e.g. gain sur 7p et perte sur 4q <sup>26</sup>. Des altérations épigénétiques par hyperméthylation de promoteur (i.e. inactivation) ont également été décrites, comme par exemple au niveau du promoteur du gène codant p16INK4A, un régulateur négatif du cycle cellulaire <sup>26</sup>.

Les voies de signalisation principalement dérégulées dans le CCI concernent l'inflammation comme IL6/STAT3, les facteurs de croissance comme EGFR et la voie KRAS/MAPK (figure 4) <sup>26</sup>. Des dérégulations des voies HGF/MET, VEGF et WNT/β-caténine ont également été décrites.

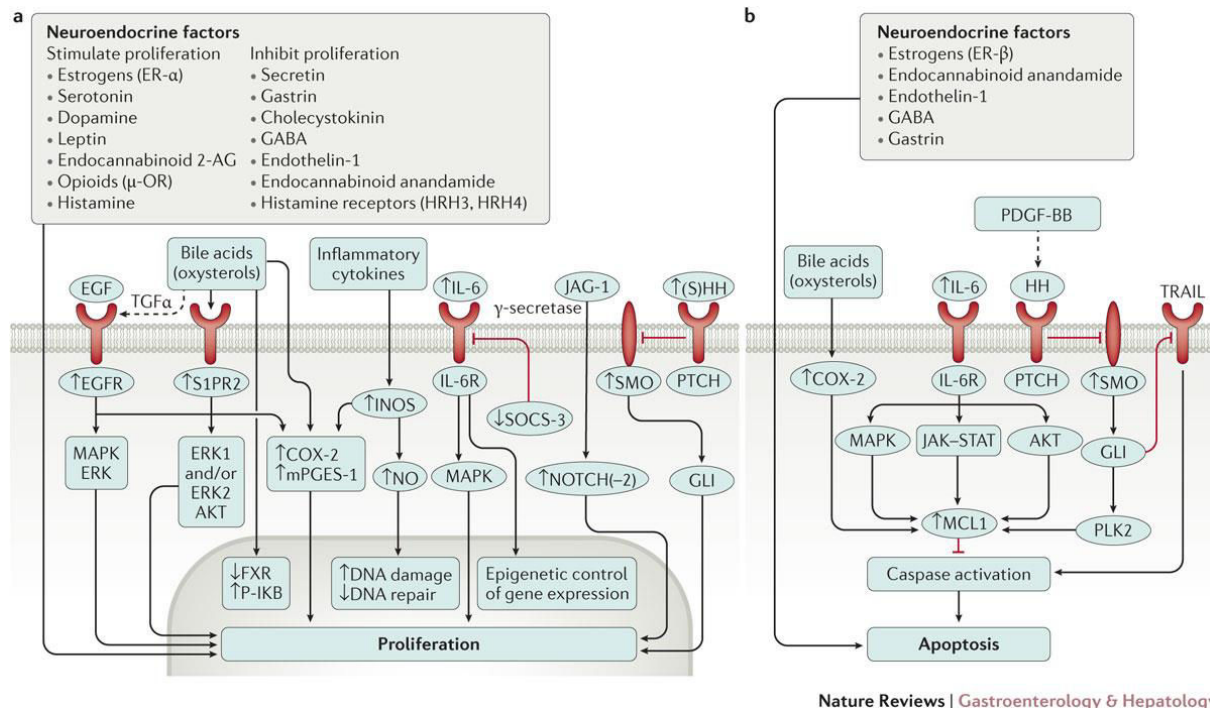


Figure 4: Voies de signalisation intracellulaires impliquées dans la prolifération et l'apoptose dans le cholangiocarcinome. Banales, *Nat Rev Gastroenterol Hepatol*, 2016<sup>5</sup>.

2-AG: 2-arachidonoylglycerol. COX-2: cyclooxygenase 2. EGF: epidermal growth factor. EGFR: epidermal growth factor receptor. ER: estrogen receptor. GABA:  $\gamma$ -aminobutyric acid. IL-6R: IL-6 receptor. NO: nitric oxide. OR: opioid receptor. TGF: transforming growth factor. iNOS: inducible nitric oxide synthase. JAG-1: Jagged1. S1PR2: Sphingosine-1-Phosphate Receptor 2. mPGES-1: microsomal prostaglandin E synthase-1. FXR: farnesoid X receptor. P-IKB: Phosphatidylinositol kinase. SOCS-3: suppressor of cytokine signaling 3. SMO: smoothened, frizzled class receptor. PTCH: patched. (S)HH: sonic hedgehog. JAK: Janus kinase. PLK2: polo like kinase 2. TRAIL: TNF-related apoptosis inducing ligand.

Différentes classifications moléculaires ont été proposées comme par exemple Sia et al. en 2013 (figure 5) <sup>27</sup>. La classe « proliférative » est plus agressive et de plus mauvais pronostic. Elle présente un enrichissement de voies de signalisation oncogéniques comme RAS, EGF, HGF/MET qui sont des altérations semblables au CHC de mauvais pronostic. La classe « inflammatoire » est de meilleur pronostic avec un enrichissement des voies de signalisation de la réponse immunitaire comme STAT3 menant à une surexpression de cytokines (e.g. IL4, IL10).

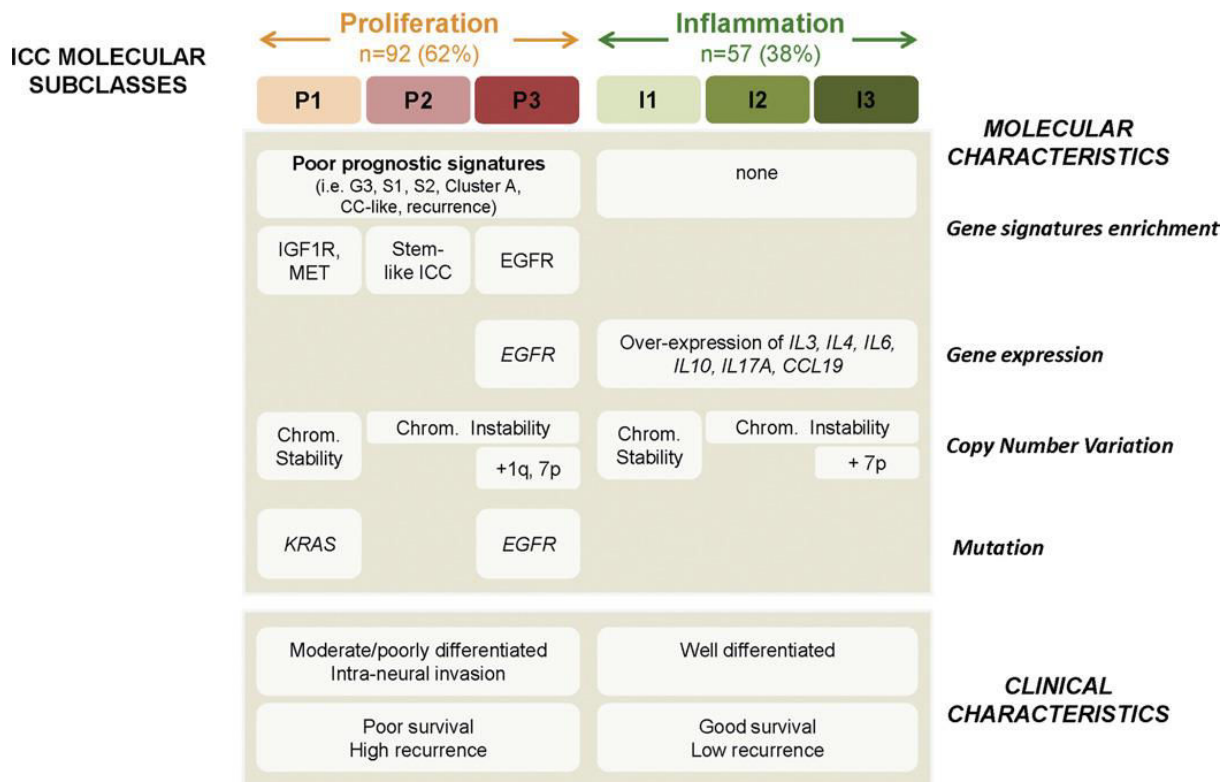


Figure 5: Résumé des classes de CCI. Les caractéristiques moléculaires et cliniques diffèrent entre les 2 classes. *Sia, Gastroenterol, 2013*<sup>27</sup>.

#### iv. Diagnostic

Le diagnostic du CCI est souvent tardif car au stade précoce les patients sont asymptomatiques. À un stade avancé, les signes sont aspécifiques : perte de poids, douleurs abdominales, hépatomégalie, plus rarement ictere. Les marqueurs tumoraux sériques actuels, CA 19-9 et ACE, manquent de spécificité pour le CCI. La sensibilité et la spécificité du CA 19-9 ne sont que de 62% et 63% respectivement<sup>2</sup>. L'obstruction biliaire peut faussement augmenter le taux de CA 19-9 mais un taux élevé pourrait être prédictif de non résécabilité et d'une moins bonne survie sans récidive après chirurgie<sup>28,29</sup>. De nombreux autres biomarqueurs sériques potentiels (e.g. CYFRA 21-1, SPP1) ont été identifiés mais sans résultats assez satisfaisants pour une application clinique actuellement<sup>30,31</sup>. Des travaux dans l'équipe avaient notamment identifié LOXL2, EPCAM et SPP1 comme biomarqueurs pronostiques indépendants au niveau tissulaire<sup>18,32,33</sup>. Dans le but d'identifier de nouveaux biomarqueurs non invasifs, Banales et al. ont isolé des vésicules extracellulaires dont la majorité étaient des exosomes<sup>34</sup>. L'analyse protéomique des

exosomes a montré des signatures potentiellement utiles à visée diagnostique pour différencier CCI, CHC et CSP.

La tomodensitométrie abdominale et l'imagerie par résonance magnétique permettent de suspecter le diagnostic. L'aspect typique est une lésion hépatique prenant le contraste au temps artériel avec une augmentation du rehaussement au temps veineux en raison d'une prise de contraste lente du stroma fibreux<sup>35</sup>. La différenciation avec un CHC est parfois difficile particulièrement pour les tumeurs de petite taille <2cm. Seule la preuve histologique fait donc le diagnostic formel.

#### v. *Traitements et pronostic*

Le pronostic du CCI est mauvais avec 50% de récidive à 1 an et une médiane de survie globale de 33 mois après chirurgie<sup>36</sup>. La chirurgie reste cependant le seul traitement potentiellement curatif pour les 30 à 40% de patients avec une tumeur résécable<sup>37</sup>. La résection ne doit pas laisser de résidu tumoral (R0) ce qui implique pour 80% des patients une hépatectomie majeure et un curage ganglionnaire dans 70% des cas<sup>13</sup>. Les facteurs de risque de récidive après résection sont l'envahissement ganglionnaire, l'invasion périneurale et la présence de nodules satellites intrahépatiques<sup>36</sup>. En l'absence de chirurgie, la médiane de survie est de 12 à 15 mois<sup>37</sup>. La transplantation hépatique (TH) pour CCI reste actuellement contre indiquée dans la plupart des équipes. La survie à 5 ans est inférieure à 50% dans les séries de patients chez lesquels l'indication pour la TH était initialement une suspicion de CHC<sup>38</sup>. Cependant, des études rétrospectives récentes analysant des groupes homogènes de patients avec des CCI uniques <2cm montrent des résultats encourageants avec des survies de 65 à 73% à 5 ans<sup>38</sup>.

Pour les patients non résécables, la chimiothérapie systémique utilisée actuellement combine gemcitabine et cisplatine. Les résultats de l'essai ABC-02 publiés en 2010 avaient montré une amélioration de la médiane de survie globale de 8.1 à 11.7 mois grâce à cette combinaison<sup>39</sup>. Un essai de seconde ligne de chimiothérapie intra artérielle (gemcitabine et

oxaliplatine) est en cours en France (GEMOXIA, FFCG 1606, clinicaltrials.gov : NCT03364530).

En situation adjuvante, les résultats récents de l'essai de phase III BILCAP ont montré une augmentation de la survie globale avec la capécitabine<sup>40</sup>. L'essai français PRODIGE12-ACCORD18 n'avait par contre pas montré d'intérêt à un traitement adjuvant par gemcitabine et oxaliplatine<sup>41</sup>.

Parmi les autres possibilités thérapeutiques en cours de développement, la radioembolisation à l'yttrium 90 combinée à la chimiothérapie permettrait un allongement de la survie globale<sup>42</sup>. Plusieurs essais de ce schéma pour les CCI non résécables sont en cours aux Etats-Unis et en Europe (clinicaltrials.gov : NCT02807181, NCT02512692).

L'essai de thérapies ciblées suite à l'identification des mutations présentes dans le CCI est en plein développement<sup>43</sup>. Pour l'instant, les différentes études de phase II et III ciblant VEGFR, EGFR, PDGFR, BRAF n'ont pas permis d'améliorer de façon significative la survie des patients<sup>26</sup>. Des inhibiteurs IDH1, IDH2 et FGFR sont en cours d'évaluation<sup>44</sup>.

Des essais d'immunothérapie sont également en cours avec le nivolumab et le pembrolizumab (clinicaltrials.gov : NCT02834013, NCT02628067), des anticorps antiPD1, qui ont déjà montré leur efficacité notamment dans le traitement du mélanome<sup>45</sup>.

## *2. Voie du « Transforming Growth Factor $\beta$ » (TGF $\beta$ )*

### *i. Voie de signalisation / Mécanisme de transduction du signal*

La voie de signalisation du TGF $\beta$  joue un rôle majeur dans le développement des mammifères via la modulation de nombreux processus cellulaires (e.g. prolifération, différenciation) qui vont influer sur l'homéostasie et la régénération tissulaire. Les dérégulations de cette voie peuvent donc être à l'origine de nombreuses pathologies dont les cancers<sup>46</sup>. La famille du TGF $\beta$  humain, qui est une cytokine pléiotropique, comprend plus de 30 membres dont les TGF $\beta$ s (isoformes 1, 2 et 3), les activines et les protéines morphogénétiques de l'os. Le ligand se fixe à son récepteur (du type sérine/thréonine kinase) à la surface cellulaire qui forme un complexe de récepteurs bi-dimérique: TGF $\beta$ RI et

TGF $\beta$ RII. L'activation de la voie canonique dite SMAD-dépendante fait suite à une cascade de phosphorylations activant les protéines SMAD dans le cytoplasme. Le complexe activé formé par SMAD2/3 phosphorylé et SMAD4 (co-SMAD) va migrer dans le noyau cellulaire pour réguler la transcription de gènes cibles de la voie avec l'aide de co-activateurs et de co-répresseurs (figure 6) <sup>47</sup>. La voie de signalisation TGF $\beta$  régule également des modifications post-transcriptionnelles via notamment la biogenèse des microARNs (figure 6).

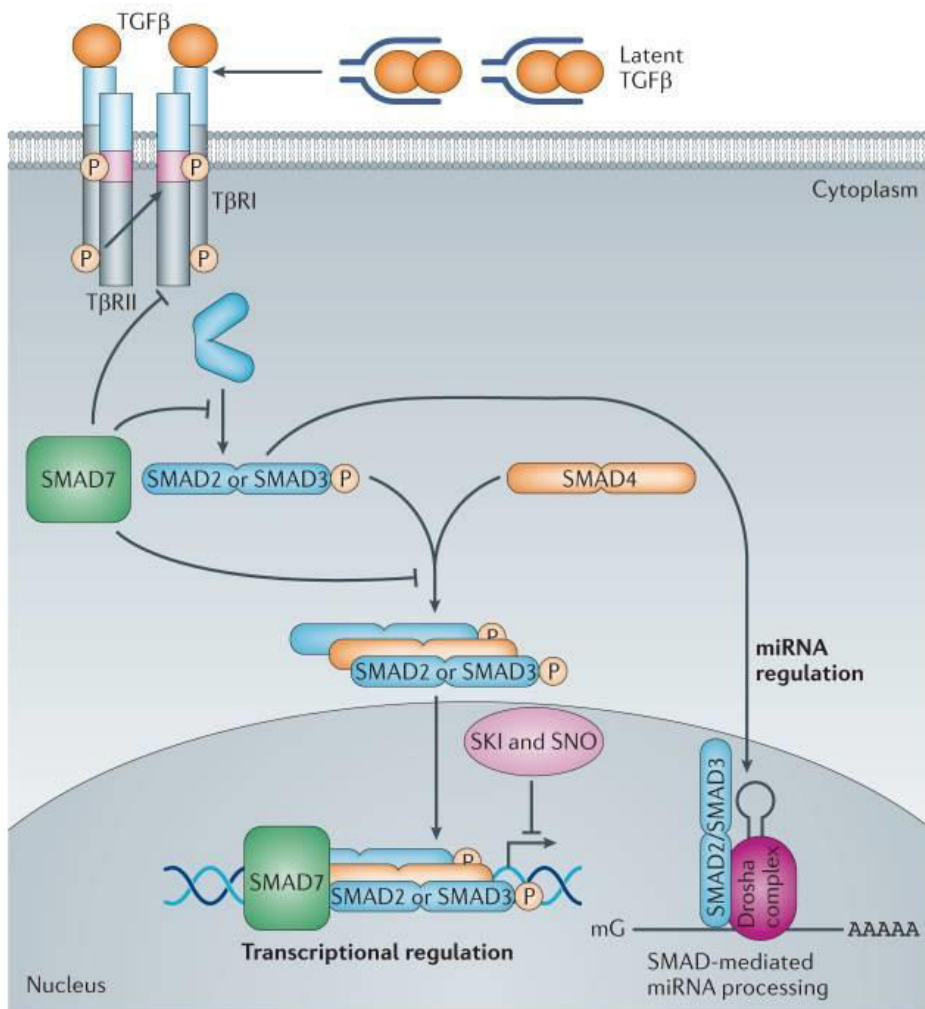


Figure 6: Représentation schématique de la voie de signalisation canonique TGF $\beta$  dépendante des SMADs. Akhurst, *Nat Rev Drug Discov*, 2012 <sup>48</sup>.  
SNO : ski-related novel gene.

L'activation de la voie SMAD indépendante (non canonique) peut se faire via le *crosstalk* avec de nombreuses autres voies dont p38 MAPK, m-TOR, RAS, RhoA, PI3K/AKT, JNK <sup>49</sup>. Les mécanismes de régulation de la voie TGF $\beta$  sont complexes. Par exemple, SMAD7 est un inhibiteur de la famille SMAD qui exerce un rétrocontrôle négatif sur la voie et agit comme

médiateur des interactions avec les autres voies de signalisation e.g. voie Wnt/β-caténine<sup>50</sup>.

Sa surexpression est fréquente quand la voie TGFβ est perturbée<sup>49</sup>.

## ii. Rôle du TGFβ dans la cancérogénèse

Le TGFβ a un rôle paradoxal dans la cancérogénèse. L'activation de la voie donne des effets opposés (suppresseur de tumeur ou tumorigénique) selon le contexte cellulaire (figure 7).

Les mécanismes orientant vers l'un ou l'autre des effets du TGFβ ne sont pas clairement identifiés<sup>51</sup>.

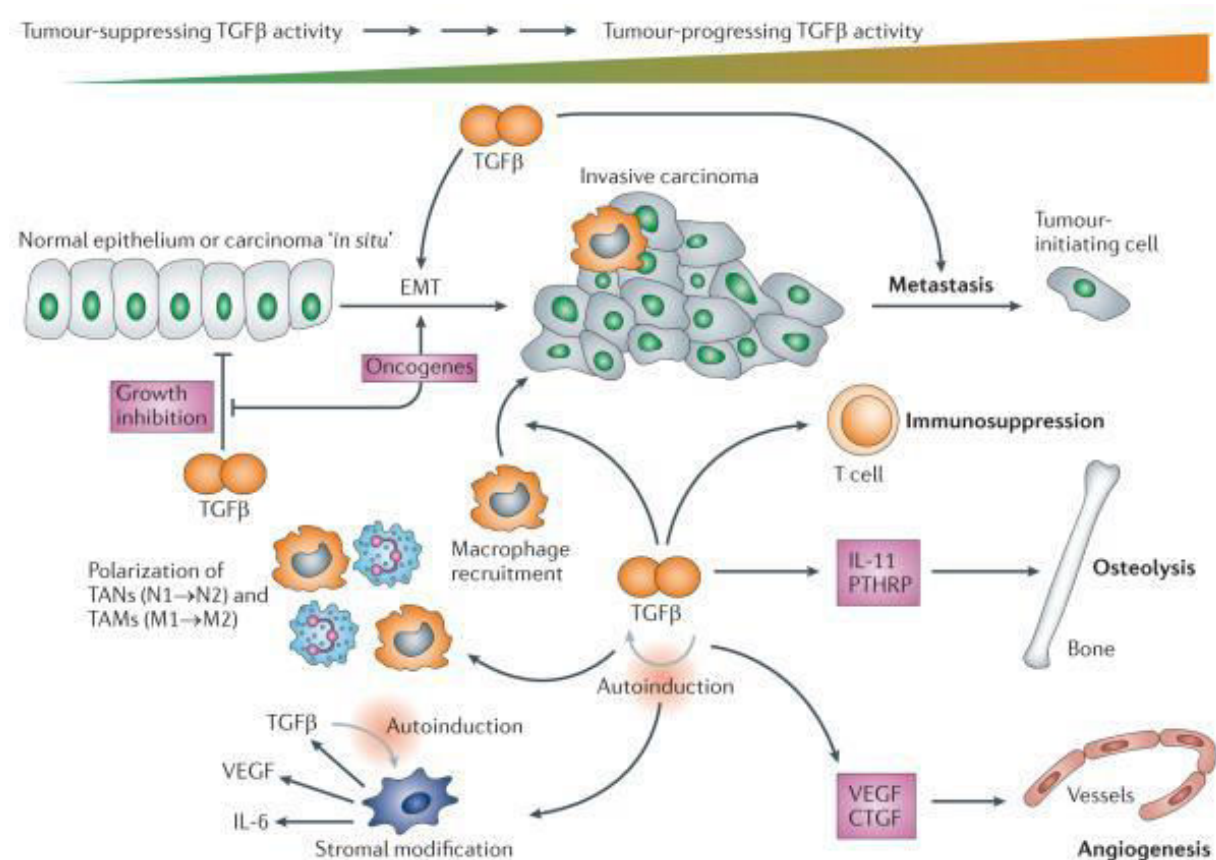


Figure 7: Schéma de l'activité biphasique de la voie TGFβ pendant la cancérogénèse: de la suppression à la promotion de la tumeur. Akhurst, *Nat Rev Drug Discov*, 2012<sup>48</sup>  
Les flèches gris clair indiquent la boucle d'activation conduisant à des niveaux plus élevés de TGFβ dans les pathologies néoplasiques et non néoplasiques.

CTGF, connective tissue growth factor; EMT, epithelial-mesenchymal transition; IL, interleukin; PTHRP, parathyroid hormone-related protein; TAMs, tumour-associated macrophages; TANs, tumour-associated neutrophils; VEGF, vascular endothelial growth factor.

A des stades précoces (prénéoplasiques ou cancer *in situ*), le TGFβ va plutôt exercer un rôle cytostatique, par exemple en contrôlant le cycle cellulaire via c-MYC, p21 et cycline D<sup>49</sup>.

Après activation de signaux oncogéniques, le TGFβ va favoriser l'apoptose et la sénescence pour limiter la prolifération cellulaire et l'apparition de néoplasie<sup>51</sup>. Cependant, nous avons

vu également précédemment le rôle profibrotique du TGF $\beta$  dans les hépatopathies chroniques. Aux stades avancés de cancer, le TGF $\beta$  va augmenter la croissance tumorale et l'invasion. Les effets tumorigéniques du TGF $\beta$  passent par l'activation de la transition épithélio-mésenchymateuse (TEM), la mobilisation de myofibroblastes et l'immunosuppression<sup>51</sup>.

La TEM est un processus dynamique réversible pendant lequel les cellules épithéliales adoptent progressivement les caractéristiques structurelles et fonctionnelles des cellules mésenchymateuses (figure 8)<sup>52</sup>. Elle est mise en évidence au niveau membranaire par la perte d'E-cadhérine et l'expression de protéines mésenchymateuses comme Vimentine, N-cadhérine et fibronectine qui vont favoriser l'invasion<sup>49</sup>. Le processus de perte d'E-cadhérine peut être régulé par les voies SMAD dépendante ou SMAD indépendante du TGF $\beta$  et des interactions entre les deux ont été montré<sup>49</sup>. Au niveau transcriptionnel, les facteurs qui régulent la TEM sont SNAIL, TWIST et ZEB<sup>53</sup>.

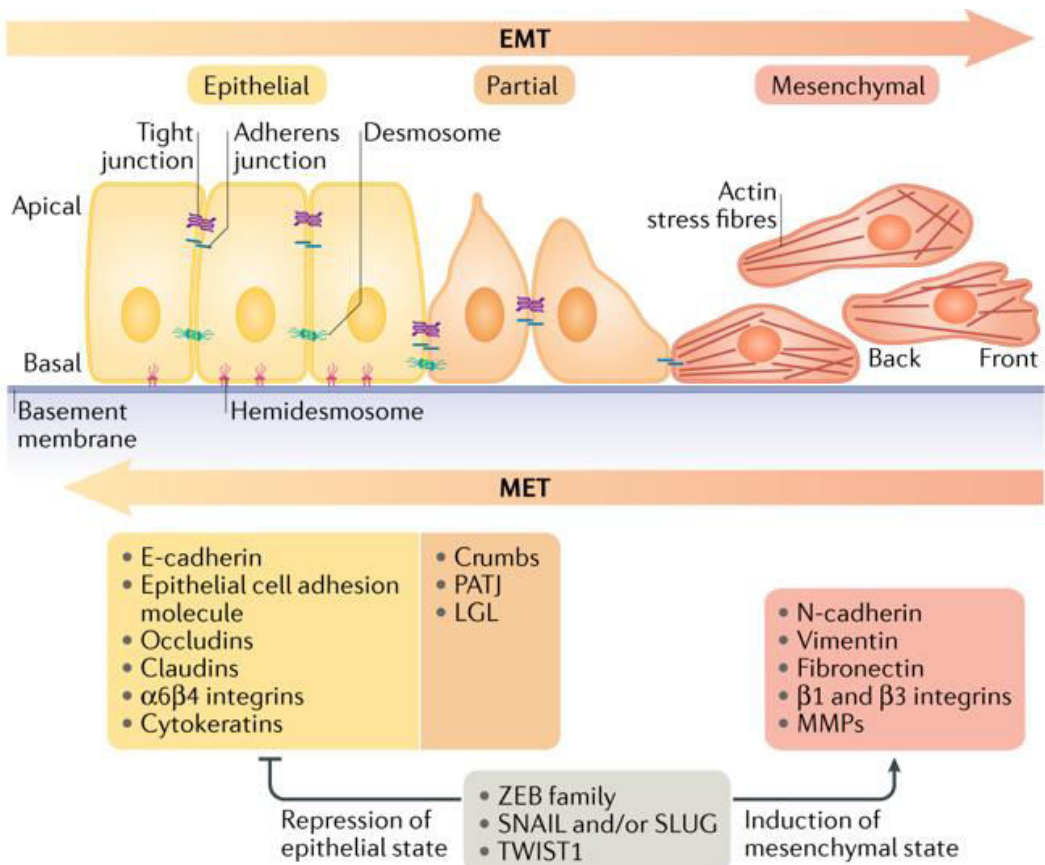


Figure 8: Schéma d'une transition épithélio-mésenchymateuse typique. *Dongre, Nat Rev Mol Cell Biol, 2019*<sup>54</sup>.

PATJ : PALS1-associated tight junction protein. LGL : lethal giant larvae. ZEB : zinc finger E-box binding.

La régulation de l'expression de marqueur de cellules souches cancéreuses comme CD133 par le TGF $\beta$  a été également été montré. Des modèles de xénogreffes CD133+ induites par le TGF $\beta$  ont montré des tumeurs plus agressives avec des cellules résistantes à la chimiothérapie et à l'apoptose<sup>55,56</sup>. À un stade tumoral avancé, le TGF $\beta$  joue aussi un rôle crucial dans la répression du système immunitaire notamment via l'inactivation des cellules T<sup>49</sup>.

Outre son rôle dans la TEM, le TGF $\beta$  exerce aussi une action prométastatique en favorisant l'angiogénèse à un stade tumoral avancé. Le TGF $\beta$  régule l'expression du VEGF ainsi que la prolifération et la migration des cellules endothéliales (figure 7)<sup>57,58</sup>.

Cependant, selon l'organe siège du cancer et le sous type tumoral, la réponse au TGF $\beta$  peut être différente. Le type de réponse des tumeurs (évolution métastatique et pronostic) au TGF $\beta$  permet de les classer en différents groupes. Par exemple dans le cancer du sein, une

signature spécifique de la réponse au TGF $\beta$  n'est pas associée au même sous type de tumeur (récepteur œstrogène + ou -) ni au même site de rechute métastatique (poumon ou os)<sup>59</sup>.

De même, des mutations des récepteurs TGF $\beta$  et de SMAD4 ont été identifiées fréquemment dans le cancer du pancréas et du colon. Cependant, ces mutations seules ne vont pas être responsables du développement tumoral. Elles s'ajoutent à des lésions déjà induites par l'oncogène KRAS ou l'inactivation du gène APC<sup>51</sup>

### *iii. TGF $\beta$ et cholangiocarcinome intrahépatique*

Le TGF $\beta$  joue un rôle majeur dans la TEM et donc le développement du microenvironnement tumoral (stroma). La richesse du stroma fibreux dans le CCI a donc fait supposer l'implication du TGF $\beta$  dans son développement. L'induction de la TEM par le TGF $\beta$  dans le CCI a été montré avec une augmentation des marqueurs mésenchymateux (VIM, S100A4, SNAI1) et une diminution des marqueurs épithéliaux (E cadhérine, CK19)<sup>60,61</sup>. La surexpression des facteurs de transcription SNAI1, TWIST et ZEB est associée à des CCI plus agressifs et de plus mauvais pronostic<sup>53</sup>. Dans les CCI présentant des caractéristiques de cellules souches cancéreuses, le profil transcriptomique a révélé un lien entre l'expression du microARN miR-200c avec la TEM. L'expression de miR-200c est inversement corrélée avec les gènes cibles de la voie TGF $\beta$ . La surexpression de miR-200c dans la lignée HuH28 induit une inhibition de la TEM avec suppression des marqueurs mésenchymateux et augmentation des marqueurs épithéliaux<sup>62</sup>. Plus récemment, des études de co-cultures chez le rat, de cellules de cholangiocarcinome avec des myofibroblastes, ont montré que la formation d'un stroma fibreux (réaction desmoplastique) était dépendante du TGF $\beta$ <sup>63</sup>. Les mécanismes de l'induction de la prolifération cellulaire par le TGF $\beta$  sont multiples. L'IL6 et la cycline D1 via miR-34a seraient impliqués<sup>64-66</sup>. Le TGF $\beta$ 1 induit également l'angiogénèse via VEGF dans le CCI<sup>67</sup>. L'expression de TGF $\beta$ 1 est corrélée à l'envahissement ganglionnaire, les métastases à distance et la récidive dans le CCI<sup>68</sup>.

Les travaux réalisés dans l'unité Inserm 1241 sur le CCI au cours des 10 dernières années ont cherché à identifier des altérations génomiques dans le stroma tumoral du CCI. Après séparation du stroma tumoral et des cholangiocytes tumoraux par microdissection laser de coupes de tumeurs humaines, une analyse transcriptomique a comparé le stroma non tumoral au stroma tumoral. L'analyse a montré une surexpression de l'ostéopontine (SPP1) mais aussi du TGF $\beta$  dans le stroma tumoral qui était corrélée à un plus mauvais pronostic <sup>18</sup>. Ces données confirmaient l'importance du microenvironnement tumoral.

Andersen et al. en 2012 avaient également montré des signatures spécifiques des compartiments épithelial et stromal du CCI avec une augmentation du TGF $\beta$  et de l'IL6 dans le stroma <sup>24</sup>.

Des mutations de composants de la voie TGF $\beta$  ont déjà été observées dans le CCI : *SMAD4*, *SMAD6*, *SMAD7* et des mutations non-sens de *TGFBR1* <sup>69,70</sup>.

Cependant, la dualité fonctionnelle du TGF $\beta$  fait qu'un traitement inhibant la voie TGF $\beta$  pour traiter une fibrose pourrait augmenter le risque de développement d'un cholangiocarcinome. Dans un modèle murin, Mu et al. ont montré que le signal TGF $\beta$  épithelial n'induisait pas la fibrose et protégerait du développement du cholangiocarcinome <sup>71</sup>.

La régulation de la voie TGF $\beta$  est un ensemble de processus complexes qui sont encore loin d'être tous identifiés. Les ARN non-codants pourraient être des acteurs de cette régulation.

### *3. ARN longs non-codants (ARNlnc)*

Le génome codant ne représente que 2% des gènes. Depuis les années 90, le nombre d'ARN non-codants identifiés est en constante augmentation et dépasse le nombre des transcrits codants connus<sup>72</sup>. Afin de simplifier leur classification, ils ont été classés arbitrairement selon leur taille. Les ARN courts ont moins de 200 nucléotides dont les microARN qui ont en moyenne 21 nucléotides et répriment la production de protéines. Les ARN circulaires (ARNcirc) constituent un groupe distinct d'ARN non-codants issus de la biogénèse et de l'épissage de transcrits linéaires, codants ou non-codants. Ils sont stables car résistants aux exonucléases en l'absence d'extrémité libre 5' ou 3'<sup>73</sup>.

#### *i. Caractéristiques des ARNlnc*

Les ARNlnc ont plus de 200 nucléotides et ont été peu étudiés jusqu'aux années 2000 contrairement aux microARNs. Ils appartiennent à une classe hétérogène d'ARN non-codants régulateurs qui influencent une large variété de processus biologiques et de voies de signalisation cellulaires. Après leur découverte dans les années 80, les ARNlnc ont initialement été peu étudiés car considérés comme du « bruit » transcriptionnel et donc non fonctionnels. Le projet *Encyclopedia of DNA elements* (ENCODE) a été initié en 2003 afin de faciliter l'identification et l'analyse de l'ensemble des éléments fonctionnels du génome. Le consortium GENCODE issu de ce projet a permis d'annoter environ 15000 transcrits correspondants à des ARNlnc. L'étude des ARNlnc a montré qu'ils sont généralement moins exprimés que les gènes codants pour des protéines et qu'ils ont des caractéristiques spécifiques d'organes<sup>74</sup>. Même si de nombreux ARNlnc ont été identifiés, leur fonction demeure inconnue pour la plupart.

Comme pour les gènes codants, plusieurs gènes donnant naissance aux ARNlnc sont conservés dans l'évolution<sup>75</sup>. Ils ont des similarités avec les ARNm: ils sont transcrits par la polymérase II, ont une extrémité 5', peuvent être épissés et polyadénylés, mais non codants. La classification courante des ARNlnc différencie 5 catégories selon leur organisation génomique : sens, antisens, bidirectionnel, intronique, et intergénique (figure 9)<sup>76</sup>.

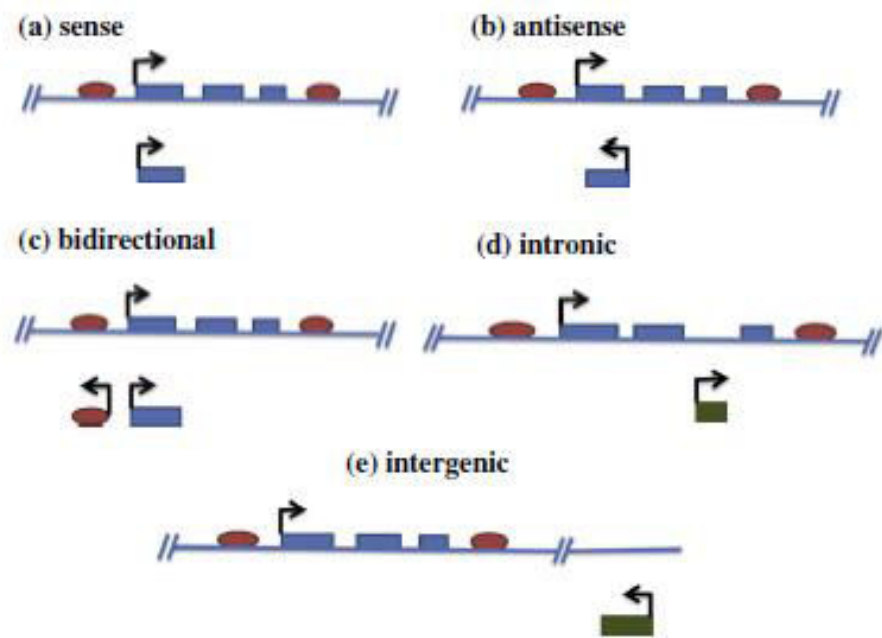


Figure 9: Classification des ARNlnc selon leur organisation génomique. He, Cancer Lett, 2014<sup>76</sup>.

Au niveau fonctionnel, les ARNlnc peuvent s'associer à de l'ADN, à d'autres ARN ou à des protéines ce qui conduira à de multiples fonctions possibles (figure 10).

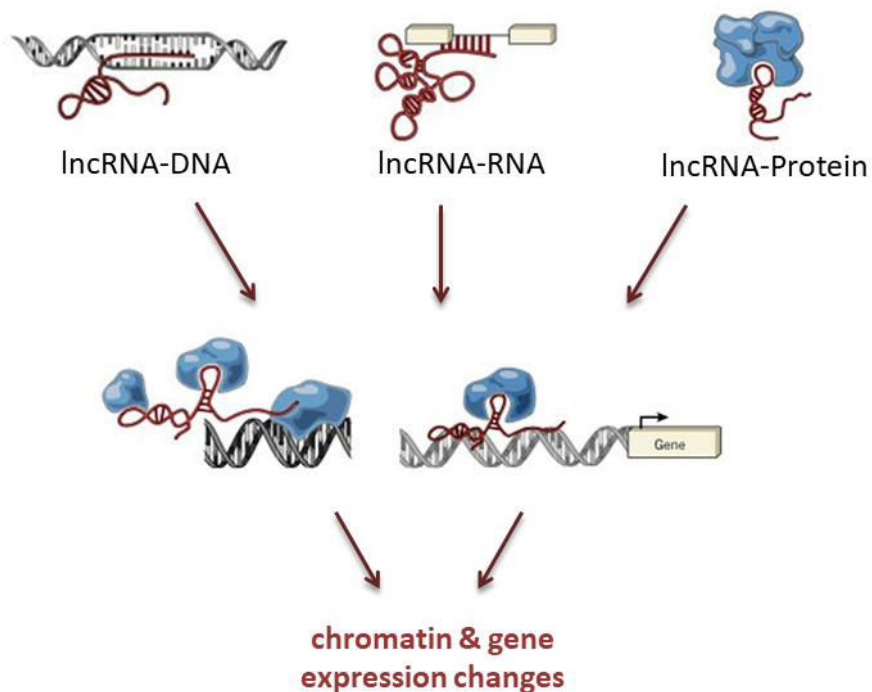


Figure 10: Associations moléculaires possibles des ARNlnc aboutissant à de multiples fonctions.

Les ARNlnc sont localisés dans des compartiments cellulaires spécifiques selon leur fonction biologique<sup>77</sup>. L'identification croissante d'ARNlnc a conduit à découvrir de nombreux modes d'action (figure 11). Le rôle d'ARNlnc a été identifié dans de nombreuses pathologies et organes différents (cœur, cerveau foie, poumon) mais surtout dans les cancers. Dans la cancérogénèse hépatique, les premières altérations d'expression d'ARNlnc ont été identifiées dans le CHC dont des exemples sont cités ci-dessous.

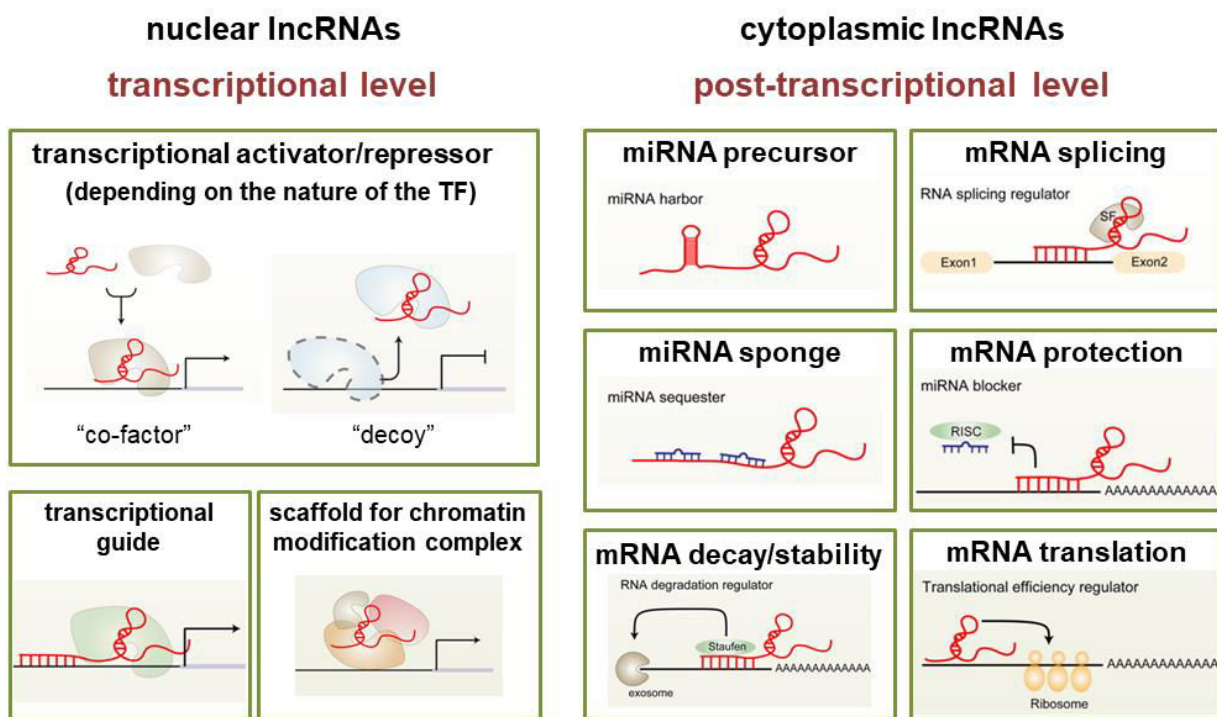


Figure 11: Exemples de description de modes d'actions des ARNlnc selon leur localisation nucléaire ou cytoplasmique.

Dans le noyau, les ARNlnc peuvent agir sur la chromatine et influencer la transcription :

- Guide : ces ARNlnc se lient à des protéines afin de former des complexes capables d'agir comme facteurs de transcription. Exemple de l'ARNlnc HOXA Distal Transcript Antisense RNA (HOTTIP) dans le CHC : HOTTIP interagit avec le complexe mixed lineage leukemia (MLL) qui conduit à la formation de H3K4me3 (triméthylation de la lysine 4 de la protéine d'histone H3) et à la transcription de gènes à proximité (figure 12)<sup>78</sup>.

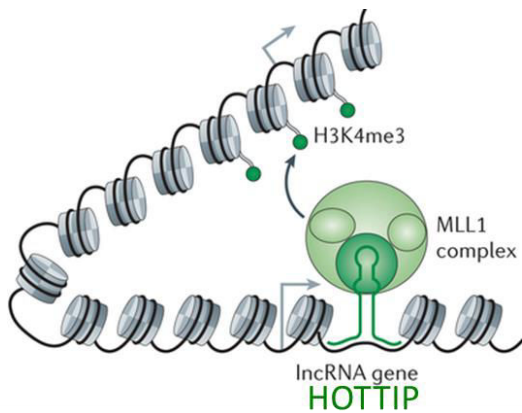


Figure 12: Schéma du mode d'action de HOTTIP. Wang, *Nature*, 2011<sup>78</sup>.  
MLL : mixed lineage leukemia.

- Echafaudage (*scaffold*) : ces ARNlnc servent de plateformes sur lesquelles différents composants moléculaires vont s'assembler. Les complexes ainsi formés vont réguler au niveau épigénétique des régions génomiques spécifiques. L'ARNlnc HOXA Transcript Antisense RNA (HOTAIR) a ainsi un rôle oncogénique en modulant les complexes d'histones comme Polycomb Repressive Complex 2 (PRC2) impliqués dans la répression de gènes suppresseurs de tumeur (figure 13)<sup>79</sup>.

**PRC2 (Polycomb Repressive Complex 2): histone methyl-transferase complex**  
« writer » of the repressive mark H3K27 trimethylation

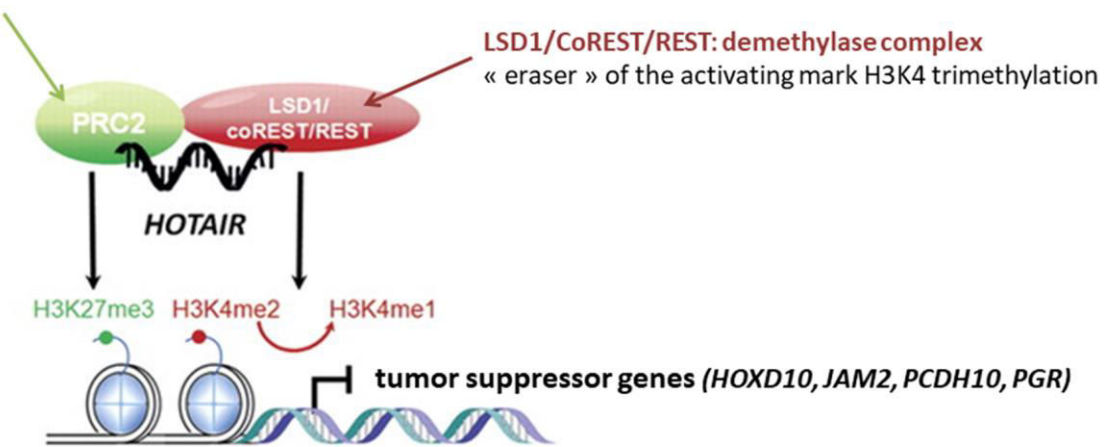


Figure 13 : Schéma du mode d'action de HOTAIR sur les complexes d'histone PRC2 et LSD1/coREST/REST. D'après Tsai, *Science*, 2010<sup>79</sup>.

PRC2 : Polycomb Repressive Complex 2. LSD1 : lysine-specific histone demethylase. REST : RE1-silencing transcription factor; 1. H3K27me3 : trimethylated lysine 27 of histone H3. H3K4me : methylated lysine 4 of histone H3. HOXD10: homeobox D10. JAM2 : junctional adhesion molecule 2. PCDH10 : protocadherin 10. PGR : progesterone receptor

- Régulateur transcriptionnel: ces ARNlnc vont être co-facteur de facteur de transcription ou répresseur en agissant comme leurre (*decoy*) pour les facteurs de transcription. L'ARNlnc p21-associated ncRNA DNA damage-activated (PANDA) limite ainsi l'apoptose en séquestrant le facteur de transcription nuclear transcription factor Y (NF-Y) (figure 14)<sup>80,81</sup>.

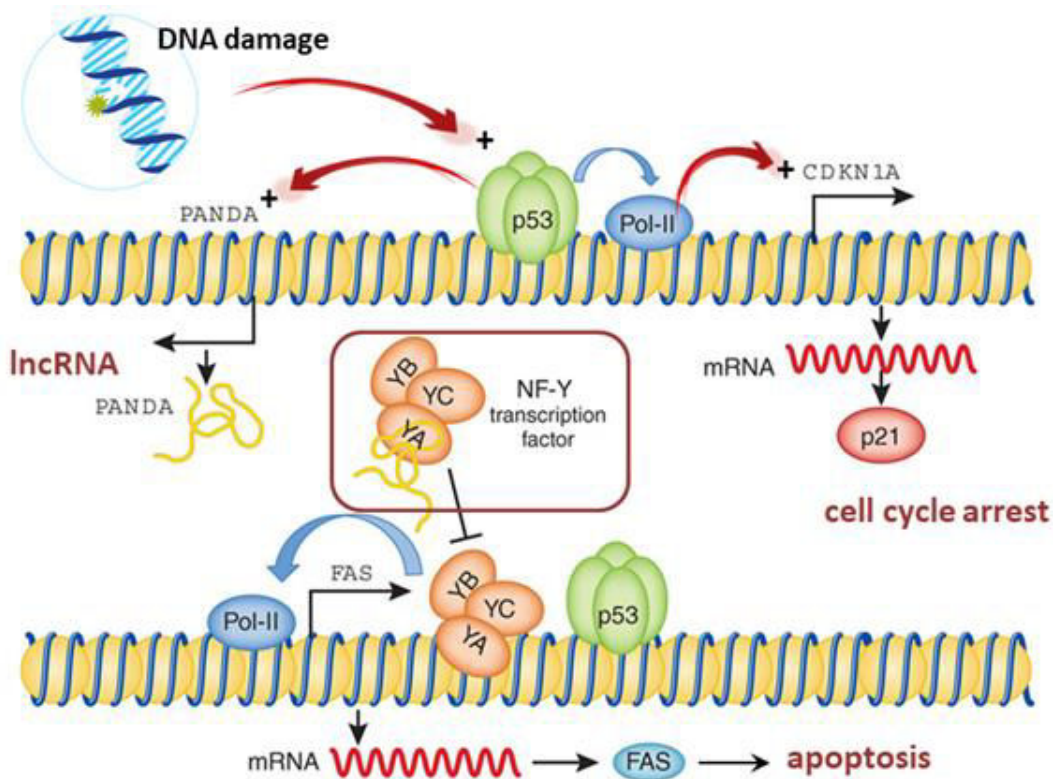


Figure 14: Schéma du mode d'action de PANDA. Sotillo, *Nat Genet*, 2011<sup>81</sup>.  
PANDA : p21-associated ncRNA DNA damage-activated. CDKN1A : cyclin-dependent kinase Inhibitor 1A. NF-Y : nuclear transcription factor Y. Pol-II : RNA polymerase II.

Dans le cytoplasme, les ARNlnc agissent au niveau post transcriptionnel (figure 11).

Sur les ARNm, les ARNlnc peuvent agir comme :

- Régulateur de l'épissage des ARNm
- Protecteur de l'action des miARN (bloqueur de miARN)
- Régulateur de la traduction
- Régulateur de la dégradation ou de la stabilité des ARNm

Sur les miARN, les ARNlnc peuvent agir comme :

- Précurseur de miARN. Exemple : l'ARNlnc H19, qui est essentiel à la croissance tumorale du CHC, a sur son exon 1 un site précurseur de miR-675 (figure 15)<sup>82,83</sup>

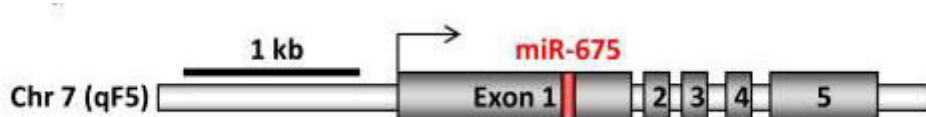


Figure 15 : Représentation schématique de l'unité transcriptionnelle de H19 avec miR-675 (en rouge) inclus dans l'exon 1 de H19. La flèche noire indique le site de départ de la transcription. *Keniry, Nat Cell Biol, 2012*<sup>83</sup>.

- Eponge à microARN, ce qui aura pour conséquence de réguler positivement leurs cibles. Exemple : l'ARNlnc phosphatase and tensin homolog pseudogene 1 (PTENP1) séquestre le microARN miR-21 (oncomiR) et l'empêche d'inhiber le suppresseur de tumeur PTEN ce qui inhibe la prolifération et bloque le cycle cellulaire via le blocage de la voie de signalisation AKT (figure 16)<sup>84</sup>.

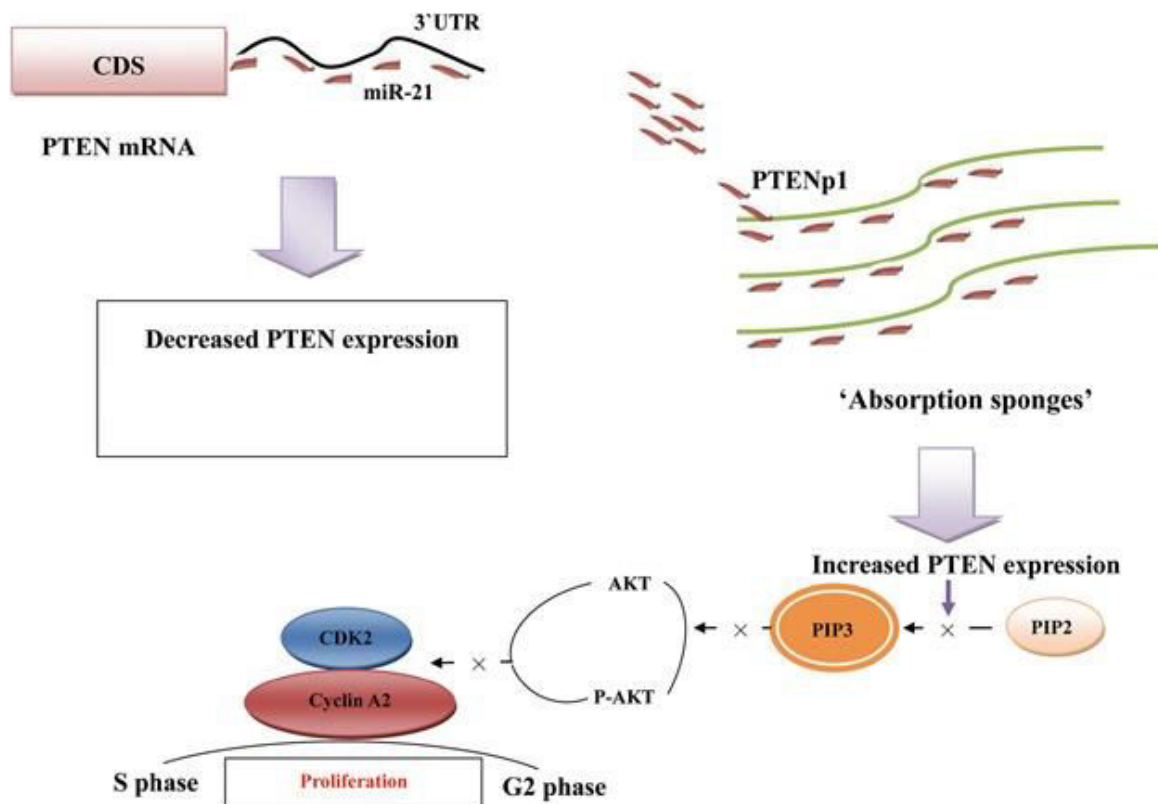


Figure 16 : Représentation schématique de l'action de PTENP1. *Gao, Mol Carcinog, 2017*<sup>84</sup>.  
CDS : coding DNA sequence. PTEN : phosphatase and tensin homolog. PIP : prolactin-inducible protein. CDK2: cyclin-dependent kinase 2.

## *ii. ARNlnc et cholangiocarcinome*

Dans le cholangiocarcinome, l'altération d'expression de plusieurs ARNlnc a également été montré<sup>85</sup>. En 2014, Wang et al. ont montré par analyse transcriptomique de 77 CCI et tissus non tumoraux adjacents humains que 2773 ARNlnc étaient surexprimés et 2392 sous exprimés<sup>86</sup>. L'analyse récente du profil d'expression des ARNlnc de CCI humains a été réalisée par plusieurs équipes à partir de la base de données *The Cancer Genome Atlas* (TCGA). Ils ont également montré une différence d'expression d'ARNlnc avec pour certains une corrélation à la survie des patients<sup>87,88</sup>. L'analyse des réseaux de co-expression des ARN codants et non-codants dans le CCI par Yang et al. en 2017 a identifié des ARNlnc impliqués dans l'inflammation et la voie PPAR qui peut réguler la TEM<sup>89</sup>.

Au niveau épigénétique, l'interaction de l'ARNlnc Small Nucleolar RNA Host Gene 1 (SNHG1) avec enhancer of zeste 2 (EZH2), la sous unité catalytique du PRC2, réduit l'expression de CDKN1A qui est suppresseur de tumeur<sup>90</sup>. L'ARNlnc nuclear paraspeckle assembly transcript 1 (NEAT1) interagit également avec EZH2 pour diminuer l'expression d'E-cadhérine et favoriser la TEM dans le CCI<sup>91</sup>.

Certains ARNlnc ont également une action directe ou indirecte sur des régulateurs oncogéniques. Ainsi, l'ARNlnc epigenetically-induced lncRNA1 (EPIC1) cible directement le facteur de transcription oncogénique MYC pour promouvoir la prolifération cellulaire<sup>92</sup>. L'ARNlnc metastasis associated lung adenocarcinoma transcript 1 (MALAT1) active la voie PI3/AKT et augmente la prolifération et l'invasion cellulaire<sup>93</sup>.

Le niveau d'expression de quelques ARNlnc est corrélé au pronostic de patients opérés de CCI constituant ainsi de potentiels biomarqueurs. Par exemple, les ARNlnc Colorectal Neoplasia Differentially Expressed (CRNDE) et taurine upregulated gene 1 (TUG1) sont surexprimés dans les CCI et leur surexpression est corrélée au mauvais pronostic<sup>94-96</sup>. Une revue de la littérature est consacrée à ce sujet dans la partie résultat de ce manuscrit.

### iii. ARNlnc et TGF $\beta$ dans la cancérogénèse hépatique

Des ARNlnc régulés par la voie TGF $\beta$  ont été identifiés dans la cancérogénèse. Au cours de la TEM, SNAI1 est un des régulateurs dont l'expression est sous la dépendance du TGF $\beta$ . L'ARNlnc ZEB2 antisense RNA (ZEB2-AS) a été identifié comme médiateur de l'action de SNAI1 sur la synthèse de ZEB2 qui est un répresseur transcriptionnel de l'E-Cadhérine (figure 17) <sup>97</sup>.

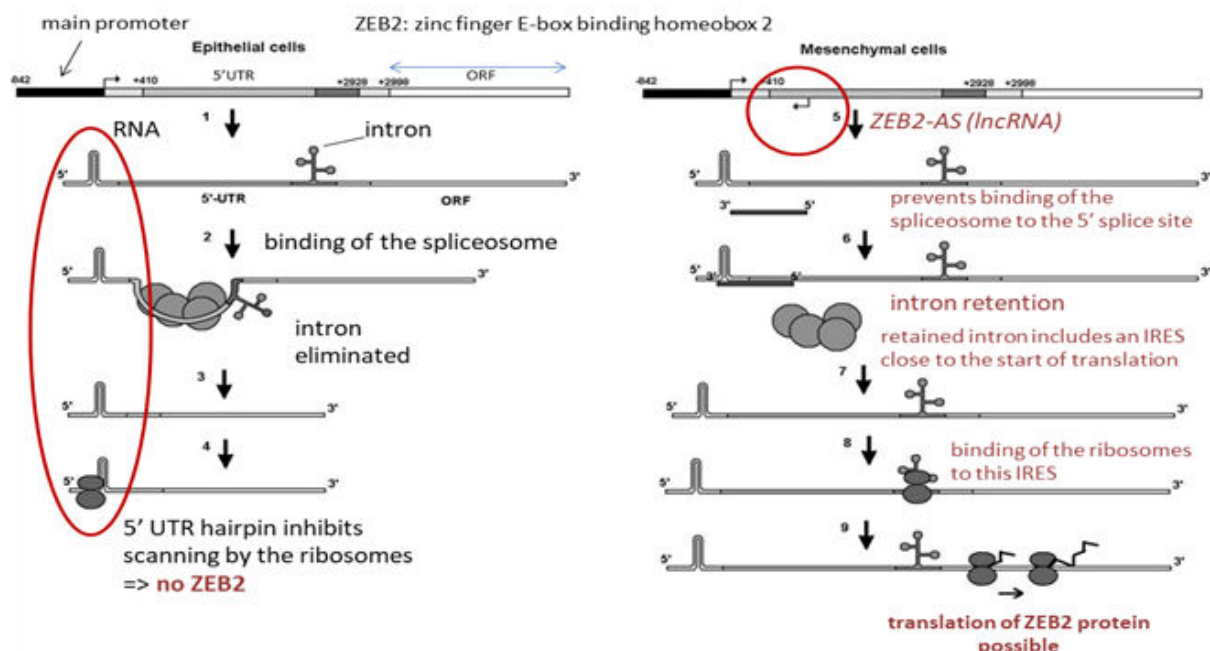


Figure 17: Schéma du mode d'action de ZEB2-AS. Beltran, Genes Dev, 2008 <sup>97</sup>.

SNAI1 n'influence pas directement la synthèse de ZEB2 mais prévient l'épissage d'un large intron situé sur son extrémité 5'UTR. L'intron contient un site d'entrée interne aux ribosomes nécessaire à l'expression de ZEB2. Le maintien de l'intron est dépendant de l'expression d'un transcript naturel antisens (ZEB2-AS) qui chevauche le site de l'intron. L'expression ectopique de ZEB2-AS dans les cellules épithéliales prévient l'épissage de l'extrémité 5'UTR de ZEB2, augmente le niveau de la protéine ZEB2 et diminue l'expression de l'E-Cadhérine. ZEB: zinc finger E-box binding.

Jusqu'à présent au niveau hépatique, des ARNlnc potentiels médiateurs de la voie TGF $\beta$  ont seulement été identifiés dans le CHC.

L'ARNlnc activated by TGF $\beta$  (ATB) est induit par le TGF $\beta$  et sa surexpression est corrélée au mauvais pronostic du CHC. ATB régule ZEB1 et ZEB2 en agissant comme éponge à miR-200 et ainsi induit la TEM et l'invasion (figure 18) <sup>98</sup>. ATB se lie également à l'IL11 ce qui induit une production autocrine d'IL11 qui va activer la voie STAT3 et le processus métastatique dans le CHC <sup>98</sup>. ATB est également surexprimé dans de nombreux autres

cancers (e.g. colorectal, gastrique, rénal, pancréatique, pulmonaire) avec une corrélation à un mauvais pronostic<sup>99</sup>.

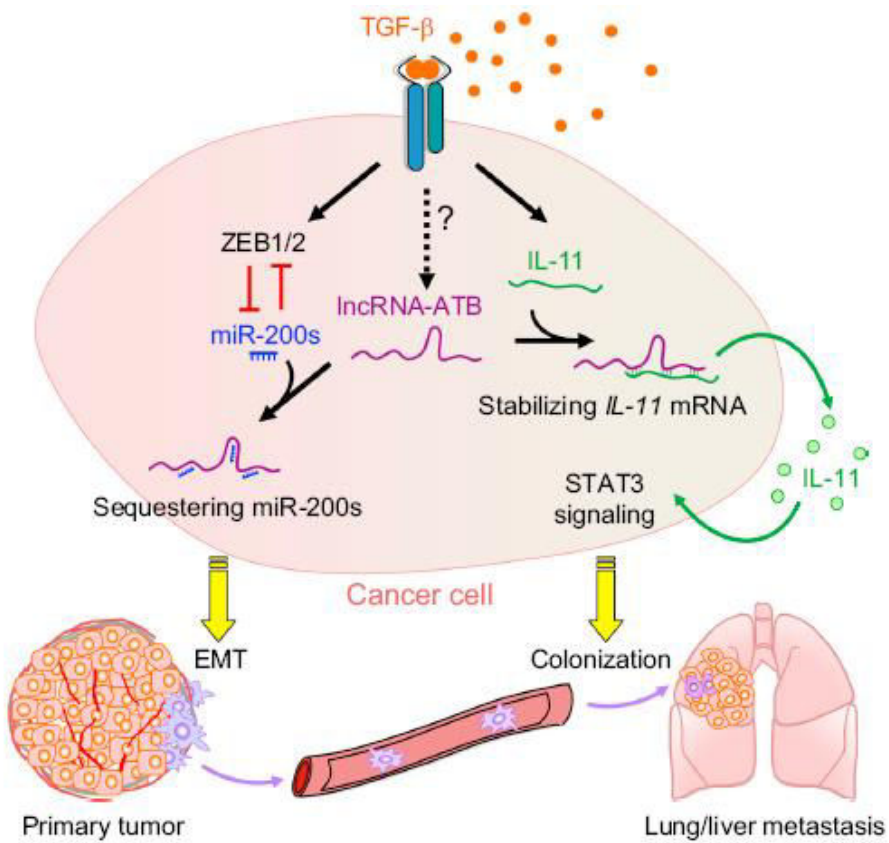


Figure 18 : Schéma du mode d'action de l'ARNlnc ATB. Yuan, *Cancer Cell*, 2014<sup>98</sup>.

Récemment, Zhang et al. ont montré que le TGF $\beta$  inhibe la transcription de l'ARNlnc H19 par l'intermédiaire du facteur de transcription SOX2 dans les hépatocytes précurseurs de tumeurs. L'ARNlnc H19 est impliqué dans la prolifération et la survie de ces hépatocytes<sup>100</sup>. Ces travaux ont donc permis d'identifier un ARNlnc, H19, comme médiateur des effets suppresseurs de tumeur du TGF $\beta$  à un stade précoce du développement du CHC.

L'ARNlnc Regulator Of Reprogramming (ROR) est induit par le TGF $\beta$  dans le CHC et intervient dans la chimiorésistance via les cellules exprimant CD133<sup>101</sup>.

Certains ARNlnc peuvent également être régulateurs de la voie TGF $\beta$ .

L'ARNlnc Maternally Expressed Gene 3 (MEG3), un ARNlnc qui interagit avec la chromatine, régule la voie TGF $\beta$  par l'intermédiaire de structures ARN-ADN<sup>102</sup>. Il joue un rôle dans le développement de la fibrose hépatique car son expression est diminuée en réponse au

TGF $\beta$  dans la lignée de cellules hépatiques étoilées humaines LX2. Sa surexpression inhibe la prolifération cellulaire induite par le TGF $\beta$  et augmente l'apoptose <sup>103</sup>. Son rôle dans le développement du CHC avait également été montré par l'intermédiaire de sa régulation par miR-29 <sup>104</sup>.

La surexpression de LINC00974 est corrélée à celle de la kératine 19 (KRT19) et à un mauvais pronostic dans le CHC. La répression de LINC00974 inhibe la prolifération cellulaire et l'invasion par l'activation de l'apoptose et de l'arrêt du cycle cellulaire. Son action est liée à son rôle d'éponge pour le miR-642 qui va induire une surexpression de KRT19 et une activation des voies de signalisation NOTCH et TGF $\beta$  <sup>105</sup>.

L'ARNlnc Plasmacytoma Variant Translocation 1 (PVT1) régule SMAD4 et les gènes associés à l'apoptose dans la voie TGF $\beta$  <sup>106</sup>. Dans le CHC, PVT1 augmente la prolifération cellulaire et l'acquisition de propriétés de cellules souches <sup>107</sup>.

L'ARNlnc Antisense Noncoding RNA In The INK4 Locus (ANRIL) est transcrit dans le sens opposé du locus INK4 codant pour les gènes suppresseurs de tumeurs p15INK4b, p14ARF et p16INK4a. ANRIL est un ARNlnc dérégulé dans les maladies cardiovasculaires et de nombreux cancers. Il recrute les complexes PRC1 et PRC2 par l'intermédiaire des protéines polycomb chromobox7 (CBX7) et PRC2 Subunit (SUZ12), respectivement (figure 19). Ces interactions épigénétiques aboutissent à la répression du locus INK4 qui induit la prolifération cellulaire. Dans les cellules de cancer de la thyroïde et de cancer épidermoïde de l'œsophage, ANRIL réduit l'expression de p15/INK4 en inhibant la voie TGF $\beta$ , ce qui aboutit à une augmentation de l'invasion et des métastases <sup>108,109</sup>.

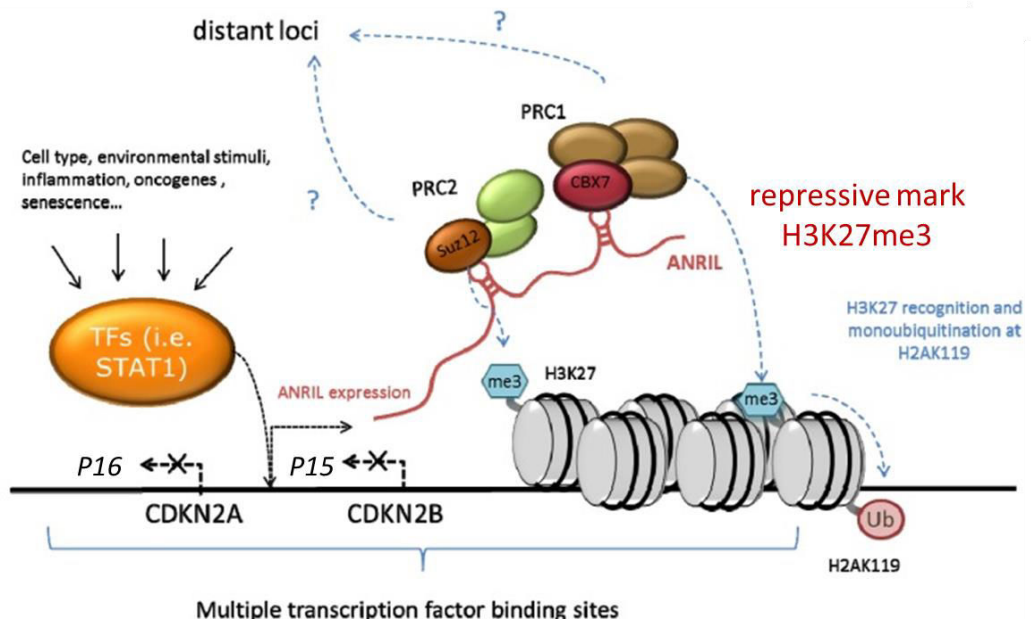


Figure 19 : Schéma du mode d'action d'ANRIL. *Congrains, Int J Mol Sci, 2013*<sup>110</sup>.

CDKN2 : Cyclin Dependent Kinase Inhibitor 2. TFs : transcription factors. CBX7 : Chromobox 7. Suz12 : Polycomb Repressive Complex 2 Subunit. H3K27me3 : trimethylated lysine 27 of histone H3.

ANRIL agit comme éponge pour plusieurs microARNs, notamment pour miR-122-5p dans le CHC. ANRIL est surexprimé dans le CHC où un lien a été observé avec une induction de la prolifération cellulaire, la capacité à former des colonies, des métastases et l'invasion<sup>111</sup>. Une partie des résultats de ce manuscrit est consacrée à l'identification d'ANRIL comme facteur prédictif de mauvais pronostic dans le CCI.

## **II. Objectifs**

Le CCI est un cancer de mauvais pronostic avec un arsenal thérapeutique limité. Après une résection chirurgicale, seul traitement potentiellement curatif, la récidive est fréquente et peu répondeuse aux chimiothérapies actuelles. Les axes de recherche actuels sur la prise en charge du CCI doivent donc se porter sur l'identification:

- des altérations d'expression génique présentes dans le CCI
- de biomarqueurs diagnostiques et pronostiques
- de potentielles cibles thérapeutiques

Des travaux antérieurs réalisés au sein de l'unité Inserm 1241 s'étaient intéressés au microenvironnement tumoral dans le CCI. L'expression de TGF $\beta$  dans le stroma tumoral était corrélée à un mauvais pronostic <sup>18</sup>. Comme décrit en introduction, plusieurs publications ont également confirmé cette implication de la voie TGF $\beta$  dans le microenvironnement tumoral du CCI. Cependant, l'impact d'un environnement riche en TGF $\beta$  sur le transcriptome des cellules de CCI a été peu étudié.

La dérégulation d'ARN non-codants dans la cancérogénèse est de plus en plus mise en évidence. La découverte de leur action régulatrice de nombreuses voies de signalisation permet d'imaginer de nouvelles cibles thérapeutiques.

L'hypothèse du projet est l'implication d'ARNInc dans le développement du CCI notamment comme médiateurs de la voie TGF $\beta$ . Les objectifs du projet se sont focalisés sur:

- l'identification des ARNInc régulés par le TGF $\beta$  dans le CCI et leur caractérisation fonctionnelle
- la recherche d'ARNInc potentiels biomarqueurs diagnostiques ou pronostiques

Les études ont été menées *in vitro* sur des lignées cellulaires de CCI et en parallèle *in vivo* sur tumeurs humaines. Les lignées cellulaires ont été choisies de phénotype différent pour étudier l'activation de la voie TGF $\beta$  dans différents contextes cellulaires. Les tumeurs humaines ont été obtenues à partir du centre de ressources biologiques local du CHU de Rennes mais aussi via le réseau national des tumeurs du foie.

### **III. Résultats**

#### **1. Article n°1**

Publié dans Hepatology Communications

#### **« TLINC : un nouvel ARNlnc induit par le TGFβ favorise un microenvironnement inflammatoire dans le cholangiocarcinome intrahépatique »**

L'objectif de ce travail était d'étudier l'impact du TGFβ sur le transcriptome des cellules de CCI. Une analyse transcriptomique par microarrays de 2 lignées cellulaires de CCI de phénotype différent, HuCCT1 (épithelial) et HuH28 (mésenchymateux), a été réalisée avec et sans traitement par le TGFβ. Une signature spécifique des gènes dérégulés par le TGFβ a été identifiée incluant des gènes cibles connus de la voie TGFβ mais également de nouveaux gènes cibles dont plusieurs ARNlnc. Nous nous sommes focalisé sur l'étude d'un ARNlnc connu sous le nom de CASC15/LINC00340, que nous avons renommé TLINC (*TGFβ induced long non coding RNA*). En effet, nous montrons que TLINC est une cible du TGFβ dans des lignées cellulaires hépatiques et non hépatiques. Dans les lignées de CCI, l'expression de 2 isoformes, longue et courte, était associée à un phénotype épithelial ou mésenchymateux respectivement. Les 2 isoformes ont été détectées dans le noyau et le cytoplasme. L'isoforme longue de TLINC était associée à un phénotype migratoire dans les lignées cellulaires de CCI et à l'induction de cytokines proinflammatoires, dont l'IL8, dans les lignées cellulaires et dans les CCI humains réséqués. TLINC a été identifié comme marqueur tumoral dans les cellules épithéliales et stromales. Dans les foies non tumoraux, TLINC est présent seulement dans les espaces portes spécifiques avec des signes de réaction et d'inflammation ductulaire. Enfin, nous avons montré expérimentalement l'existence d'isoformes circulaires de TLINC dans les lignées cellulaires traitées avec le TGFβ et dans les CCI humains réséqués.

# A Novel Transforming Growth Factor Beta-Induced Long Noncoding RNA Promotes an Inflammatory Microenvironment in Human Intrahepatic Cholangiocarcinoma

Aude Merdrignac,<sup>1</sup> Gaëlle Angenard,<sup>1</sup> Coralie Allain,<sup>1</sup> Kilian Petitjean,<sup>1</sup> Damien Bergeat,<sup>1</sup> Pascale Bellaud,<sup>1</sup> Allain Fautrel,<sup>1</sup> Bruno Turlin,<sup>1</sup> Bruno Clément,<sup>1</sup> Steven Dooley,<sup>2</sup> Laurent Sulpice,<sup>1</sup> Karim Boudjema,<sup>1</sup> and Cédric Coulouarn<sup>1</sup>

Intrahepatic cholangiocarcinoma (iCCA) is a deadly liver primary cancer associated with poor prognosis and limited therapeutic opportunities. Active transforming growth factor beta (TGF $\beta$ ) signaling is a hallmark of the iCCA microenvironment. However, the impact of TGF $\beta$  on the transcriptome of iCCA tumor cells has been poorly investigated. Here, we have identified a specific TGF $\beta$  signature of genes commonly deregulated in iCCA cell lines, namely HuCCT1 and Huh28. Novel coding and noncoding TGF $\beta$  targets were identified, including a TGF $\beta$ -induced long noncoding RNA (TLINC), formerly known as cancer susceptibility candidate 15 (CASC15). TLINC is a general target induced by TGF $\beta$  in hepatic and nonhepatic cell types. In iCCA cell lines, the expression of a long and short TLINC isoform was associated with an epithelial or mesenchymal phenotype, respectively. Both isoforms were detected in the nucleus and cytoplasm. The long isoform of TLINC was associated with a migratory phenotype in iCCA cell lines and with the induction of proinflammatory cytokines, including interleukin 8, both *in vitro* and in resected human iCCA. TLINC was also identified as a tumor marker expressed in both epithelial and stroma cells. In nontumor livers, TLINC was only expressed in specific portal areas with signs of ductular reaction and inflammation. Finally, we provide experimental evidence of circular isoforms of TLINC, both in iCCA cells treated with TGF $\beta$  and in resected human iCCA. Conclusion: We identify a novel TGF $\beta$ -induced long noncoding RNA up-regulated in human iCCA and associated with an inflammatory microenvironment. (*Hepatology Communications* 2018;2:254–269)

## Introduction

Cholangiocarcinomas (CCAs) comprise heterogeneous hepatobiliary tumors with cholangiocyte differentiation features. CCAs are classified as intrahepatic (iCCA), perihilar, and distal, based on their anatomic location.<sup>(1,2)</sup> In the liver,

iCCA accounts for 5%–10% of all malignant primary cancers and ranks second after hepatocellular carcinoma (HCC). Importantly, both incidence and mortality rates of iCCA have increased significantly worldwide during the past decades.<sup>(2)</sup> To date, surgery is the best potentially curative treatment for iCCA but is feasible in less than 40% of cases. For these

**Abbreviations:** CASC15, cancer susceptibility candidate 15; CCA, cholangiocarcinoma; circRNA, circular RNA; EMT, epithelial to mesenchymal transition; GSEA, gene set enrichment analysis; HCC, hepatocellular carcinoma; iCCA, intrahepatic cholangiocarcinoma; IL8, interleukin 8; ISH, *in situ* hybridization; LCM, laser capture microdissection; lncRNA, long non coding RNA; miRNA, miR, micro RNA; Q-RT-PCR, quantitative reverse-transcription polymerase chain reaction; RNase, ribonuclease; SMAD, SMAD family member; SNAI1, snail family transcriptional repressor 1; TGF $\beta$ , transforming growth factor beta; TLINC, transforming growth factor beta-induced long noncoding RNA; TLINC-L, long TLINC isoform; TLINC-S, short TLINC isoform.

Received November 1, 2017; accepted December 8, 2017.

Additional Supporting Information may be found at [onlinelibrary.wiley.com/doi/10.1002/hep4.1142/full](http://onlinelibrary.wiley.com/doi/10.1002/hep4.1142/full).

Supported by INSERM, University of Rennes 1, Institut National du Cancer (INCa, Cancéropôles Ile-de-France and Grand-Ouest), Ligue contre le cancer (cd35, cd44, cd49), Novartis Oncology, and Association Française pour l'Etude du Foie, France (to L.S., C.C.); and by Deutsche Forschungsgemeinschaft DFG DO373/13-1 (to S.D.).

resectable early stage iCCAs, 5-year survival is about 40%. However, for unresectable advanced iCCA, the median survival is less than 15 months.<sup>(2)</sup> Although significant progress in understanding the molecular basis of iCCA pathogenesis has been achieved by high throughput strategies, including the identification of genetic, epigenetic, and genomic alterations (e.g., KRAS proto-oncogene guanosine triphosphatase [*KRAS*], isocitrate dehydrogenase 1/2 [*IDH1/2*] mutations, fibroblast growth factor receptor 2 [*FGFR2*] fusions), there is no approved molecular targeted therapy that significantly improves patient survival in iCCA.<sup>(1,3)</sup> Thus, iCCA remains characterized by limited therapeutic options and very poor prognosis.<sup>(1,3)</sup> One histologic feature of iCCA is the presence of a prominent desmoplastic stroma that is known to contribute to tumor onset and progression.<sup>(4,5)</sup> While previous studies largely focused on identifying molecular alterations in tumor cells, we recently characterized genomic alterations that occur in the tumor microenvironment of iCCA.<sup>(6)</sup> Thus, by combining laser microdissection and gene expression profiling, we demonstrated that the expression of transforming growth factor beta (TGF $\beta$ ) in the stroma of iCCA predicts a poor prognosis, suggesting that TGF $\beta$  may represent a potential therapeutic target in iCCA.<sup>(6)</sup>

TGF $\beta$  is a pleiotropic cytokine that controls fundamental cellular processes associated with carcinogenesis (e.g., proliferation, apoptosis, invasion, angiogenesis, immunity).<sup>(7)</sup> However, the actions of TGF $\beta$  in cancer are complex because TGF $\beta$  exhibits either tumor-suppressive or tumor-promoting properties, depending

on the tumor stage. At an early stage, TGF $\beta$  exerts potent antiproliferative properties on precancerous epithelial cells, notably by inducing genes with cytostatic actions (e.g., cyclin-dependent kinase inhibitor 1A [*CDKN1A*]). At an advanced stage, cells become resistant to the cytostatic effects of TGF $\beta$ , which then promotes tumor growth and metastatic progression, particularly as a potent inducer of epithelial–mesenchymal transition (EMT).<sup>(7,8)</sup> To date, the molecular mechanisms switching the TGF $\beta$  actions from tumor suppression toward tumor promotion are not fully understood and may depend on the cellular context.<sup>(9,10)</sup> Gene mutations in the canonical TGF $\beta$  signaling (e.g., SMAD family member 4 [*SMAD4*]) and crosstalk with proliferative pathways have been proposed to contribute to the loss of the tumor suppressor arm of TGF $\beta$  in several cancers.<sup>(9)</sup> In addition, recent evidence demonstrated that long noncoding RNA (lncRNA) could mediate the prometastatic properties of TGF $\beta$ .<sup>(11,12)</sup> LncRNAs form a large and diverse class of long RNA molecules (>200 nucleotides) that do not encode proteins. LncRNAs emerged as key regulators involved in human carcinogenesis, including liver cancers.<sup>(13,14)</sup> Here, we characterized the transcriptional response of iCCA cell lines to TGF $\beta$  and identified novel TGF $\beta$ -regulated genes, including a lncRNA that we named TGF $\beta$ -induced lncRNA (*TLINC*, formerly known as *LINC00340* and cancer susceptibility candidate 15 [*CASC15*]). *TLINC* is induced by TGF $\beta$  in several settings, and the expression of specific isoforms correlates with an EMT phenotype. *TLINC* is strongly up-regulated in human

Copyright © 2018 The Authors. *Hepatology Communications* published by Wiley Periodicals, Inc., on behalf of the American Association for the Study of Liver Diseases. This is an open access article under the terms of the Creative Commons Attribution-NonCommercial-NoDerivs License, which permits use and distribution in any medium, provided the original work is properly cited, the use is non-commercial and no modifications or adaptations are made.

*View this article online at* [wileyonlinelibrary.com](http://wileyonlinelibrary.com).

DOI 10.1002/hep4.1142

Potential conflict of interest: Nothing to report.

## ARTICLE INFORMATION:

From the <sup>1</sup>Institut National de la Santé et de la Recherche Médicale, INRA, Université de Rennes, CHU Rennes, UMR 1241, Nutrition Metabolisms and Cancer, Service de Chirurgie Hépatobiliaire et Digestive, Biosit, Biogenouest, Core Facility H2P2 and CRB Santé, Rennes, France; <sup>2</sup>Department of Medicine II, Medical Faculty Mannheim, Heidelberg University, Mannheim, Germany.

## ADDRESS CORRESPONDENCE AND REPRINT REQUESTS TO:

Cédric Coulouarn, Ph.D.  
INSERM UMR 1241, CHU Pontchaillou  
2 rue Henri Le Guilloux

F-35033 Rennes, France  
E-mail: cedric.coulouarn@inserm.fr  
Tel: +33-2-2323-3881

iCCA and is associated with an enhanced expression of proinflammatory cytokines, including interleukin 8 (*IL8*). Finally, circular isoforms of *TLINC* are highlighted as promising biomarkers in patients with iCCA.

## Materials and Methods

### CELL CULTURE AND REAGENTS

HuCCT1 (RCB-1960) and Huh28 (RCB-1943) CCA cell lines were purchased at the RIKEN BioResource Center (Tsukuba-shi, Japan). Cells were grown in Roswell Park Memorial Institute 1640 medium (HuCCT1) or minimal essential medium (Huh28) supplemented with 100 U/mL penicillin, 100 µg/mL streptomycin, and 10% fetal bovine serum. HCC cell lines were purchased from ATCC and cultured as described.<sup>(15)</sup> LX2 cells were grown as described.<sup>(16)</sup> Freshly isolated human hepatocytes were purchased from Biopredic International (St. Grégoire, France). Cells were cultured at 37 °C in a 5% CO<sub>2</sub> atmosphere, and overnight serum starvation was performed before each treatment. Unless otherwise specified, cells were treated with 1 ng/mL recombinant human TGFβ (R&D Systems, Minneapolis, MN) and 10 µM TGFβ inhibitors (Sigma-Aldrich, St. Louis, MO).

### TGF $\beta$ SENSOR CELL LINES AND LUCIFERASE ACTIVITY

Stable TGF $\beta$  sensor cell lines were generated by using a pCignal Lenti-SMAD Reporter assay (Qiagen, Courtabeuf, France) according to the manufacturer's instructions. Briefly, cells were transduced with lentiviral particles (multiplicity of infection, 10; 8 µg/mL SureENTRY transduction reagent) and selected with 1 µg/mL puromycin for 5 days. Luciferase activity was determined with the Firefly Luciferase Assay System (Promega, Madison, WI) and normalized by the number of viable cells evaluated by a PrestoBlue cell viability reagent (Invitrogen, Carlsbad, CA).

### DNA TRANSFECTION

DNA constructs were kindly provided by Dr. Kristina A. Cole (Children's Hospital of Philadelphia, Philadelphia, PA) and Dr. Sumio Sugano (University of Tokyo, Tokyo, Japan). All constructs were amplified by transformation of One Shot TOP10 *Escherichia coli* (Invitrogen) and validated by DNA sequencing

(Supporting Table S1) after DNA purification (Nucleobond Xtra plasmid maxiprep kit; Macherey Nagel, Hoerdt, France). DNA transfection was performed by using Lipofectamine 2000 (Invitrogen).

### PROTEIN ANALYSIS

A Quantikine enzyme-linked immunosorbent assay human TGF $\beta$ 1 immunoassay (R&D Systems) was used to evaluate the expression of TGF $\beta$  in the supernatant of cell cultures collected 24 hours after serum starvation. Protein analysis by immunoblotting was performed as described.<sup>(17)</sup> Human anti-E-cadherin (CDH1) (AF648; R&D Systems) and anti-vimentin (VIM) (B01P; Abnova) antibodies were used.

### GENE EXPRESSION PROFILING

Total RNA, including lncRNA and micro RNA (miRNA, miR), was purified with an miRNAeasy kit (Qiagen). Genome-wide expression profiling was performed using the low-input QuickAmp labeling kit and human SurePrint G3 8x60K probes pangenomic microarrays (Agilent Technologies, Santa Clara, CA) as described.<sup>(15)</sup> These microarrays include 26,083 Entrez genes and 30,606 lncRNAs. Gene expression data were processed using Feature Extraction and GeneSpring software (Agilent Technologies). Microarray data sets have been deposited into the public Gene Expression Omnibus database under accession numbers GSE102109 and GSE102110. Gene set enrichment analysis (GSEA) was performed using the Java tool developed at the Broad Institute (Cambridge, MA). The Enrichr algorithm (<http://amp.pharm.mssm.edu/Enrichr>) was also used to identify key genes associated with relevant signaling pathways.

### QUANTITATIVE REVERSE-TRANSCRIPTION POLYMERASE CHAIN REACTION

Quantitative reverse-transcription polymerase chain reaction (Q-RT-PCR) was performed as described<sup>(16)</sup> by using a SYBR Green master mix (Applied Biosystems, Carlsbad, CA). A mixture of deoxythymidine oligomer (250 ng) and random hexamers (100 ng) was used to prime the RT reaction of 1 µg total RNA (Superscript III RT; Invitrogen). A list of DNA primers used in this study is provided in Supporting Table S2.

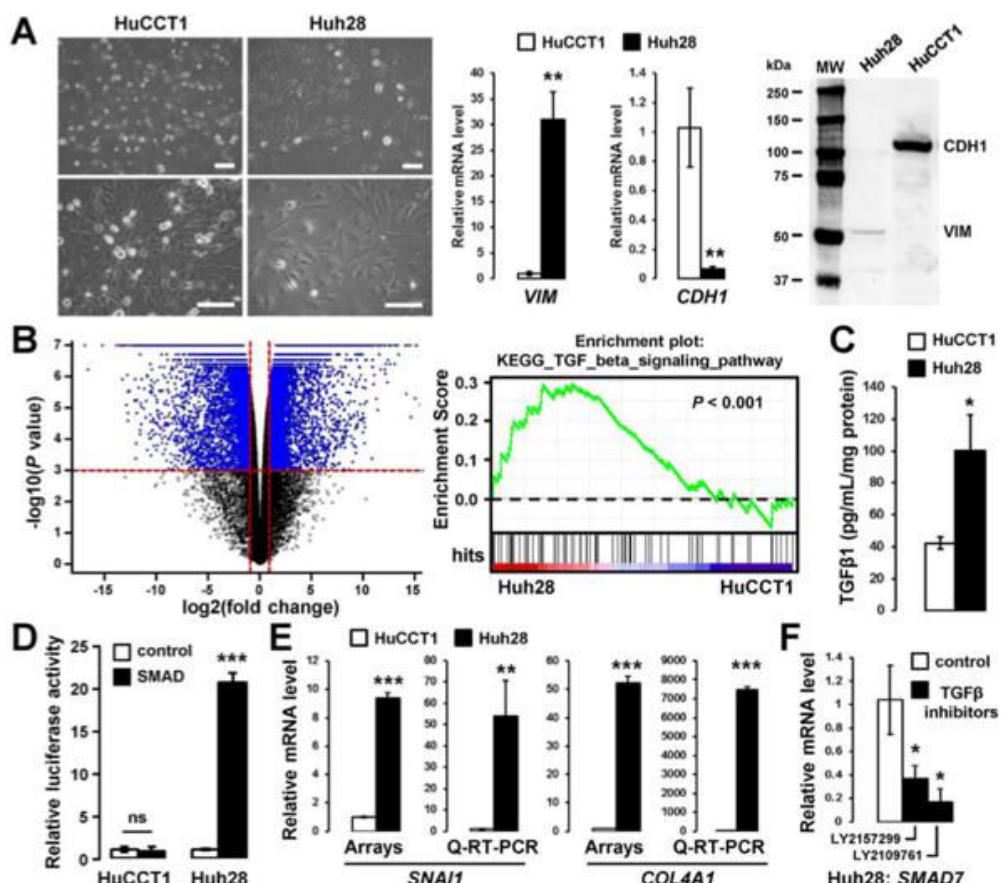


**FIG. 1.** HuCCT1 and Huh28 cell lines exhibit an epithelialoid and a mesenchymal-like phenotype respectively, the later correlating with endogenous activation of the TGF $\beta$  pathway. (A) Phase contrast micrographs of HuCCT1 and Huh28 cells (left panel; scale bar, 100  $\mu$ m) and expression of vimentin and E-cadherin at the RNA (middle panel) and protein level (right panel). (B) Volcano plot of genes differentially expressed between HuCCT1 and Huh28 (left panel) and GSEA highlighting a TGF $\beta$  signature enriched in the gene expression profile of Huh28. (C) Enzyme-linked immunosorbent assay demonstrating increased secretion of TGF $\beta$ 1 in the supernatant of Huh28 cells 24 hours after overnight serum starvation. (D) Relative luciferase activity of HuCCT1 and Huh28 engineered cell lines in which a luciferase gene is under the transcriptional control of a TATA box alone (white bars) or with SMAD responsive elements (black bars). Luciferase activity was measured at the basal level without exogenous addition of TGF $\beta$  after overnight serum starvation. (E) Gene expression analysis of TGF $\beta$  target genes in HuCCT1 and Huh28 cells at the basal level by microarray and Q-RT-PCR. (F) Q-RT-PCR analysis of TGF $\beta$  target gene SMAD7 in Huh28 cells treated with 10  $\mu$ M TGF $\beta$  inhibitors (black bars). Statistical analysis was performed by *t* test (\* $P < 0.05$ ; \*\* $P < 0.01$ ; \*\*\* $P < 0.001$ );  $n \geq 3$  replicates. Data represent mean  $\pm$  SD. Abbreviations: mRNA, messenger RNA; MW, molecular weight.

## FUNCTIONAL TESTS

Cell viability was evaluated using a PrestoBlue reagent (Invitrogen). Data were expressed as relative cell viability compared to untreated cells transfected with the control plasmid set as 1. Cell migration and invasion were evaluated using BD BioCoat Matrigel Invasion Chambers (BD Biosciences) as described.<sup>(16)</sup> Briefly,  $4 \times 10^4$  cells were plated in serum-free medium either on an 8- $\mu$ m pore-size positron emission tomography membrane insert coated with a layer

of matrigel basement membrane matrix (invasion test) or on an 8- $\mu$ m pore-size positron emission tomography control membrane insert (migration test). The lower compartment contained medium with 10% fetal bovine serum as a chemoattractant. After incubation for 48 hours, we removed the cells remaining on the upper surface of the membrane with a cotton swab, fixed cells in 4% paraformaldehyde that had passed through to the lower surface of the membrane, and stained the fixed cells with 1% crystal violet. We scored invasive and migrating cells per membrane under a

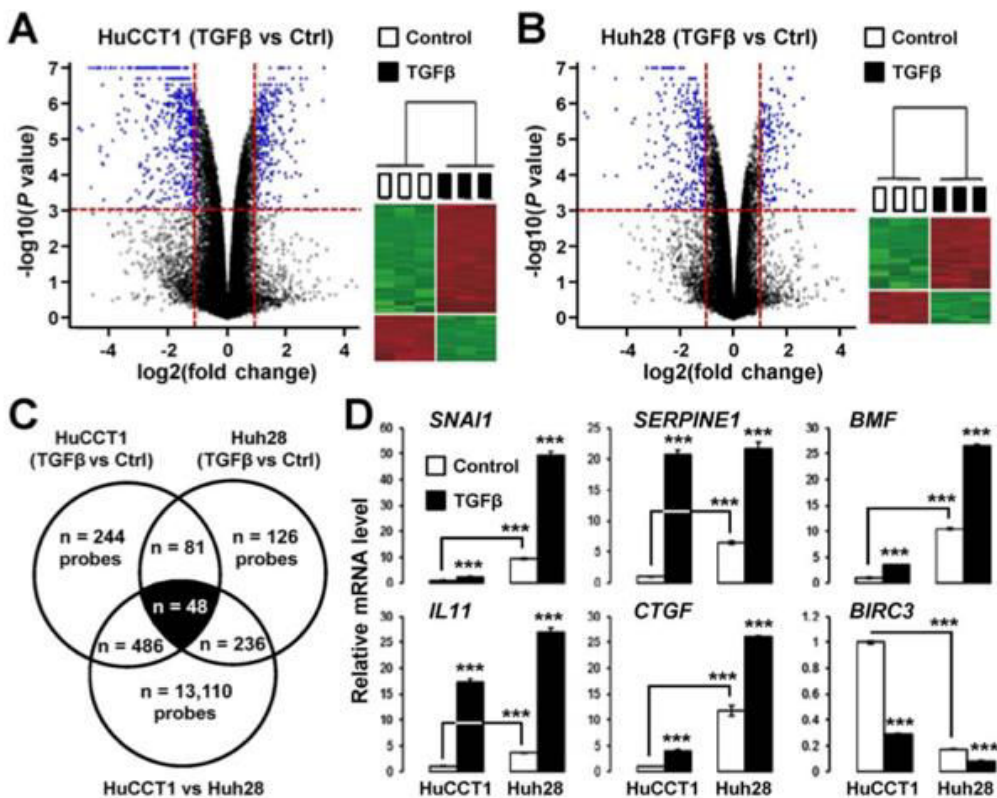


**FIG. 2.** A TGF $\beta$ -specific gene expression signature in cholangiocarcinoma cell lines. (A,B) Volcano plot and hierarchical clustering of genes differentially expressed by TGF $\beta$  (1 ng/mL, 16 hours) in (A) HuCCT1 and (B) Huh28 cells. Horizontal dashed lines on volcano plots,  $P < 0.001$ ; vertical dashed lines, fold change  $> 2$ . (C) Venn diagram analysis of genes differentially expressed by TGF $\beta$  in HuCCT1 and Huh28 cells. A common TGF $\beta$  signature made of 48 probes (42 nonredundant well-annotated genes) was identified. (D) Expression of six well-known TGF $\beta$  target genes in HuCCT1 and Huh28 cells after 16 hours of culture in absence (white bars) or presence (black bars) of 1 ng/mL TGF $\beta$ . Statistical analysis was performed by  $t$  test (\* $P < 0.05$ ; \*\* $P < 0.01$ ; \*\*\* $P < 0.001$ );  $n \geq 3$  replicates. Data represent mean  $\pm$  SD. Abbreviation: Ctrl, control.

light microscope at a  $5 \times$  magnification ( $n = 3$  independent experiments). The number of migrating and invasive cells after transfection of TLINC was normalized relative to the number of migrating and invasive cells after transfection of the control plasmid, which was set to 1.

## HUMAN iCCA SAMPLES AND TISSUE MICROARRAY

Freshly frozen and formalin-fixed paraffin-embedded human iCCA samples were obtained through the national liver biobanks network. Written informed consent was obtained from all patients. The study protocol fulfilled national laws and regulations and was approved by the local ethics committee and the institutional review board of the Institut National de la Santé

et de la Recherche Médicale (IRB00003888). Tissue microarrays were performed using a Minicore 3 Tissue Arrayer (Excilone, Vicq, France) as described.<sup>(6)</sup>

## LASER CAPTURE MICRODISSECTION

Laser capture microdissection (LCM) was performed using an Arcturus Veritas Microdissection system (Applied Biosystems) as described.<sup>(6)</sup> Briefly, serial sections of 10- $\mu$ m frozen tissues were mounted onto PEN membrane glass slides prior to LCM of biliary epithelial cells and fibrous tissue from tumor and nontumor parts. Total RNA was purified using an Arcturus Picopure RNA isolation kit (Applied Biosystems).

TABLE 1. TGF $\beta$  SIGNATURE IN CHOLANGIOMA CELL LINES(A) Genes induced by TGF $\beta$ 

Agilent Probe	Gene Name	Gene Symbol	Accession No.	HuCC1 (TGF $\beta$ /Ctrl)		HuH28 (TGF $\beta$ /Ctrl)		HuH28/HuCC1		Known TGF $\beta$ Target
				P Value	FC	P Value	FC	P Value	FC	
A_24_P411561	Hepatitis A virus cellular receptor 2	HAVCR2	NM_0327782	1.00E-07	38.46	5.00E-07	7.14	1.40E-06	11.26	yes
A_24_P158089	Serpin peptidase inhibitor, clade E (nexin, plasminogen activator inhibitor type 1), member 1	SERPINE1	NM_000602	<1e-07	20.83	7.00E-07	3.33	1.00E-07	6.63	yes
A_21_P0011334	na	XLOC_12_004757	BC043257	4.50E-06	18.52	<1e-07	5.88	8.21E-04	5.20	no
A_33_P3243887	Interleukin 11	IL11	NM_000641	<1e-07	17.24	<1e-07	7.14	1.40E-06	3.54	yes
A_21_P001676	na	XLOC_000166	na	<1e-07	15.15	5.10E-06	2.08	<1e-07	300.67	no
A_23_P153571	IGF-like family member 2	IGFL2	NM_00102915	3.40E-06	12.82	5.35E-05	2.27	4.69E-05	5.42	no
A_33_P3243454	IGF-like family member 3	IGFL3	NM_207393	5.30E-06	11.76	1.00E-07	3.70	4.00E-07	57.37	no
A_33_P3255384	BPI fold containing Family C Collagen, type XX, alpha 1	BPIFC	NM_174932	1.00E-07	10.20	7.56E-06	2.78	2.00E-07	12.20	no
A_32_P185637	Leukocyte cell-derived chemotaxin 2	COL20A1	NM_020882	1.50E-06	10.10	<1e-07	6.25	3.10E-06	8.09	no
A_23_P110777	Keratin 14	LECT2	NM_002302	2.57E-04	8.33	1.23E-06	7.69	2.30E-06	7.21	no
A_33_P345534	Keratin 17	KRT14	NM_000526	1.00E-07	7.69	9.30E-06	2.70	1.00E-07	10.82	no
A_23_P96158	na	KRT17	NM_000422	<1e-07	7.69	8.70E-06	2.63	<1e-07	9.50	no
A_24_P887857	Solute carrier family 46, member 3	SLC46A3	NM_181785	3.15E-04	7.69	1.66E-05	2.70	1.00E-07	9.67	no
A_23_P205074	na	SLC46A3	NM_000526	1.00E-06	2.33	3.55E-04	7.54	no	no	no
A_24_P882732	na	XLOC_12_006021	DR007925	<1e-07	7.14	2.28E-05	2.70	1.00E-07	9.50	no
A_21_P0011578	Keratin 42 pseudogene	KRT42P	DB117598	3.00E-07	7.14	3.00E-06	2.70	4.00E-07	8.77	no
A_33_P3857239	na	XLOC_003415	NR_033415	<1e-07	6.67	9.70E-06	2.86	1.00E-07	8.69	no
A_33_P3235905	na	na	na	6.20E-05	6.67	6.82E-05	2.44	3.22E-04	3.90	no
A_21_P0008663	Keratin 16 pseudogene 2	KR116P2	NR_029392	1.00E-07	5.88	2.19E-06	2.70	3.00E-07	19.21	no
A_32_P62963	Long intergenic nonprotein coding RNA 313	LINC00313	NR_026863	4.10E-06	5.88	8.91E-05	2.08	4.00E-07	5.88	no
A_23_P381489	Long intergenic nonprotein coding RNA 312	LINC00312	NR_024065	3.06E-06	4.17	1.00E-07	5.00	1.36E-04	2.86	no
A_23_P166779	Connective tissue growth factor	CTGF	NM_001901	4.00E-07	4.00	1.91E-05	2.22	1.00E-07	11.67	yes
A_23_P19663	na	XLOC_12_010751	na	1.56E-04	4.00	3.60E-06	3.03	5.06E-05	5.57	no
A_19_P00321671	na	na	na	1.20E-06	4.00	6.60E-06	3.03	5.00E-07	5.23	no
A_21_P0012601	na	na	CR597597	1.00E-07	3.70	2.60E-06	2.78	3.00E-07	4.00	no
A_32_P76627	Bcl2 modifying factor	BMF	NM_001003940	1.66E-05	3.57	3.00E-07	2.56	8.00E-07	10.75	yes
A_23_P379649	na	XLOC_012049	NR_015410	1.72E-04	3.45	1.06E-05	3.03	2.81E-05	5.86	no
A_21_P0009087	Long intergenic nonprotein coding RNA 340	LINC00340	2.06E-06	3.33	8.60E-06	2.27	1.00E-07	19.17	no	no
A_19_P00318323	na	na	na	na	na	na	na	na	na	no
A_23_P107744	Sphingosine-1-phosphate receptor 5	S1PR5	NM_030760	6.04E-04	3.03	1.50E-06	3.57	1.35E-05	12.24	no
A_32_P309404	Solute carrier family 22 (extraneuronal monoamine transporter), member 3	SLC22A3	NM_021977	5.00E-07	3.03	1.78E-05	2.04	1.60E-06	3.48	no
A_24_P838448	Long intergenic nonprotein coding RNA 340	LINC00340	NR_015410	1.04E-04	2.86	1.30E-06	2.44	2.00E-07	12.50	no

TABLE 1. CONTINUED

(A) Genes induced by TGF $\beta$ 

Agilent Probe	Gene Name	Gene Symbol	Accession No.	HuCCT1 (TGF $\beta$ /Ctrl)			HuH28 (TGF $\beta$ /Ctrl)			HuH28/HuCCT1		
				P Value	FC	P Value	FC	P Value	FC	P Value	FC	Known TGF $\beta$ Target
A_23_P124642	RAS guanyl releasing protein 1 (calcium and DAG-regulated Synaptojanin)	RASGRP1	NM_005739	1.40E-05	2.70	1.32E-05	2.08	<1e-07	27.00			no
A_23_P344531	Nucleolar protein 4-like	SYNPO	NM_007286	7.10E-06	2.50	1.60E-06	2.56	<1e-07	24.38			no
A_23_P303548	Growth arrest and DNA-damage-inducible, beta	NOL4L	XM_003403733	2.34E-04	2.44	5.14E-05	2.08	4.81E-04	2.31			no
A_24_P239606	DNA-damage-inducible, beta	GADD45B	NM_015675	3.00E-06	2.33	6.10E-05	2.44	3.69E-05	2.93			yes
A_23_P131846	Small homolog 1 ( <i>Drosophila</i> )	SNAI1	NM_005985	4.20E-06	2.33	1.00E-07	5.26	<1e-07	9.48			yes
A_21_P0009196	no	XLOC_012515	na	6.91E-04	2.27	2.06E-05	2.08	8.00E-06	7.67			no

(B) Genes repressed by TGF $\beta$ 

Agilent Probe	Gene Name	Gene Symbol	Accession No.	HuCCT1 (TGF $\beta$ /Ctrl)			HuH28 (TGF $\beta$ /Ctrl)			HuH28 / HuCCT1		
				P Value	FC	P Value	FC	P Value	FC	P Value	FC	Known TGF $\beta$ Target
A_33_P3663974	Thyroid hormone receptor beta	THRB	NM_001128177	8.10E-06	0.49	1.75E-04	0.47	1.70E-06	0.42			no
A_21_P0010449	no	XLOC_014399	XR_109732	2.70E-06	0.47	1.05E-04	0.38	1.00E-07	0.08			no
A_21_P000841	Hypothetical LOC100505483	LOC100505483	NR_038926	7.60E-06	0.45	3.13E-05	0.40	2.25E-05	0.43			no
A_23_P121064	Pentoxin 3, long	PTX3	NM_002852	1.50E-06	0.45	2.00E-06	0.32	4.90E-06	0.42			yes
A_23_P121657	Heparan sulfate (glucosamine) 3-O-sulfotransferease 1	HS3ST1	NM_006114	3.00E-07	0.42	3.07E-04	0.45	<1e-07	0.00			no
A_23_P52266	Interferon-induced protein with tetratricopeptide repeats 1	IFT1	NM_001548	1.19E-04	0.40	1.66E-05	0.36	1.72E-05	0.27			no
A_23_P345460	Pleckstrin homology domain-containing, family G (with RhoGef domain) member 4	PLEKHG4	NM_015432	6.00E-07	0.36	2.90E-04	0.50	1.00E-07	0.21			no
A_23_P98350	Baculoviral inhibitor of apoptosis protein repeat-containing 3	BIRC3	NM_001165	1.00E-07	0.29	2.70E-06	0.45	<1e-07	0.17			yes
A_33_P3398181	Hypothetical LOC100127909	LOC100127909	XR_111781	8.81E-05	0.26	7.13E-05	0.35	1.89E-05	0.27			no
A_23_P415021	Methyltransferase-like 7A	METTL7A	NM_014033	2.00E-07	0.22	4.00E-06	0.32	1.00E-07	0.19			no

Abbreviations: Ctrl, control; FC, fold change; na, not applicable.

## IN SITU HYBRIDIZATION

Specific *in situ* hybridization (ISH) riboprobes were designed to evaluate the expression of TLINC-S and TLINC-T transcripts (Supporting Table S1). Sense and antisense riboprobes were generated by *in vitro* transcription from PCR products incorporating the promoter of T7 RNA polymerase. *In vitro* transcription was performed with 40 units T7 RNA Polymerase (Agilent) in the presence of 0.35 mM digoxigenin-11-UTP (Roche Diagnostics, Meylan, France). ISH was performed on the Discovery Automated IHC Stainer using the Ventana Detection Kit (Ventana Medical Systems, Tucson, AZ). Staining was performed using an anti-digoxigenin-horseradish peroxidase antibody (Roche Diagnostics), and signal detection was performed using a nitro-blue tetrazolium/5-bromo-4-chloro-3'-indolylphosphate or a Discovery purple kit (Ventana Medical Systems).

## CIRCULAR RNA ANALYSIS

RT-PCR using convergent and divergent primers combined with ribonuclease (RNase) R (Epicentre, Middleton, WI) treatment (1 μ/μg, 37 °C, 1 hour) was used to detect linear and circular transcripts of *TLINC* and actin beta (*ACTB*). The sequence of DNA primers is provided in Supporting Table S2.

## Results

### ENDOGENOUS TGF $\beta$ ACTIVATION IN Huh28 CELLS

HuCCT1 and Huh28 cells were used to study the impact of TGF $\beta$  on iCCA cells. The two cell lines have different phenotypic features that reflect tumor heterogeneity. HuCCT1 cells exhibit an epithelioid-like phenotype associated with a cobblestone-like morphology and numerous cell-to-cell junctions compared to Huh28 cells, which exhibit a mesenchymal-like phenotype associated with a spindle and polygonal morphology together with prominent cytoskeleton fibers (Fig. 1A). Epithelioid and mesenchymal-like phenotypes were further characterized by the expression of *CDH1* and *VIM* markers in HuCCT1 cells and Huh28 cells, respectively, both at the RNA and protein level (Fig. 1A). Marked differences in pangenomic expression profiles were also highlighted between HuCCT1 and Huh28 cells and validated by Q-RT-PCR (Fig. 1B; Supporting Fig. S1A).

Interestingly, GSEA, using the Kyoto Encyclopedia of Genes and Genomes signaling pathways, demonstrated that a TGF $\beta$  signature was significantly enriched ( $P < 0.001$ ) at the basal level in mesenchymal Huh28 cells (Fig. 1B). Endogenous activation of the TGF $\beta$  pathway in Huh28 cells was further validated by a significantly enhanced secretion of TGF $\beta$  (Fig. 1C) that correlated with enhanced luciferase activity as detected in engineered SMAD sensor cell lines (Fig. 1D). A higher expression of TGF $\beta$  target genes (e.g., snail family transcriptional repressor 1 [*SNAI1*], collagen type IV alpha 1 chain [*COL4A1*], *SMAD7*) in Huh28 cells was also validated by Q-RT-PCR (Fig. 1E; Supporting Fig. S1A) as well as a reduced expression of *SMAD7*, a well-known TGF $\beta$  transcriptional target, when cells were cultured in the presence of TGF $\beta$  inhibitors (Fig. 1F). Altogether, these data demonstrate that Huh28 cells exhibit a mesenchymal phenotype associated with basal and endogenous activation of the TGF $\beta$  pathway.

### NEW TGF $\beta$ TARGET GENES IN iCCA CELLS

HuCCT1 and Huh28 cells were treated with 1 ng/mL TGF $\beta$  for 16 hours. Gene expression profiling using pangenomic microarrays identified 859 probes in HuCCT1 cells (Fig. 2A) and 491 probes in Huh28 cells (Fig. 2B) that were significantly deregulated by TGF $\beta$  ( $P < 0.001$ ; fold change  $>2$ ). A Venn diagram analysis, including genes differentially expressed between HuCCT1 and Huh28 cells at a basal level (Fig. 1B), identified a set of 48 probes (42 nonredundant annotated genes) that were recurrently deregulated by TGF $\beta$  in all three experimental settings (Fig. 2C; Table 1). The deregulation of well-known positive (e.g., serpin family E member 1 [*SERPINE1*], connective tissue growth factor [*CTGF*]) and negative (e.g., baculoviral inhibitor of apoptosis protein repeat containing 3 [*BIRC3*]) TGF $\beta$  target genes was confirmed by Q-RT-PCR on independent RNA samples (Fig. 2D; Supporting Fig. S1B). GSEA was also performed in all specific gene subsets and demonstrated that the 42 common genes were significantly associated with TGF $\beta$  and SMAD2/3 and related to EMT (Supporting Fig. S2). Importantly, this common signature comprised genes not known to be regulated by TGF $\beta$ , including several lncRNAs (e.g., *LINC00312*, *LINC00340*). Notably, two microarray probes for *LINC00340* were induced by TGF $\beta$  (Table 1).

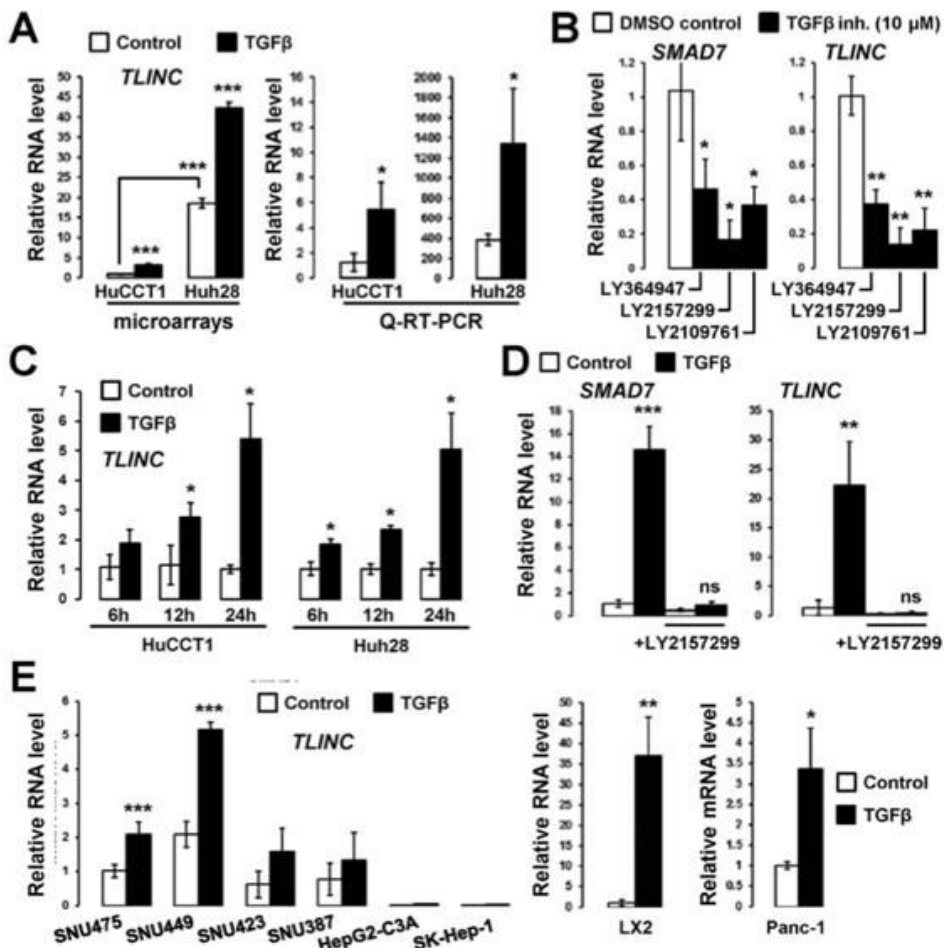


**FIG. 3.** LINC00340/CASC15/TLINC is a novel TGF $\beta$ -induced lncRNA. (A) Analysis of *LINC00340* expression in HuCCT1 and Huh28 cells after 16 hours of culture in absence (white bars) or presence (black bars) of 1 ng/mL TGF $\beta$ , as evaluated by microarray and Q-RT-PCR. (B) Analysis of *SMAD7* and *LINC00340* expression in Huh28 cells after 72 hours treatment with 10  $\mu$ M TGF $\beta$  inhibitors. (C) Time-course analysis of *LINC00340* expression in HuCCT1 and Huh28 cells (1 ng/mL TGF $\beta$ ). (D) Analysis of *SMAD7* and *LINC00340* expression in primary human hepatocytes ( $n = 3$  independent donors) in the presence of 1 ng/mL TGF $\beta$  and 10  $\mu$ M TGF $\beta$  inhibitor LY2157299 for 16 hours. (E) Analysis of *LINC00340* expression in HCC cell lines (left panel) and LX2 and Panc-1 (pancreatic cancer) cells (right two panels) (1 ng/mL TGF $\beta$  for 16 hours). Statistical analysis was performed by *t* test (\* $P < 0.05$ ; \*\* $P < 0.01$ ; \*\*\* $P < 0.001$ );  $n \geq 3$  replicates. Data represent mean  $\pm$  SD. Abbreviations: DMSO, dimethyl sulfoxide; inh., inhibitor; mRNA, messenger RNA; ns, not significant.

## LINC00340/CASC15/TLINC IS A NOVEL TGF $\beta$ -INDUCED lncRNA

*LINC00340* is known as cancer susceptibility candidate 15 (*CASC15*) located on chromosome 6p22. *CASC15* was reported to act as a tumor suppressor in neuroblastoma<sup>(18)</sup> and to promote tumor progression and phenotype switching in melanoma.<sup>(19)</sup> To further characterize *LINC00340* biological activities in iCCA, we first validated the microarray expression data by Q-RT-PCR. *LINC00340* was induced by TGF $\beta$  in

both HuCCT1 and Huh28 cells, and a significant higher expression in Huh28 cells at the basal level was confirmed (Fig. 3A). Repression of *LINC00340* and *SMAD7* was observed in Huh28 cells treated with inhibitors of the TGF $\beta$  pathway (Fig. 3B). Time-course experiments also demonstrated increased expression of *LINC00340* by TGF $\beta$ , both in HuCCT1 and Huh28 cells (Fig. 3C). Interestingly, *LINC00340* was induced by TGF $\beta$  in nontransformed human primary hepatocytes, and the induction was abolished in the presence of a TGF $\beta$  inhibitor

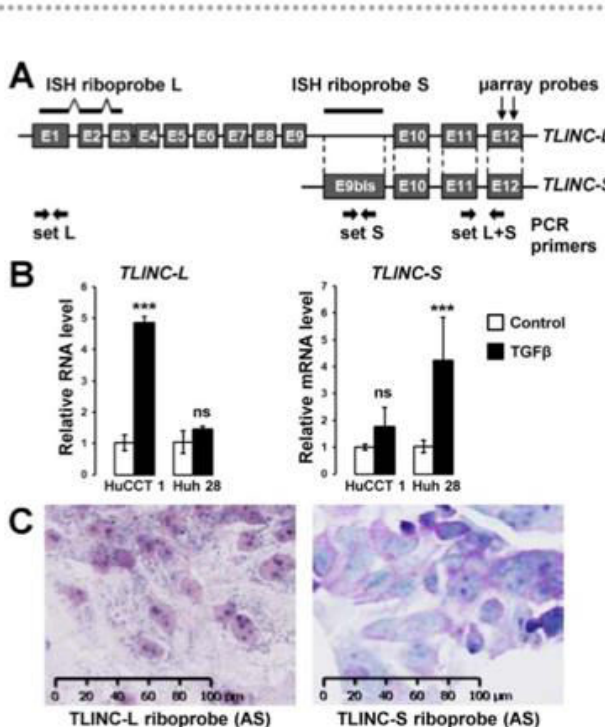


**FIG. 4.** Expression and cellular localization of TLINC isoforms. (A) Simplified representation of TLINC locus highlighting two reported isoforms: TLINC-L and TLINC-S. ISH riboprobes, sets of PCR primers, and microarray probes are also represented. (B) Analysis of TLINC-L and TLINC-S expression in HuCCT1 and Huh28 cells after 16 hours of culture in the absence (white bars) or presence (black bars) of 1 ng/mL TGFβ, as evaluated by Q-RT-PCR using specific sets of primers. (C) *In situ* hybridization using TLINC-L and TLINC-S riboprobes highlights a nuclear and cytoplasmic location of both TLINC isoforms (HuCCT1 cells treated with 1 ng/mL TGFβ). Scale, 100 μm. Statistical analysis was performed by *t* test (\*P < 0.05; \*\*P < 0.01; \*\*\*P < 0.001); n ≥ 3 replicates. Data represent mean ± SD. Abbreviations: (AS), anti-sense; mRNA, messenger RNA; ns, not significant.

(Fig. 3D). In addition, *LINC00340* was induced by TGFβ in several human HCC cell lines as well as in LX2-activated hepatic stellate cells (Fig. 3E). Finally, induction by TGFβ occurred also in nonhepatic cell lines, such as pancreatic Panc-1 (Fig. 3E). Altogether, these data demonstrate that *LINC00340* is a novel and general transcriptional target of TGFβ. We therefore named it TGFβ-induced lncRNA or *TLINC*.

## INDUCTION OF TWO TLINC ISOFORMS LINKED TO AN EMT PHENOTYPE

Previous studies demonstrated that *TLINC* is located on a complex locus that produces multiple

mRNAs by alternative splicing, including a short (TLINC-S) and a long (TLINC-L) isoform, as shown in Fig. 4A.<sup>(18,19)</sup> These two isoforms have been functionally associated with either tumor suppressive (TLINC-S)<sup>(18)</sup> or tumor promoting (TLINC-L)<sup>(19)</sup> functions in neuroblastoma and melanoma, respectively. Because our previous gene expression analysis by microarray (Fig. 2) and Q-RT-PCR (Fig. 3) could not distinguish the two isoforms (primer set L + S), we next evaluated TLINC-S and TLINC-L with specific sets of primers (Fig. 4A). TLINC-L was induced by TGFβ in HuCCT1 cells and TLINC-S in Huh28 cells, as demonstrated by Q-RT-PCR (Fig. 4B). ISH demonstrated that the two isoforms were expressed in both the cytoplasm and the nucleus (Fig. 4C).

## FUNCTIONAL CHARACTERIZATION OF TLINC ISOFORMS

Gain of function experiments were performed using DNA constructs designed to specifically overexpress TLINC-L and TLINC-S (Supporting Fig. S3A-C). No significant effect was observed on cell viability (Supporting Fig. S3D) and cell invasion (Fig. 5A); however, overexpression of TLINC-L increased cell migration (Fig. 5A). In order to get insights into the molecular mechanisms involved, gene expression profiling was performed on HuCCT1 cells after TLINC-L overexpression. Numerous genes were repressed (Fig. 5B), whereas several inflammation-associated genes, including cytokines and chemokines (e.g., *IL6*, *IL8*, C-X-C motif chemokine ligand 1 [*CXCL1*]) were induced together with *LINC00340/TLINC* (Fig. 5B). Accordingly, an immune response gene signature was significantly enriched in the gene expression profiles of HuCCT1 cells overexpressing TLINC-L (Fig. 5C; Supporting Table S3). The enrichment of a described<sup>(20)</sup> cell migration signature supported the phenotype observed after TLINC-L overexpression (Fig. 5C). Although no obvious change was observed on cell morphology after TLINC-L transfection, EMT-associated *SNAI2* was enriched in the gene expression profiles of TLINC-L transfected cells (Supporting Table S4). A significant enrichment of TGFβ target genes was also observed, suggesting that TLINC-L may act as a feedback regulator of the TGFβ pathway (Fig. 5C). However, experimental data using SMAD sensor cell lines refuted this hypothesis (Supporting Fig. S3E). In agreement

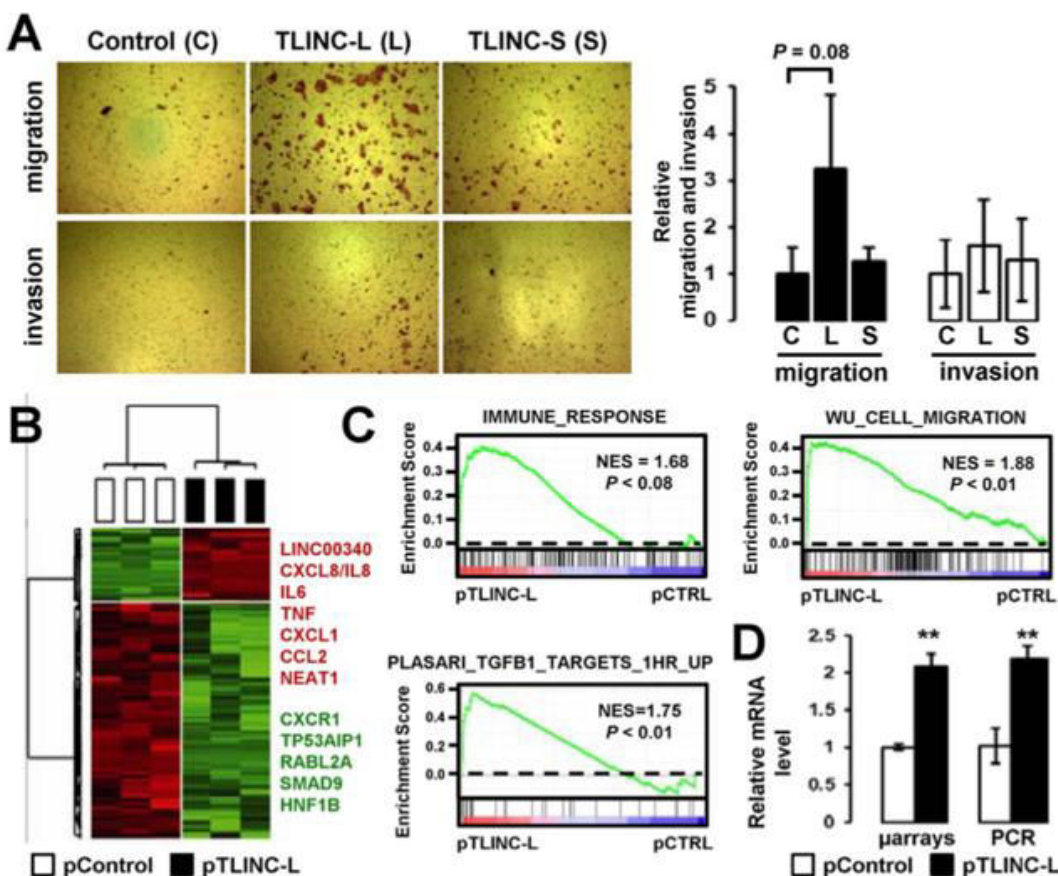


**FIG. 5.** Functional analysis of TLINC. (A) Effects of TLINC-L and TLINC-S overexpression on migration and invasion of HuCCT1 cells 48 hours after transfection of the DNA constructs. (B) Gene expression analysis of HuCCT1 cells 24 hours after transfection of the *TLINC-L* DNA construct. Hierarchical clustering was based on the expression of 431 genes ( $P < 0.01$ ; fold change  $>1.5$ ). (C) GSEA of specific signatures significantly enriched in the gene expression profile of HuCCT1 cells overexpressing TLINC-L. (D) Analysis of *IL8* expression in HuCCT1 cells after transfection of the *TLINC-L* DNA construct, as evaluated by microarray and Q-RT-PCR. Statistical analysis was performed by *t* test (\* $P < 0.05$ ; \*\* $P < 0.01$ ; \*\*\* $P < 0.001$ );  $n \geq 3$  replicates. Data represent mean  $\pm$  SD. Abbreviations: C, control; CCL2, chemokine (C-C motif) ligand 2; CTRL, control; CXCR1, chemokine (C-X-C motif) receptor 1; HNF, hepatocyte nuclear factor; L, long; mRNA, messenger RNA; NES, normalized enrichment score; p, plasmid [for pControl and pTLINC-L]; RABL2A, RAB, member of RAS oncogene family like 2A; S, short; TP53AIP1, tumor protein p53 regulated apoptosis inducing protein 1; TNF, tumor necrosis factor.

with the identified immune signature, increased expression of *IL8* was confirmed after TLINC overexpression (Fig. 5D). As a potent inducer of cell motility, *IL8* may contribute to the observed phenotype by creating a gradient for the migration of cancer cells.

## INCREASED EXPRESSION OF TLINC IN HUMAN iCCA

We next evaluated the clinical relevance of TLINC expression in human resected iCCA. TLINC was shown to be induced both in tumor biliary epithelial

cells and in the stroma compared to their nontumor counterparts (Fig. 6A). Overexpression of TLINC in iCCA tumors was validated by ISH on tissue microarrays (Fig. 6A). Interestingly, Q-RT-PCR on 22 resected human iCCA demonstrated that the expression of TLINC-L and TLINC-S was tightly correlated (Fig. 6B). A detailed analysis by ISH on human resected iCCA confirmed that both TLINC isoforms were expressed in tumor cholangiocytes and in cells from the tumor microenvironment. In the nontumor liver, TLINC was only expressed in remodeled portal areas with signs of ductular reaction and inflammation (Fig. 6C; Supporting Fig. S4).

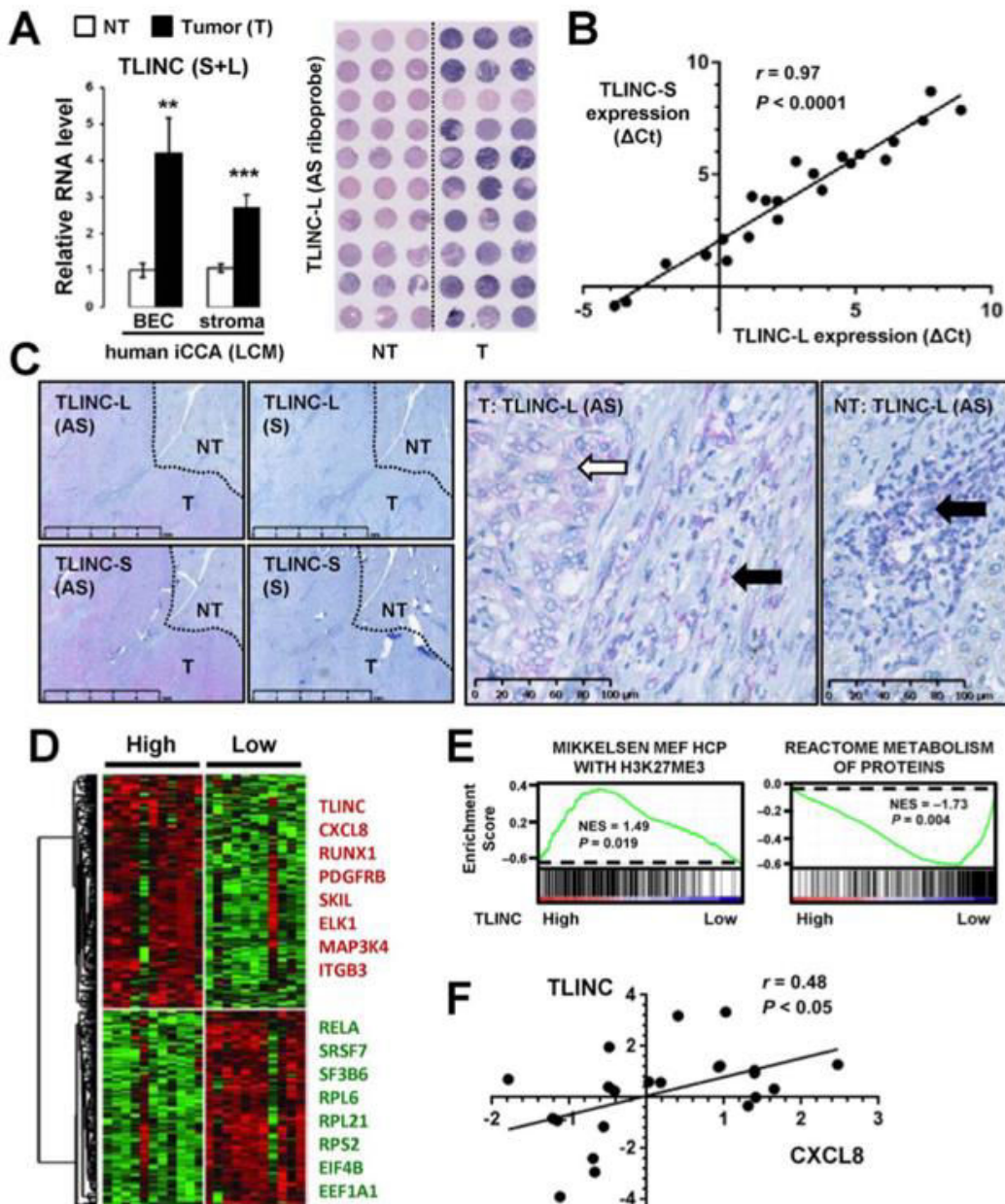


**FIG. 6.** Clinical relevance of *TLINC* expression in human resected iCCA. (A) Analysis of *TLINC* expression in biliary epithelial cells and stroma isolated by laser capture microdissection from nontumor (white bars) and tumor (black bars) tissues (n = 10 patients, left panel). Data represent mean  $\pm$  SD. ISH on human iCCA tissue microarrays using *TLINC*-L antisense riboprobes demonstrating higher expression in the tumor than in the nontumoral tissues (tissue microarray, right panel). (B) Correlation between *TLINC*-L and *TLINC*-S expression in human iCCA resected tumors, evaluated by Q-RT-PCR (n = 22 patients). (C) ISH analysis of *TLINC*-L and *TLINC*-S expression using specific antisense and sense riboprobes. In the tumor part, *TLINC* was expressed in both epithelial cells (white arrow) and in the stroma (black arrow). In the nontumor part, *TLINC* was only expressed in remodeled portal areas with signs of ductular reaction. Scale bars: 5 mm (left panels) and 100  $\mu$ m (right panels). (D) Expression of *TLINC* identifies human iCCA with specific gene expression profiles. Median expression of *TLINC* was used to define high and low expression groups (n = 22 patients). (E) Example of signatures significantly enriched in the gene expression profiles of iCCA with high versus low *TLINC* expression, as evaluated by GSEA. (F) Correlation between the expression of *TLINC* and CXCL8 in 22 human iCCAs. Abbreviations: (AS), antisense; BEC, biliary epithelial cells; EEF1A1, eukaryotic translation elongation factor 1 alpha 1; EIF4B, eukaryotic translation initiation factor 4B; ELK1, ELK1, ETS transcription factor; ITGB3, integrin subunit beta 3; HCP, high-CpG-density promoters; MAP3K4, mitogen-activated protein kinase kinase kinase 4; MEF, mouse embryonic fibroblast; NF- $\kappa$ B subunit; NES, normalized enrichment score; NT, nontumor; PDGFRB, platelet derived growth factor receptor beta; RELA, RELA proto-oncogene; RPL6, ribosomal protein L6; RPL21, ribosomal protein L21; RPS2, ribosomal protein S2; RUNX1, runt related transcription factor 1; (S), sense; SF3B6, splicing factor 3b subunit 6; SKIL, SKI like proto-oncogene; SRSF7, serine and arginine rich splicing factor 7; T, tumor.

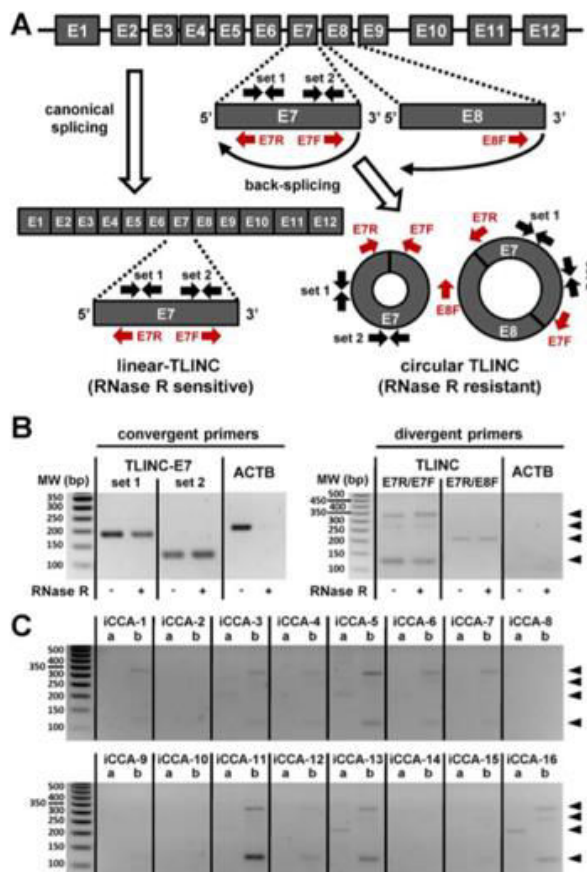


**FIG. 7.** Experimental evidence of TLINC circular isoforms. (A) Schematic representation of TLINC RNA processing into linear RNA (canonical splicing) or circular RNA (back-splicing). Several sets of convergent and divergent PCR primers were designed to detect specific linear and circular isoforms. (B) RNA was extracted from Huh28 cells after 16 hours of treatment with 1 ng/mL TGF $\beta$ . RNase R treatment was performed prior to RT-PCR analysis. Convergent primers (left panel) detected specific TLINC-E7 transcripts in both RNase R untreated and treated samples. For ACTB (a housekeeping gene highly expressed), no amplification was observed after RNase R treatment. By using a specific set of divergent primers located on exons E7 and E8, several TLINC circular isoforms were highlighted (black arrowheads). (C) RNAs were extracted from 16 human iCCA tumors. RT-PCR analysis was performed using a specific set of divergent primers located on exons E7 and E8, as indicated at the top of the panels (a, E7R/E8F; b, E7R/E7F). Black arrowheads highlight TLINC circular isoforms. Abbreviations: bp, base pair; MW, molecular weight.

## TLINC EXPRESSION DEFINES SPECIFIC SUBSETS OF HUMAN iCCA

Gene expression profiling was performed on 22 resected human iCCA, and a specific signature was

defined on the basis of TLINC expression (Fig. 6D). High expression of TLINC correlated with a high expression of TGF $\beta$  target genes and inflammation-associated genes, as previously observed in cell lines (Fig. 6D; Supporting Fig. S5). In addition, GSEA demonstrated that up-regulated genes in high-TLINC-expressing tumors were significantly associated with the H3K27Me3 repressive epigenetic mark signature, while down-regulated genes were linked to protein metabolism and included numerous genes encoding ribosomal components (Fig. 6D,E; Supporting Fig. S6). Among the chemokines induced in HuCCT1 cells directly overexpressing TLINC (Fig. 5B) and possibly contributing to a migration phenotype, IL8 was found to be significantly correlated with TLINC expression in human iCCA tumors (Fig. 6F).

## EXPERIMENTAL EVIDENCE OF TLINC CIRCULAR ISOFORMS

A genome-wide bioinformatic analysis of RNA-seq data previously reported a 204-nucleotide circular isoform of LINC00340/TLINC, probably derived from exon E7. This isoform was one of the most highly expressed circular RNAs (circRNAs) in H1-human embryonic stem cells.<sup>(21)</sup> To evaluate the putative expression of such circular isoforms in iCCA, we designed specific sets of convergent and divergent primers from exons E7 and E8 of TLINC (Fig. 7A). ACTB was used as a housekeeping gene control that was highly expressed and without prior evidence of a circular isoform. Interestingly, by combining RNase R treatment and RT-PCR experiments, we provide evidence of the existence of several RNase R-resistant circular TLINC isoforms not only in iCCA cells treated with TGF $\beta$  (Fig. 7B) but also in resected human iCCA tumors (Fig. 7C).

## Discussion

The molecular mechanisms involved in iCCA carcinogenesis are complex and involve multiple interactions between tumor cells and their microenvironment.<sup>(1)</sup> We previously demonstrated that active TGF $\beta$  signaling is an important feature in the iCCA microenvironment<sup>(6)</sup>; however, a deep characterization of the impact of TGF $\beta$  on tumor cells at the transcriptome level was lacking in iCCA. In this study, we first validated suitable experimental cellular models to study TGF $\beta$  signaling in iCCA cells. Particularly, we provided strong experimental evidence that Huh28 cells

exhibit an endogenous activation of TGF $\beta$ , which correlates with a mesenchymal phenotype. This cell line may thus be relevant to test TGF $\beta$  inhibitors for therapeutic purposes, as was suggested in liver cancers.<sup>(22)</sup> In addition, we provided the first TGF $\beta$  transcriptome signature in iCCA cells, which allowed us to identify novel TGF $\beta$  transcriptional targets, including coding and noncoding genes, both *in vitro* and in resected human iCCA.

Few studies have reported a deregulation of lncRNA in iCCA.<sup>(23,24)</sup> As an example, oncogenic metastasis-associated lung adenocarcinoma transcript 1 (MALAT1) lncRNA was shown to promote proliferation and invasion of CCA cell lines by activating the phosphoinositide 3-kinase/protein kinase B signaling pathway.<sup>(24)</sup> Here, we provide the first report of lncRNA directly regulated by TGF $\beta$  in iCCA, supporting the previous description of TGF $\beta$ -regulated lncRNA in other cancer types.<sup>(11,12)</sup> Notably, lncRNA activated by TGF- $\beta$  was shown to induce EMT and to promote HCC cell invasion through a TGF $\beta$ /miR-200/zinc finger E-box binding axis.<sup>(12)</sup> Similarly, TGF $\beta$ -induced lncRNA-HIT was shown to promote EMT in breast cancer, notably by decreasing the expression of CDH1.<sup>(11)</sup> By comparing the transcriptome profiles of HuCCT1 and Huh28 cells at the basal level and after TGF $\beta$  treatment, we identified a robust signature made of 42 nonredundant genes. This signature was validated by including well-known TGF $\beta$  target genes (e.g., SERPINE1, IL11, CTGF, BCL2 modifying factor [BMF], SNAI1) reported in multiple cell types, including hepatocytes.<sup>(25)</sup> Importantly, this approach highlighted several novel TGF $\beta$ -induced lncRNA, including LINC00312, LINC00313, and LINC00340 (TLINC), possibly involved in TGF $\beta$  signaling. LINC00312 has been reported to inhibit the migration and invasion of bladder cancer cells by targeting miR-197-3p.<sup>(26)</sup> High expression of LINC00313 has been associated with a poor prognosis and metastasis in lung cancer.<sup>(27)</sup> Experimental data on TLINC were more complex given that several isoforms were reported to exhibit either tumor-suppressive or tumor-promoting features in various types of cancer.<sup>(18,19)</sup> Thus, in neuroblastoma, a short isoform was associated with tumor suppression by hampering cell growth and migration, and a lower expression of this short isoform was found in advanced tumors associated with a poor survival.<sup>(18)</sup> Conversely, a long isoform of TLINC was reported in metastatic melanoma and associated with tumor progression.<sup>(19)</sup> The differences in the basal expression

and induction by TGF $\beta$  of TLINC isoforms in HuCCT1 and Huh28 cell lines suggest that the function of TLINC is highly dependent on the cellular context, as known for several TGF $\beta$  target genes.<sup>(10)</sup>

Although TLINC deregulation has been reported in cancer,<sup>(18,19)</sup> we provide the first evidence that TLINC is a common transcriptional target of TGF $\beta$  not only in liver cancer (iCCA and HCC) but also in other cancer types, including pancreatic cancer. Interestingly, we demonstrated that TLINC is also up-regulated by TGF $\beta$  in cells from the tumor microenvironment, as evidenced by the analysis of its expression in activated hepatic stellate cells (LX2) and in human iCCA tumors by ISH and LCM of the stroma. These data suggest that TLINC may play a role in TGF $\beta$ -induced remodeling of the tumor microenvironment. Supporting this hypothesis, our experimental data show that ectopic expression of TLINC directly impacts the expression of several inflammatory mediators, including chemokine IL8. Increased expression of IL8 has been reported in cancer and is associated with important changes within the tumor microenvironment, including promotion of angiogenesis, infiltration of neutrophils and tumor-associated macrophages, and migration of cancer cells.<sup>(28,29)</sup> Interestingly, a functional link has been established between the expression of IL8 and nuclear paraspeckle assembly transcript 1 [NEAT1], another lncRNA that we found to be induced in cells transfected with the TLINC DNA construct (Fig. 5B). Indeed, it was demonstrated that NEAT1-dependent relocation of a splicing factor proline/glutamine-rich from the promoter region of the IL8 gene to paraspeckle led to the transcriptional activation of IL8.<sup>(30)</sup> One can hypothesize that TLINC acts as a structural component of paraspeckles and that interaction with NEAT1 may result in IL8 expression. This hypothesis is in agreement with the partial nuclear location of TLINC. The enrichment of a gene signature associated with repressive marks H3K27me3 in iCCA tumors characterized by a high expression of TLINC may also suggest a role of TLINC in epigenetic silencing, as was described for other lncRNAs, such as Kcnq1ot1 antisense.<sup>(31)</sup> Similarly, enrichment of a gene signature associated with protein metabolism in iCCA with low TLINC expression together with the cytoplasmic expression of TLINC may suggest a role of TLINC in translation, as described for lncRNA growth arrest specific 5 (GAS5), which interacts with the translational machinery to inhibit c-Myc translation.<sup>(32)</sup> Another interesting aspect is the restricted expression of TLINC in remodeled portal areas with

signs of ductular reaction in nontumor livers. These areas are usually associated with activation of the cancer stem cell compartment.<sup>(33)</sup> Supporting a putative role of TLINC in cancer stem cell biology, TLINC has been reported to be highly expressed in human embryonic stem cells.<sup>(21,34)</sup> At the functional level, we showed that TLINC-L overexpression in HuCCT1 cells resulted in increased cell migration. Although the underlying molecular mechanisms are still to be clarified, *SNAI2* was found to be enriched in the gene expression profiles of TLINC-L transfected cells, suggesting that the type of migration could be partly related to EMT. Other genes found to be tightly correlated with TLINC expression in human iCCA tumors may also contribute to the observed phenotypes. As an example, platelet-derived growth factor receptor beta (*PDGFRB*) has been associated with the aggressive behavior of several types of tumors.<sup>(35)</sup> Notably, *PDGFRB* has been shown to promote liver metastasis formation of mesenchymal-like colorectal tumor cells.<sup>(36)</sup>

Finally, we provide experimental evidence of circular isoforms of TLINC that may represent putative, relevant, noninvasive biomarkers for iCCA. Indeed, recent data demonstrated that circRNAs are enriched in extracellular vesicles, including exosomes, compared to their linear counterparts.<sup>(37,38)</sup> The circular structure of circRNAs renders them more stable and resistant to degradation by exonucleases. Thus, pangenomic profiling of circRNA abundance is emerging in cancer, and several expression signatures have been reported, notably in HCC.<sup>(39)</sup> Our study provides the first report of circRNA expression in iCCA. The function of circRNA-TLINC remains to be explored, but several experimental data demonstrated that circRNAs may act as sponges for miRNA and RNA binding proteins. With respect to the TGF $\beta$  pathway, circRNA\_010567 has been recently shown to promote TGF $\beta$ -induced myocardial fibrosis by directly suppressing miR-141, which naturally targets TGF $\beta$ .<sup>(40)</sup>

In conclusion, our study identifies novel TGF $\beta$  transcriptional target genes in iCCA, including an lncRNA that may represent a promising biomarker for iCCA.

**Acknowledgment:** We thank the core facilities of Bio-sit and Biogenouest (CRB Santé BB-0033-00056, GEH, H<sup>2</sup>P<sup>2</sup>, ImPACcell) and the French liver cancer biobanks network (BB-0033-00085), including Beaujon, Bordeaux, Mondor, Nantes, Paris-Sud, and Rennes biobanks. C.C. thanks K.A. Cole (Children's

Hospital of Philadelphia) and S. Sugano (University of Tokyo) for providing the CASC15 DNA constructs; S. Dréano (Institut de génétique et développement de Rennes [IGDR]) for DNA sequencing; and C. Père for reporter sensor cell line analysis. We thank D. Gilot, M.D. Galibert (IGDR, Rennes), B. Fromenty (NuMeCan, Rennes), and S. Diederichs (German Cancer Research Center [DKFZ], Heidelberg) for helpful discussions.

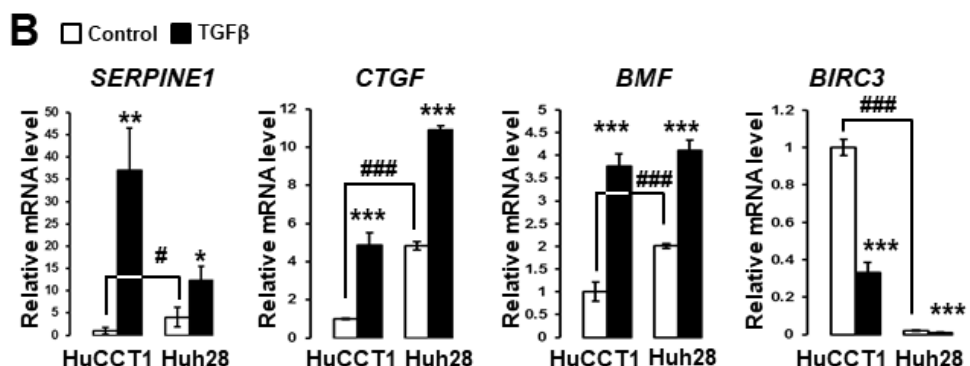
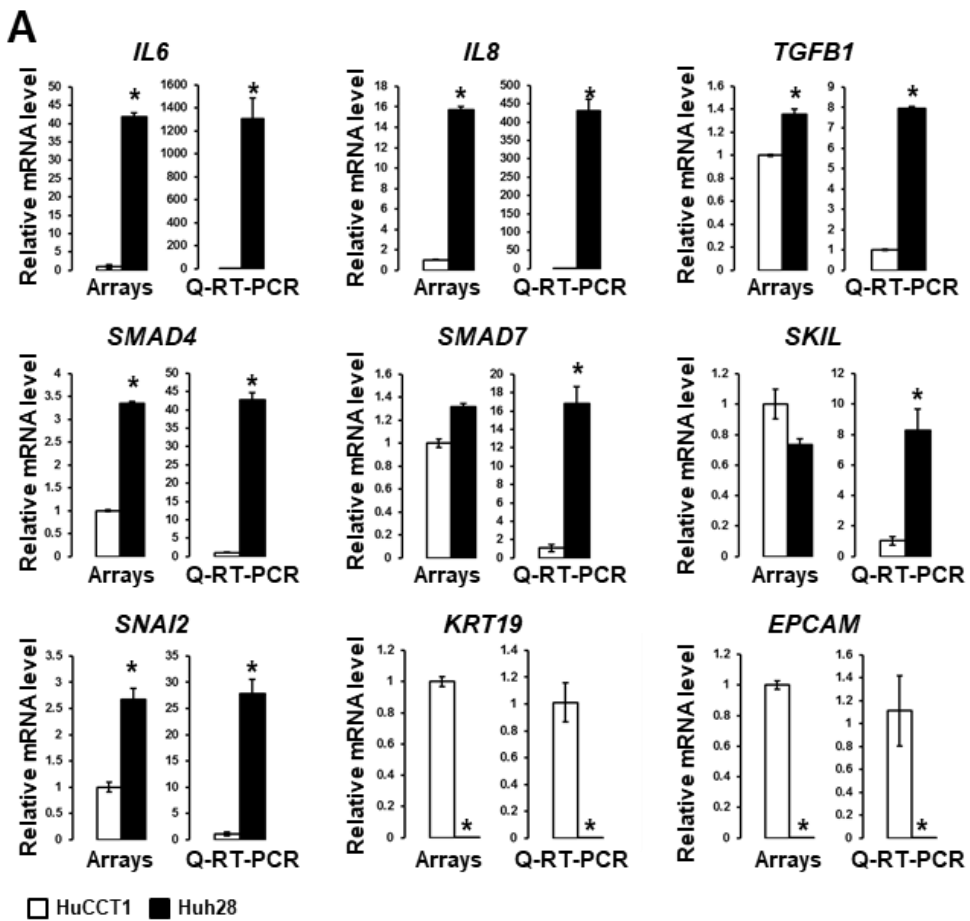
## REFERENCES

- Banales JM, Cardinale V, Carpino G, Marzoni M, Andersen JB, Invernizzi P, et al. Expert consensus document: cholangiocarcinoma: current knowledge and future perspectives consensus statement from the European Network for the Study of Cholangiocarcinoma (ENS-CCA). *Nat Rev Gastroenterol Hepatol* 2016;13:261-280.
- Bridgewater J, Galle PR, Khan SA, Llovet JM, Park JW, Patel T, et al. Guidelines for the diagnosis and management of intrahepatic cholangiocarcinoma. *J Hepatol* 2014;60:1268-1289.
- Moeini A, Sia D, Bardeesy N, Mazzaferro V, Llovet JM. Molecular pathogenesis and targeted therapies for intrahepatic cholangiocarcinoma. *Clin Cancer Res* 2016;22:291-300.
- Sirica AE. The role of cancer-associated myofibroblasts in intrahepatic cholangiocarcinoma. *Nat Rev Gastroenterol Hepatol* 2011;9:44-54.
- Rizvi S, Gores GJ. Pathogenesis, diagnosis, and management of cholangiocarcinoma. *Gastroenterology* 2013;145:1215-1229.
- Sulpice L, Rayar M, Desille M, Turlin B, Fautrel A, Boucher E, et al. Molecular profiling of stroma identifies osteopontin as an independent predictor of poor prognosis in intrahepatic cholangiocarcinoma. *Hepatology* 2013;58:1992-2000.
- Massague J. TGF $\beta$  in cancer. *Cell* 2008;134:215-230.
- Nieto MA, Huang RY, Jackson RA, Thiery JP. EMT: 2016. *Cell* 2016;166:21-45.
- Ikushima H, Miyazono K. TGF $\beta$  signalling: a complex web in cancer progression. *Nat Rev Cancer* 2010;10:415-424.
- Massague J. TGF $\beta$  signalling in context. *Nat Rev Mol Cell Biol* 2012;13:616-630.
- Richards EJ, Zhang G, Li ZP, Permuth-Wey J, Challa S, Li Y, et al. Long non-coding RNAs (lncRNA) regulated by transforming growth factor (TGF) beta. LncRNA-HIT-mediated TGF-induced epithelial to mesenchymal transition in mammary epithelia. *J Biol Chem* 2016;291:22860.
- Yuan JH, Yang F, Wang F, Ma JZ, Guo YJ, Tao QF, et al. A long noncoding RNA activated by TGF-beta promotes the invasion-metastasis cascade in hepatocellular carcinoma. *Cancer Cell* 2014;25:666-681.
- Klingenberg M, Matsuda A, Diederichs S, Patel T. Non-coding RNA in hepatocellular carcinoma: mechanisms, biomarkers and therapeutic targets. *J Hepatol* 2017;67:603-618.
- Prensner JR, Chinaiyan AM. The emergence of lncRNAs in cancer biology. *Cancer Discov* 2011;1:391-407.
- Allain C, Angenard G, Clement B, Coulouarn C. Integrative genomic analysis identifies the core transcriptional hallmarks of human hepatocellular carcinoma. *Cancer Res* 2016;76:6374-6381.

- 16) Couloarn C, Corlu A, Glaise D, Guenon I, Thorgeirsson SS, Clement B. Hepatocyte-stellate cell cross-talk in the liver engenders a permissive inflammatory microenvironment that drives progression in hepatocellular carcinoma. *Cancer Res* 2012;72:2533-2542.
- 17) Dubois-Pot-Schneider H, Fekir K, Couloarn C, Glaise D, Aninat C, Jarnouen K, et al. Inflammatory cytokines promote the retrodifferentiation of tumor-derived hepatocyte-like cells to progenitor cells. *Hepatology* 2014;60:2077-2090.
- 18) Russell MR, Penikis A, Oldridge DA, Alvarez-Dominguez JR, McDaniel L, Diamond M, et al. CASC15-S is a tumor suppressor lncRNA at the 6p22 neuroblastoma susceptibility locus. *Cancer Res* 2015;75:3155-3166.
- 19) Lessard L, Liu M, Marzese DM, Wang H, Chong K, Kawas N, et al. The CASC15 long intergenic noncoding RNA locus is involved in melanoma progression and phenotype switching. *J Invest Dermatol* 2015;135:2464-2474.
- 20) Wu Y, Siadat MS, Berens ME, Hampton GM, Theodorescu D. Overlapping gene expression profiles of cell migration and tumor invasion in human bladder cancer identify metallothionein 1E and nicotinamide N-methyltransferase as novel regulators of cell migration. *Oncogene* 2008;27:6679-6689.
- 21) Salzman J, Chen RE, Olsen MN, Wang PL, Brown PO. Cell-type specific features of circular RNA expression. *PLoS Genet* 2013;9:e1003777.
- 22) Giannelli G, Mikulits W, Dooley S, Fabregat I, Moustakas A, ten Dijke P, et al. The rationale for targeting TGF-beta in chronic liver diseases. *Eur J Clin Invest* 2016;46:349-361.
- 23) Yang W, Li Y, Song X, Xu J, Xie J. Genome-wide analysis of long noncoding RNA and mRNA co-expression profile in intrahepatic cholangiocarcinoma tissue by RNA sequencing. *Oncotarget* 2017;8:26591-26599.
- 24) Wang C, Mao ZP, Wang L, Wu GH, Zhang FH, Wang DY, et al. Long non-coding RNA MALAT1 promotes cholangiocarcinoma cell proliferation and invasion by activating PI3K/Akt pathway. *Neoplasma* 2017;64:725-731.
- 25) Couloarn C, Factor VM, Thorgeirsson SS. Transforming growth factor-beta gene expression signature in mouse hepatocytes predicts clinical outcome in human cancer. *Hepatology* 2008;47:2059-2067.
- 26) Wang YY, Wu ZY, Wang GC, Liu K, Niu XB, Gu S, et al. LINC00312 inhibits the migration and invasion of bladder cancer cells by targeting miR-197-3p. *Tumour Biol* 2016;37:14553-14563.
- 27) Li M, Qiu M, Xu Y, Mao Q, Wang J, Dong G, et al. Differentially expressed protein-coding genes and long noncoding RNA in early-stage lung cancer. *Tumour Biol* 2015;36:9969-9978.
- 28) Waugh DJ, Wilson C. The interleukin-8 pathway in cancer. *Clin Cancer Res* 2008;14:6735-6741.
- 29) Liu Q, Li A, Tian Y, Wu JD, Liu Y, Li T, et al. The CXCL8-CXCR1/2 pathways in cancer. *Cytokine Growth Factor Rev* 2016;31:61-71.
- 30) Imamura K, Imamachi N, Akizuki G, Kumakura M, Kawaguchi A, Nagata K, et al. Long noncoding RNA NEAT1-dependent SFPQ relocation from promoter region to paraspeckle mediates IL8 expression upon immune stimuli. *Mol Cell* 2014;53:393-406.
- 31) Pandey RR, Mondal T, Mohammad F, Enroth S, Redrup L, Komorowski J, et al. Kcnq1ot1 antisense noncoding RNA mediates lineage-specific transcriptional silencing through chromatin-level regulation. *Mol Cell* 2008;32:232-246.
- 32) Hu G, Lou Z, Gupta M. The long non-coding RNA GAS5 cooperates with the eukaryotic translation initiation factor 4E to regulate c-Myc translation. *PLoS One* 2014;9:e107016.
- 33) Marquardt JU, Andersen JB, Thorgeirsson SS. Functional and genetic deconstruction of the cellular origin in liver cancer. *Nat Rev Cancer* 2015;15:653-667.
- 34) Tang X, Hou M, Ding Y, Li Z, Ren L, Gao G. Systematically profiling and annotating long intergenic non-coding RNAs in human embryonic stem cell. *BMC Genomics* 2013;14(Suppl. 5):S3.
- 35) Demoulin JB, Essaghir A. PDGF receptor signaling networks in normal and cancer cells. *Cytokine Growth Factor Rev* 2014;25:273-283.
- 36) Steller EJ, Raats DA, Koster J, Rutten B, Govaert KM, Emmink BL, et al. PDGFRB promotes liver metastasis formation of mesenchymal-like colorectal tumor cells. *Neoplasia* 2013;15:204-217.
- 37) Lasda E, Parker R. Circular RNAs co-precipitate with extracellular vesicles: a possible mechanism for circRNA clearance. *PLoS One* 2016;11:e0148407.
- 38) Li Y, Zheng Q, Bao C, Li S, Guo W, Zhao J, et al. Circular RNA is enriched and stable in exosomes: a promising biomarker for cancer diagnosis. *Cell Res* 2015;25:981-984.
- 39) Han D, Li J, Wang H, Su X, Hou J, Gu Y, et al. Circular RNA circMTO1 acts as the sponge of miR-9 to suppress hepatocellular carcinoma progression. *Hepatology* 2017;66:1151-1164.
- 40) Zhou B, Yu JW. A novel identified circular RNA, circRNA\_010567, promotes myocardial fibrosis via suppressing miR-141 by targeting TGF-beta1. *Biochem Biophys Res Commun* 2017;487:769-775.

## Supporting Information

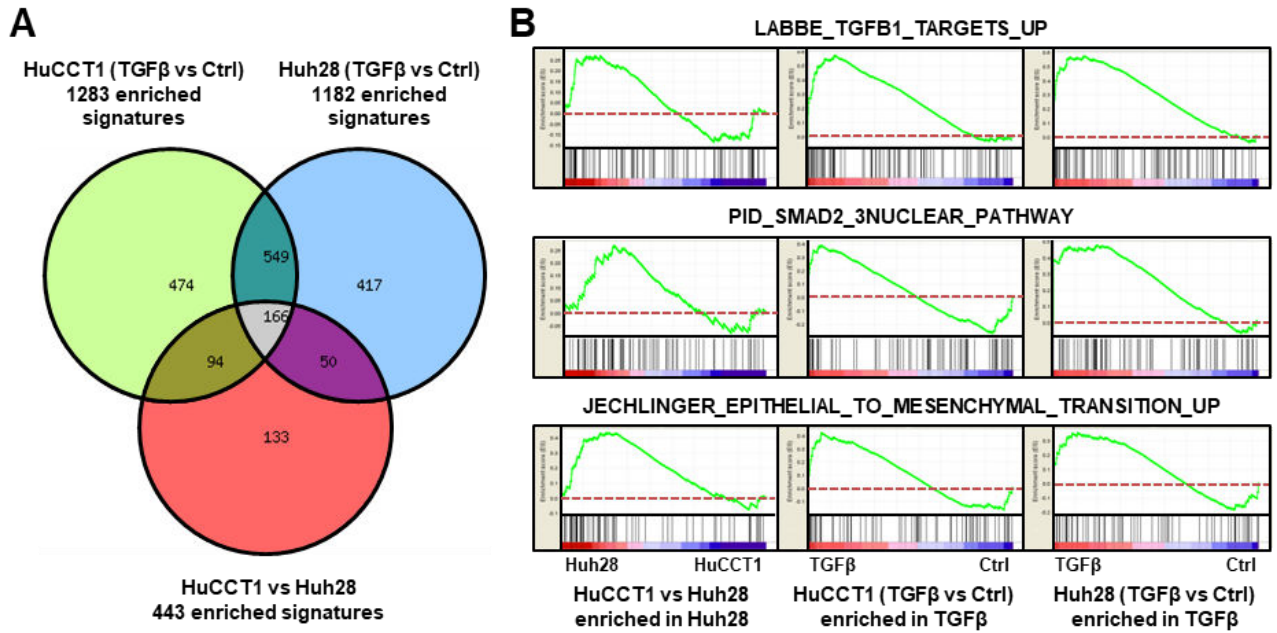
Additional Supporting Information may be found at [onlinelibrary.wiley.com/doi/10.1002/hep4.1142/full](http://onlinelibrary.wiley.com/doi/10.1002/hep4.1142/full).



**SI Figure 1: Expression of TGF $\beta$  target genes in HuCCT1 and Huh28 cells at basal condition and after a 16hrs TGF $\beta$  treatment**

**A:** Expression of TGF $\beta$  target genes in HuCCT1 (white bars) and Huh28 (black bars) cells at basal level, as evaluated by DNA microarrays (left panels) and Q-RT-PCR (right panels). Statistical analysis was performed by a t-test (\* P<0.05; n=3 replicates)

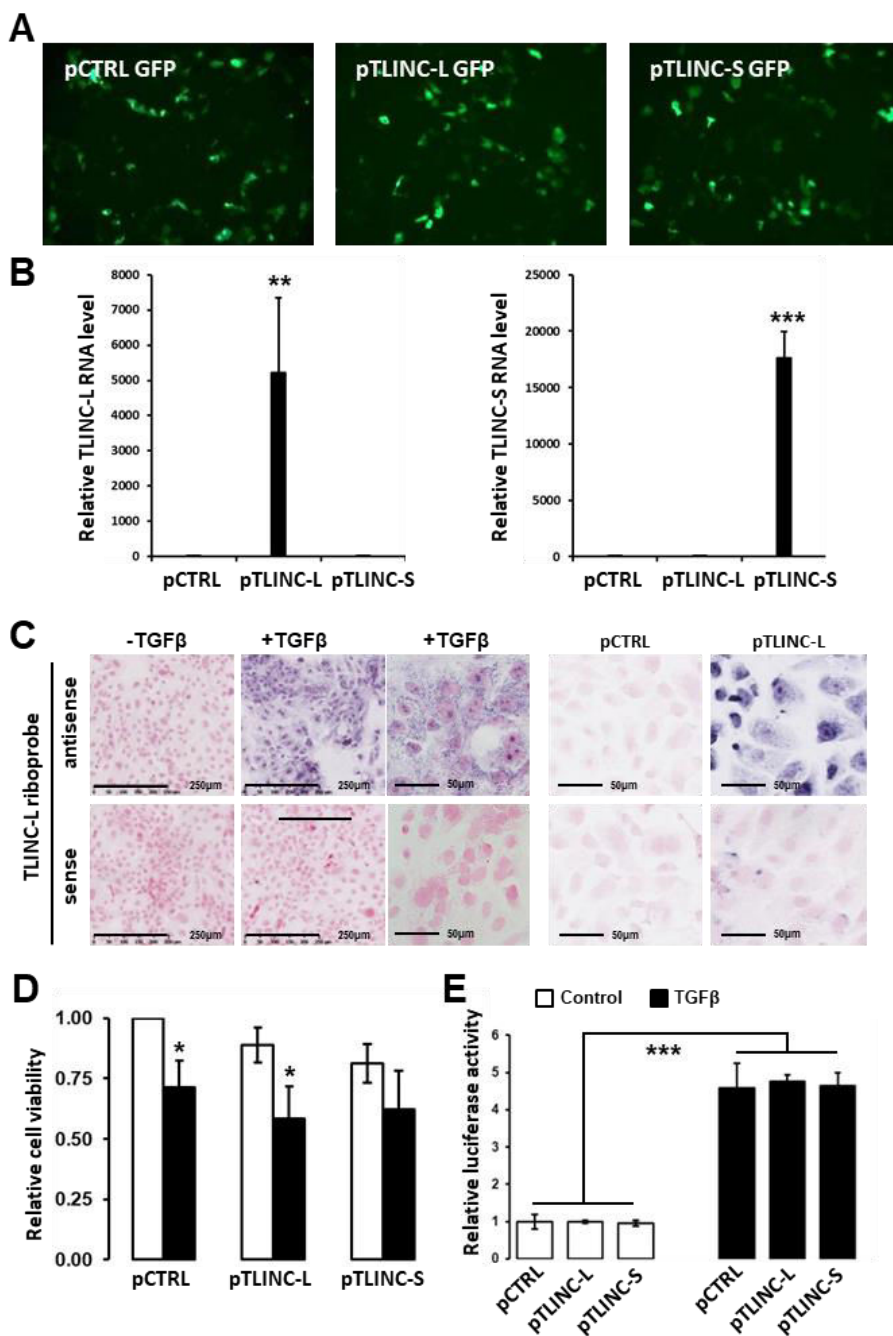
**B:** Expression of well-known TGF $\beta$  target genes in HuCCT1 and Huh28 cells after 16hrs of culture in absence (white bars) or presence (black bars) of 1ng/mL TGF $\beta$ , as evaluated by Q-RT-PCR. Statistical analysis was performed by a t-test (TGF $\beta$  vs Control: \* P<0.05; \*\* P<0.01; \*\*\* P<0.001 / HuCCT1-Control vs Huh28-Control: # P<0.05; ### P<0.001) ; n=3 replicates.



**SI Figure 2: Enrichment of specific gene expression signatures in TGF $\beta$ -associated gene sets identified in HuCCT1 and Huh28 cholangiocarcinoma cell lines**

**A:** Venn diagram analysis of gene signatures significantly enriched ( $P<0.05$ ) in TGF $\beta$ -associated gene sets identified in HuCCT1 and Huh28 (as in the main Figure 2), evaluated by unsupervised GSEA.

**B:** Examples of 3 gene signatures associated with TGF $\beta$ , SMAD2/3 and EMT, significantly enriched in Huh28 at basal level as compared to HuCCT1 (left panels), or in TGF $\beta$ -treated HuCCT1 (middle panels) and Huh28 (right panels) cells, as compared to untreated cells.



**SI Figure 3. Functional analysis of TLINC-L and TLINC-S isoforms**

**A:** Green fluorescent protein (GFP) image analysis ( $\lambda=509\text{nm}$ ) of HuCCT1 cells transfected with specific DNA constructs designed to overexpressed TLINC-L and TLINC-S isoforms with GFP (100ng plasmid / 24hrs post-transfection).

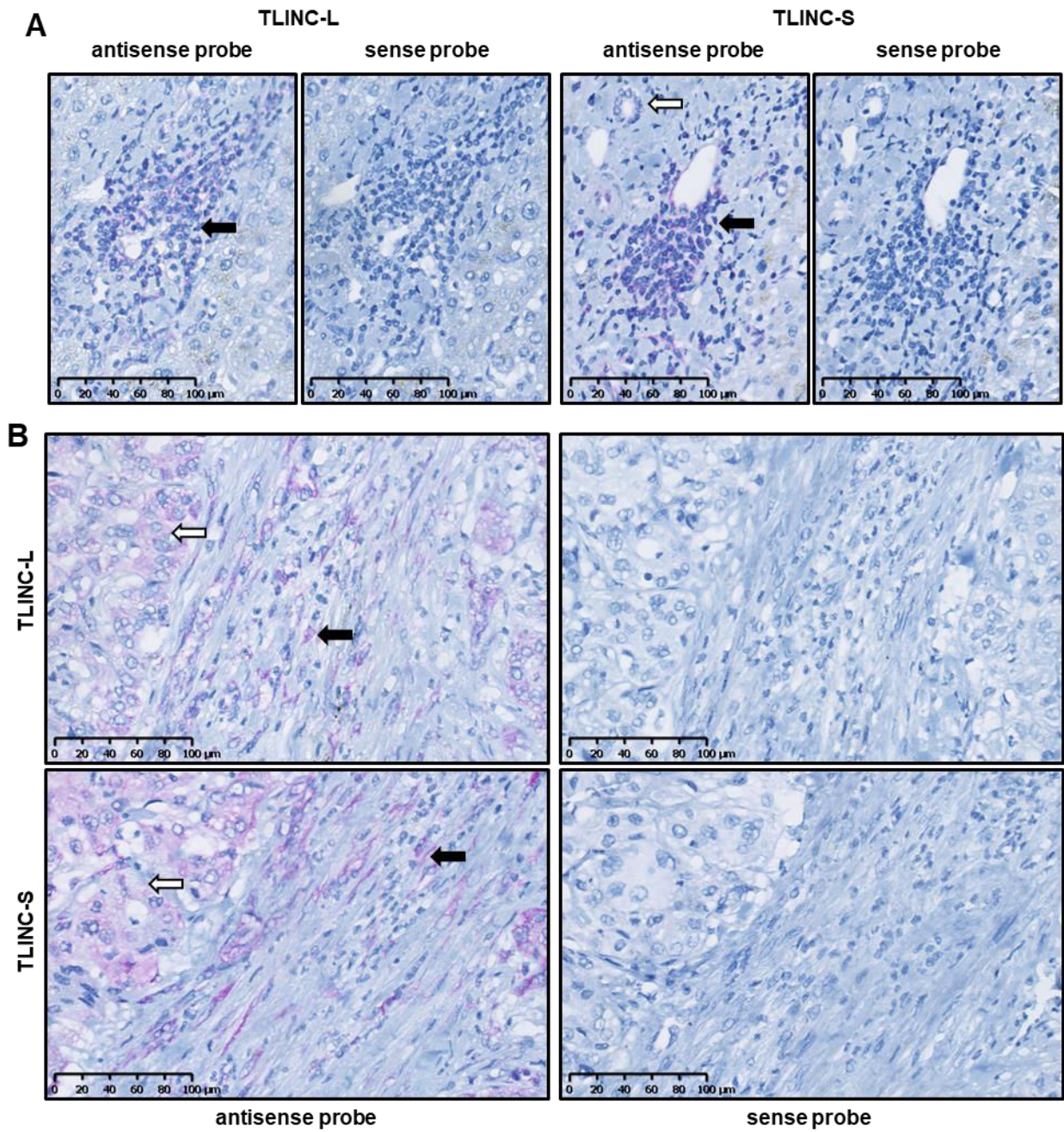
**B:** Validation of specific TLINC-L and TLINC-S overexpression by Q-RT-PCR using specific sets of primers, as in Figure 4A.

**C:** ISH using TLINC-L riboprobes (antisense, upper panels ; sense, lower panels) on HuCCT1 cells transfected with pTLINC-L DNA construct demonstrating a similar localization than after a treatment with TGF $\beta$  (Figure 4).

**D:** Cell viability of HuCCT1 cells transfected with pLINC DNA constructs after 72hrs of culture in absence (white bars) or presence (black bars) of 1ng/mL TGF $\beta$ .

**E:** Luciferase activity of HuCCT1 engineered cell lines in which a luciferase gene is under the transcriptional control of SMAD responsive elements. Luciferase activity was measured in cells transfected with TLINC-L and TLINC-S DNA constructs in absence (white bars) or presence (black bars) of TGF $\beta$ . No significant difference was observed between the different TLINC DNA constructs.

Statistical analysis was performed by a t-test (\* P < 0.05; \*\* P < 0.01; \*\*\* P < 0.001) ; n=3 replicates.



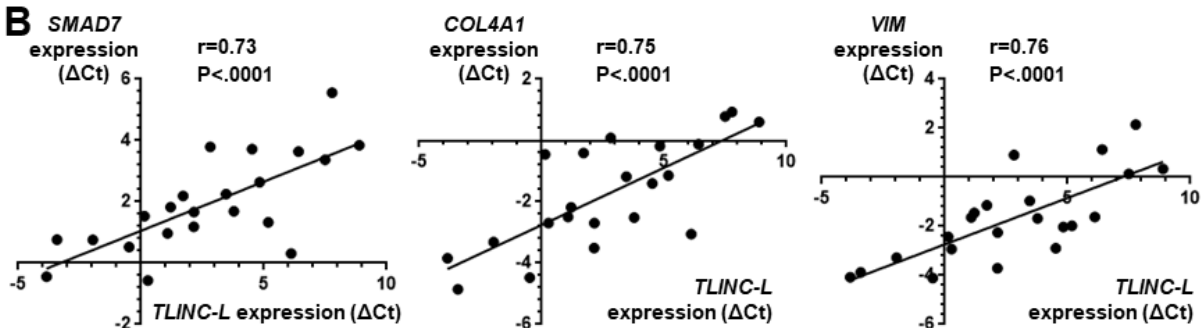
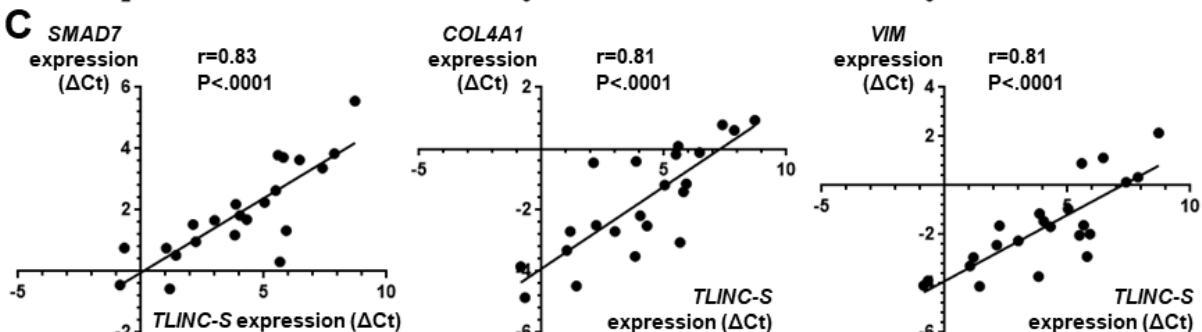
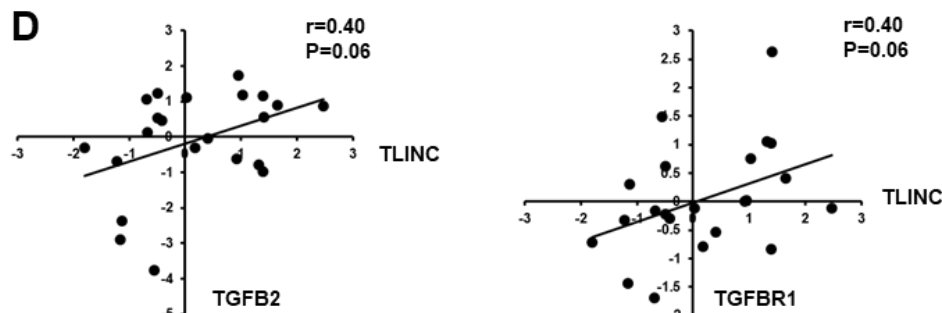
**SI Figure 4: Analysis of *TLINC-L* and *TLINC-S* expression by ISH on human resected iCCA**

**A:** ISH analysis of *TLINC-L* and *TLINC-S* expression using specific antisense and sense riboprobes in non-tumor liver. Signal was observed in remodeled portal areas (black arrow) but not in normal bile ducts (white arrow) or normal hepatocytes. No signal was observed with the sense riboprobes.

**B:** ISH analysis of *TLINC-L* and *TLINC-S* expression using specific antisense and sense riboprobes in the tumor part. *TLINC* was expressed in both epithelial cells (white arrow) and in the stroma (black arrow). No signal was observed with the sense riboprobes. Scale bar: 100μm.

**A**

	SMAD7	COL4	VIM	TLINC-L	TLINC-S
SMAD7	1.00	0.82	0.81	0.73	0.83
COL4		1.00	0.84	0.75	0.81
VIM			1.00	0.76	0.81
TLINC-L				1.00	0.97
TLINC-S					1.00

**B****C****D**

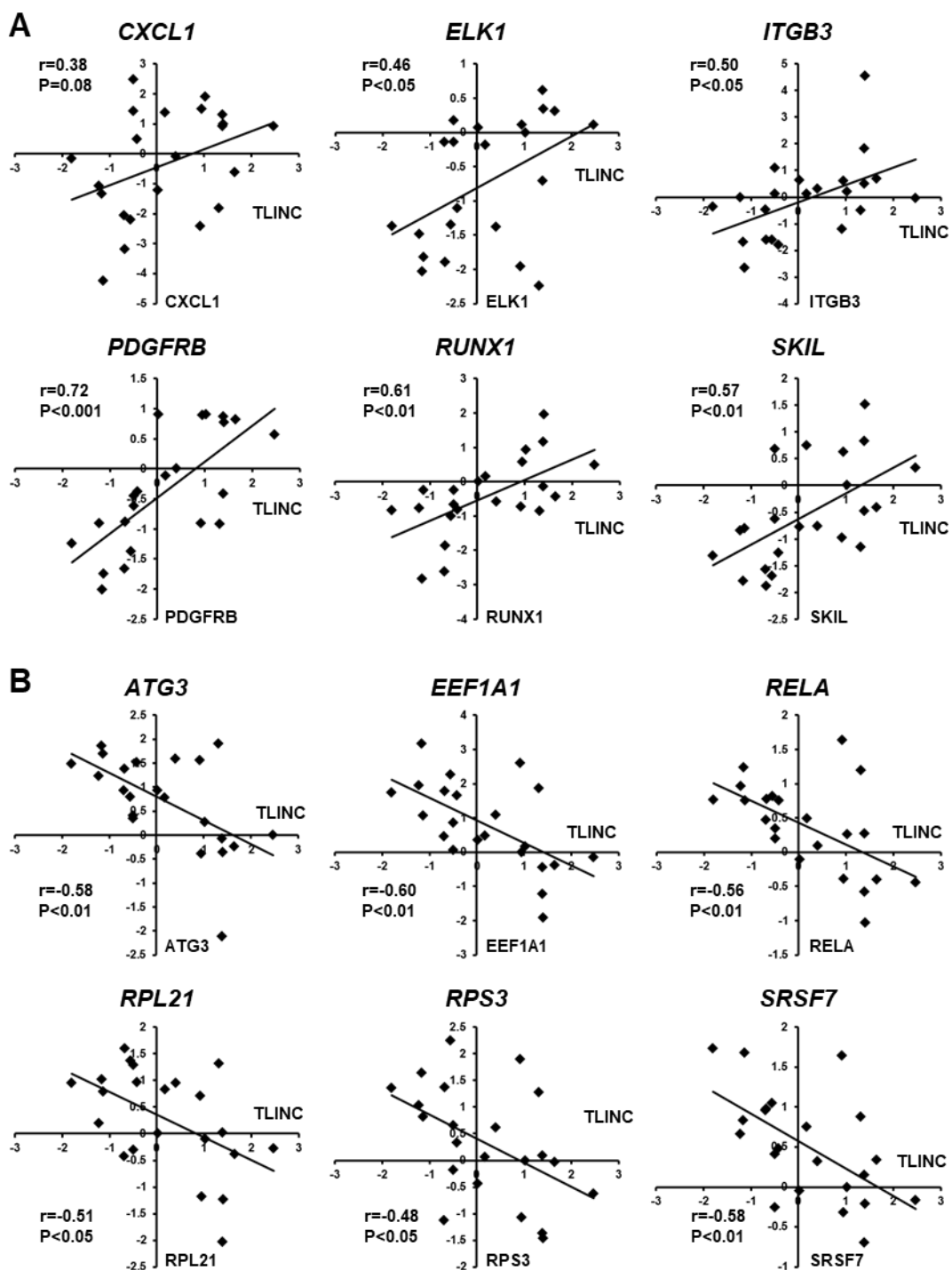
**SI Figure 5: Correlation of gene expression between TLINC isoforms and TGF $\beta$  target genes in resected human iCCA tumors**

**A:** Correlation coefficient between the expression of TLINC-L, TLINC-S and TGF $\beta$ -associated genes, as detected by Q-RT-PCR in 22 resected human iCCA tumors;  $P<0.001$  for all correlations.

**B:** Correlation plot between the expression of TLINC-L and well-known TGF $\beta$  target genes, as detected by Q-RT-PCR in 22 resected human iCCA tumors.

**C:** Correlation plot between the expression of TLINC-S and well-known TGF $\beta$  target genes, as detected by Q-RT-PCR in 22 resected human iCCA tumors.

**D:** Correlation plot between the expression of TLINC and TGFB2 and TGFBR1, as detected by microarray in 22 resected human iCCA tumors.



**SI Figure 6: Correlation of gene expression between TLINC and genes significantly induced or repressed in resected human iCCA tumors characterized by high and low TLINC expression**

**A:** Examples of genes positively correlated with TLINC.

**B:** Examples of genes negatively correlated with TLINC.

n=22 human iCCA

**Supplementary Table 1. Sequence of TLINC-L and TLINC-S isoforms**

Alternating of black and blue colors delineates successive exons. Underlined nucleotides refer to the sequence of riboprobes used for in situ hybridization experiments.

**A) Sequence of TLINC-Long isoform (TLINC-L): E1-E2-E3-E4-E5-E6-E7-E8-E9-E10-E11-E12**

GTCTGCTCCGGGACTTGGAAACAAAGGGGGAACTCTGATGAACTCTTCCTCCCCCTCCCCCGGACGC  
CGGGGTATCCCTCTCGCAACTTGCCGCCGACTTCTGCTGTCAAGGCCGGAAAAAGTGTCCGAA  
CGCCTCGTGGACTGCAGCGGGGAAATGCCCCTAAAAGTGCAGAAGTGGGGAGAAGGTGAATTACT  
ATTATCAGCATCTAGAACGATCATGAATTGCTGGAGTACTTCCTAGCACTGACCTCCTCATTCTGCCTTGT  
TCTTACTGGATCTTCATCAGCCAACAATATGGAAGTACCAATACAAGGTCAATCATTCTGGATTCTG  
GAGTTGCTTAAAGTAAATCATGGAATTGGATTTGATGATACTTCTATATGGATTACAATTGATCGCTGG  
AATTCTCCACCTTAAAGAAGTACCCCTCAGGTGACTACAGATGTGTAACACCCAGCATGTTCCGGTAGGAGA  
CTTCTGGATGGGAAGATTCCAGGAATTGGCAACAAAGCTCATTCACTGGTGGGTTGCTGAAGCATTATC  
ACAAGACAGTCAGAATGACTGATGAGTGCCTTCAGGTGAATCATGGAATACAGTGAAGACAGTGAATT  
ACTGCTTTGAGGGCGTGCATGTATGATTAACGGATGGAAGTGCAGGACTCCAAGAGATTACTCCCTCCCT  
TTCCAGCAGAATTACCTGAGACGAGTAAATCTACTGGTGGAGTCACTCATTATTCTATCTGGAGATCT  
AGATCTTGATTGAAAGTTCTGAGAAAATCTCAGCTCAGACTTGAGGGCAACTTACAGCTGAAGGATC  
TGCAATTACTGCTCAACCACATCTAATTGATGTCCTCTGCAGATTAAAATGTTGCTGCCTTCTTCCGTCA  
AAGTCATCCCTGGGTTACTACTGAACATCCTCTCAATTCCCCCGACCCATGGATGGCTGTTCTCCATTGTC  
TGTTCACCAGATGTCCTCAAAACAAACAGACAGAAGAAGGAAGTGGCTAATGAGCTGTGGAGTCCAAGTG  
TGACTGCCAAGAGGAATCCAGCAAAGCCAAAAGCCAAAGCATGTAGCCTGCCAGCACGCCACACGC  
ATGGAAAACCCAGAGGAAATGAGTGAGGATCAATGGGAAGAAGAGAGCCAGGAAGTTGAAGATTGT  
CCAGGAGCAGATAGCTGAAGAGAGAGAGAGAGAGAACGGCTTACAGCTCAGGTCTCTCCATGC  
TTAGGAACCAACTACAATGCTACTGCCTTGAGTCTCATTGTTCCCTCTGGAAACCACATGTTGACTCTGTT  
TGCAACAGTATGGGCTCACAGGCCAGAGAATTTCCTGTCTGGATGAGACTTTGACTGGACTTTGGG  
TTAAGTTCTGGAGACCAGAAGGCCAAAATCAAAAGTATGGCAGGCTGATTCTTAAAGACTCCAGCGG  
AGAAACTGTGTCCTCTGCTCTGATTCTACATCTCCATGGCCACTGTTCACTGCAACCTCAGCCAGTG  
AACACAACCTCAGCCAAGAAGAGTATGCAGAGAAAGGGAGTCCCCTACCTGCCACAAAAGTGTGCTGAAA  
CTGTCATATTGTCATAAGTTGTCATTGTAATTAGACCTGTTAACATGTAATCTGCAACATGCTCA  
CTGCTAATTTCAGAGCCCTCATATAAGGAACTGTATTATGGTATAATCATCATGGTAAGAAGTTGGTA  
TGTGGGGAGAGATGACAGAACAGAGAGTAAGTCAGAGCTGGCTGCCTGACAGATAAAAGGAAATGACC  
AA

**B) Sequence of TLINC-Short isoform (TLINC-S): E9bis-E10-E11-E12**

GGGCACGCAAGCTCCCTGGTACCTGAGCTGCTCTGCCGCTCCGCCCTGGGCTTCGCCGTGGTCAC  
CCGATCCCGGAATCGTGCCTGCGCCCTGCGAAAGAAGGACCTGCTGGCGAGCTCCGGCCGGGGTCTC  
CTGCCTCGCAGCTGGCGAGGGGACTGGAGGACAGGGTGAAGCTGCAGAAGACCTGGGTGGGATGGCT  
AGAGAGGACGCCAAGGACTGGGAAGGGGAAGTGTAGGAATACCTTACATCCAATGCCACCCGTGCTCCGC  
AGGGCAAGGGCAGCCGTCGCCCTGGCCCGTGCACCCAGCTCAGGCTGTTCCAGGGATTAGTCTGGGG  
GGACAACCCATGGCGAGATGTGGTGCATTTCACCTCAGAGTGGAGCTGAAGATGGATAAACAGGTATCTG  
ATGTATCTGCTGAGAAGGCAGAGCTGGAGAAAGGGAGCGAGGGAGCGCGTGAAGAAAGAAAGAGATGCC  
GAATGCCGGGTGATTGCTGCCGCTGCTGCATTCTCATTCTAGGGAGGATGGCATAATTATAACCCAG  
CACATGGATAGAGGAACTGTAAATTGTAAGTCTGGATGTCCCCGGCGCTGTCAGCAAGGAACACTGATGGGCT  
AGGCTCACAGGCAGAAGGAATTTCCTGTCTGGATGAGACTTTGACTGGACTTTGGGTTAAGTTCTGG  
AGACCAAGAAGGCCAAATCAAAAGTATGGCAGGCTGATTCTTAAAGAAGACTCCAGCGGAGAACTGTGTC  
TCCTGCTCTGATTCTACATCTCCATGGCCACTGTTCACTGCAACCTCAGCCAGTGCAACACACACCTC  
AGCCAAGAAGAGTATGCAGAGAAAGGAGTCCCCTACCTGCCACAAAAGTGTGCTGAAAAGTGTCTCATATT  
GTCTCAAGTTGTCATTGTAATTAGACCTGTTAACATGTAATCTGCAACATGCTCACTGTCTAATTTC  
CAGAGCCCTCATATAAGGAACTGTATTATGGTATAATCATCATGGTAAGAAGTTGGTATGTGGGGAGA  
GATGACAGAACAGAGAGTAAGTCAGAGCTGGCTGCCTGACAGATAAAAGGAAATGACCAA

**Supplementary Table 2. Sequence of DNA primers used in the study**

Gene	Forward primer (5' to 3' sequence)	Reverse primer (5' to 3' sequence)
ACTB	GGACTTCGAGCAAGAGATGG	AGCACTGTGTTGGCGTACAG
BIRC3	TTTCCGTGGCTCTTATTCAAAC	GCACAGTGGTAGGAACCTCTCAT
BMF	GCGCGGAGCCCTGGCATCAC	GCTGGTGGCTGCACATGAAGCCG
CDH1	CGAGAGCTACACGTTACCGG	GGGTGTCGAGGGAAAAATAGG
CDKN1A	GGCGTTGGAGTGGTAGAA	TGTCACTGTCTGTACCCCTG
COL4A1	ACTCTTTGTGATGCACACCA	AAGCTGTAAGCGTTGCGTA
CTGF	TCACTGACCTGCCTGTAG	GCTGAGTCTGCTGTTCTG
CXCL8	CTGGCCGTGGCTCTCTTG	CCTTGGCAAAACTGCACCTT
GAPDH	GACCACAGTCCATGCCATCA	TCCACCACCCCTGTTGCTGTA
EPCAM	CCTGCTCTGAGCGAGTGAGAAC	GATCTCCTCTGAAGTGCAGTCCGC
IL11	ACAGCTGAGGGACAAATTCC	AGCTGTAGAGCTCCCAGTGC
IL6	ACCCCAAAGTTGCTCAAGGA	AAAGCAGAACAGCACTCCCA
KRT19	TTTGAGACGGAACAGGCTCT	AATCCACCTCCACACTGACC
NEAT1	GCTCACTCCACCCCTTCTTC	CACATTCACTCCCCACCCCTC
SERPINE1	AAGCCTAATCAGCCCACCAT	TAGCATTGACACCACCCCT
SKIL	CAGATGCACCACAGGAATG	TTGCCTCTGTCTTGTGAGC
SMAD4	GCTGCTGGAATTGGTGGATG	AGGTGTTCTTGATGCTCTGTCT
SMAD7	CCAACTGCAGACTGTCCAGA	GGGCTCCTGGACACAGTAGA
SNAI1	CACTATGCCCGCGCTTT	GGCTGCTGGAAGGTAAACTC
SNAI2	TCGGACCCACACATTACCTT	TTGGAGCAGTTTGACTG
TBP	GAGCTGTGATGTGAAGTTCC	TCTGGGTTGATCATTCTGTAG
TGFB1	CACGTGGAGCTGTACCAAGAA	CCGGTAGTGAACCCGTTGAT
TLINC (S+L)	CAAGAGGAATCCAGCAAAGC	AGCATGGAGAGAGGACCTGA
TLINC-S	GAGAAGGCAGAGCTGGAGAA	CTAGCCCACAGTTCCCTCG
TLINC-L	CAAAAGGGGAACTCTGATG	CCTGACAGCAGAGAAAGTCG
VIM	GACGCCATCAACACCGAGTT	CTTGTGTTGGTTAGCTGGT

**Primers used to detect circular isoforms of TLINC (as in Figure 7)**

Forward	primer (5' to 3' sequence)	Reverse primer (5' to 3' sequence)
<b>Convergent primers</b>		
TLINC-E7 set1	GATCTGCATTTACTGCTCAACC	TGTTTGTGTTGAGGACATCTGG
TLINC-E7 set2	CCTGGGTTACTACTGAACATCC	TGTCTTCTCCTTCACCGATTAC
<b>Divergent primers</b>		
E7F/E7R	GACAGAAGAAGGAAGTGGCTAA	GTAGTAACCCAGGGATGACTTG
E8F/E7R	CAAGAGGAATCCAGCAAAGC	GTAGTAACCCAGGGATGACTTG

**Supplementary Table 3. Data mining of genes differentially expressed by TLINC-L**

**A) Enrichment of KEGG pathways and genes involved**

Name of KEGG pathway	P-value	Z-score	Combined score
Cytokine-cytokine receptor interaction_Homo sapiens_hsa04060	0.000067	-1.88	18.03
TNF signaling pathway_Homo sapiens_hsa04668	0.000134	-1.89	16.83
Rheumatoid arthritis_Homo sapiens_hsa05323	0.000139	-1.72	15.25
Salmonella infection_Homo sapiens_hsa05132	0.000533	-1.64	12.33
Toll-like receptor signaling pathway_Homo sapiens_hsa04620	0.002089	-1.77	10.9
NOD-like receptor signaling pathway_Homo sapiens_hsa04621	0.001387	-1.65	10.86
Chemokine signaling pathway_Homo sapiens_hsa04062	0.002517	-1.77	10.61
Hematopoietic cell lineage_Homo sapiens_hsa04640	0.002915	-1.58	9.24
Legionellosis_Homo sapiens_hsa05134	0.006526	-1.54	7.75
Chagas disease (American trypanosomiasis)_Homo sapiens_hsa05142	0.007288	-1.56	7.68

**Genes involved**



## B) Enrichment of GO Biological Process and genes involved

Name of GO pathway	P-value	Z-score	Combined score
inflammatory response	1.70E-07	-3.71	57.9
inflammatory response to wounding	1.70E-07	-3.71	57.86
acute inflammatory response	1.83E-07	-3.73	57.85
chronic inflammatory response	1.70E-07	-3.71	57.82
thrombopoietin-mediated signaling pathway	1.13E-07	-2.53	40.4
chemokine-mediated signaling pathway	1.911E-06	-3.05	40.15
chemokine (C-C motif) ligand 5 signaling pathway	8.83E-07	-2.51	34.99
C-C chemokine receptor CCR4 signaling pathway	8.83E-07	-2.51	34.97
chemokine (C-C motif) ligand 21 signaling pathway	8.83E-07	-2.5	34.88
chemokine (C-C motif) ligand 19 signaling pathway	8.83E-07	-2.5	34.84

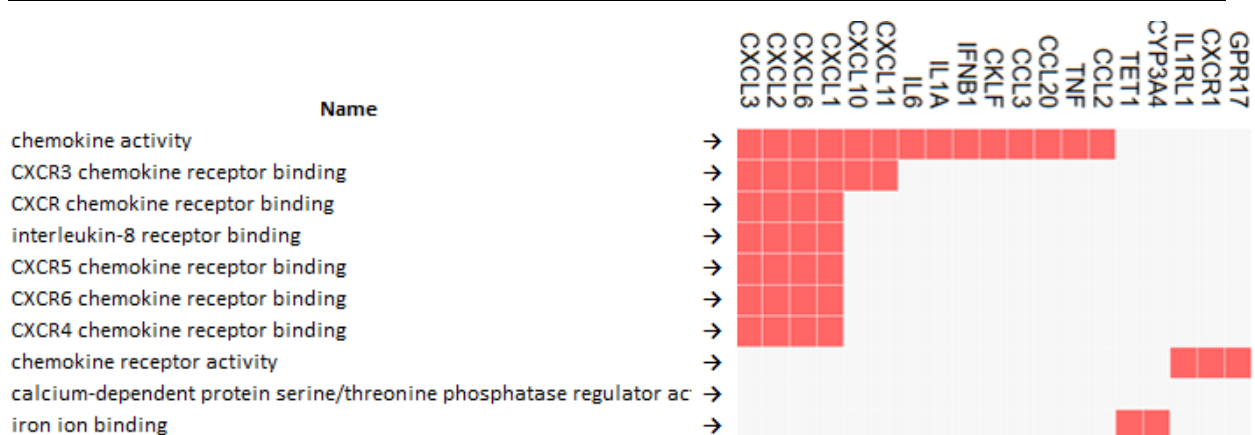
### Genes involved



### C) Enrichment of GO Molecular Function and genes involved

Name of GO pathway	P-value	Z-score	Combined score
chemokine activity	4.713E-06	-2.59	31.8
CXCR3 chemokine receptor binding	2.51E-07	-1.16	17.62
CXCR chemokine receptor binding	0.000315	-1.26	10.2
interleukin-8 receptor binding	0.000062	-0.82	7.97
CXCR5 chemokine receptor binding	0.000040	-0.75	7.62
CXCR6 chemokine receptor binding	0.000024	-0.69	7.33
CXCR4 chemokine receptor binding	0.000024	-0.69	7.3
chemokine receptor activity	0.02398	-1.83	6.81
calcium-dependent protein serine/threonine phosphatase regulator activity	0.01981	-1.62	6.36
iron ion binding	0.03363	-1.69	5.74

#### Genes involved



**Supplementary Table 4. Migration-related genes significantly enriched in the gene expression profile of HuCCT1 cells overexpressing TLINC-L**

GENE SYMBOL	RANK IN GENE LIST	RANK METRIC SCORE	RUNNING ES	CORE ENRICHMENT *
<a href="#"><u>OLR1</u></a>	6	4.458	0.0679	Yes
<a href="#"><u>NEDD9</u></a>	46	2.793	0.1086	Yes
<a href="#"><u>PTGS2</u></a>	47	2.772	0.151	Yes
<a href="#"><u>HIST1H2BK</u></a>	53	2.681	0.1917	Yes
<a href="#"><u>CYR61</u></a>	62	2.576	0.2307	Yes
<a href="#"><u>TXNIP</u></a>	84	2.359	0.2656	Yes
<a href="#"><u>UGCG</u></a>	89	2.337	0.3012	Yes
<a href="#"><u>MT1E</u></a>	96	2.282	0.3358	Yes
<a href="#"><u>MT2A</u></a>	204	1.7	0.3561	Yes
<a href="#"><u>CXCL1</u></a>	236	1.62	0.3793	Yes
<a href="#"><u>IL1A</u></a>	247	1.582	0.4029	Yes
<a href="#"><u>SNAI2</u></a>	365	1.346	0.4173	Yes
<a href="#"><u>MSN</u></a>	371	1.331	0.4374	Yes

\* from Wu et al., Oncogene, 2008

## 2. Article n°2

Accepté pour publication dans « Digestive Liver Disease »

### **« L'expression de l'ARNlnc ANRIL prédit un mauvais pronostic dans le CCI »**

Le but de ce travail était d'identifier des ARNlnc dont l'expression était significativement associée à la survie des patients opérés d'une résection chirurgicale curative d'un CCI.

Le profil d'expression génique et des q-RT-PCR ont été effectuées sur l'ARN extrait de 39 CCI issus d'une cohorte avec les données cliniques correspondantes. Un modèle de Cox univarié avec statistique de Wald a été utilisé pour identifier les ARNlnc significativement associés à la survie sans récidive et la survie globale des patients. Une méta-analyse des bases de données du TCGA a été réalisée pour évaluer la pertinence clinique de l'expression des ARNlnc dans d'autres cancers.

Une signature de 9 ARNlnc a été identifiée comme significativement associée ( $p<0.05$ ) avec la survie sans récidive et la survie globale. Parmi ces ARNlnc, quatre d'entre eux (Inc-CDK9-1, XLOC\_I2\_009441, CDKN2B-AS1, HOXC13-AS) étaient très exprimés dans les CCI de mauvais pronostic et cinq d'entre eux (Inc-CCHCR1-1, Inc-AF131215.3.1, Inc-CBLB-5, COL18A1-AS-2, Inc-RELL2-1) plus exprimés dans les CCI de meilleur pronostic. Nous avons validé CDKN2B-AS1, aussi connu sous le nom d'ANRIL, comme biomarqueur de mauvais pronostic, non seulement dans le CCI mais aussi dans le CHC, le cancer du rein à cellules claires et le carcinome de l'endomètre.



Contents lists available at ScienceDirect

## Digestive and Liver Disease

journal homepage: [www.elsevier.com/locate/dld](http://www.elsevier.com/locate/dld)



### Oncology

## Expression of long non-coding RNA ANRIL predicts a poor prognosis in intrahepatic cholangiocarcinoma

Q3 Gaëlle Angenard, Aude Merdrignac, Corentin Louis, Julien Edeline, Cédric Coulouarn\*

Inserm, Univ Rennes, Inra, Institut NuMeCan (Nutrition Metabolisms and Cancer), CHU Rennes, Centre de Lutte contre le Cancer Eugène Marquis, Rennes, France

### ARTICLE INFO

#### Article history:

Received 7 February 2019

Accepted 22 March 2019

Available online xxx

#### Keywords:

ANRIL

Cholangiocarcinoma

Long non-coding RNA

Prognosis

### ABSTRACT

Q4 **Background:** Intrahepatic cholangiocarcinoma (iCCA) is a deadly cancer worldwide associated with an increased incidence, limited therapeutic options and absence of reliable prognostic biomarkers. Long non-coding RNAs (lncRNA) emerge as relevant biomarkers in cancer being associated with tumor progression.

Q5 However, lncRNA have been poorly investigated in iCCA.

**Aim:** To identify lncRNA significantly associated with the survival of patients with iCCA after tumor resection for curative intent.

**Methods:** Gene expression profiling and Q-RT-PCR were performed from a cohort of 39 clinically well-annotated iCCA. Univariate Cox proportional hazards model with Wald Statistic was used to identify lncRNA significantly associated with overall (OS) and/or disease-free (DFS) survival.

**Results:** A signature made of 9 lncRNA was identified to be significantly ( $P < 0.05$ ) associated with OS and DFS, including 4 lncRNA (lnc-CDK9-1, XLOC\_12\_009441, CDKN2B-AS1, HOXC13-AS) highly expressed in poor prognosis iCCA and 5 lncRNA (lnc-CCHCR1-1, lnc-AF131215.3.1, lnc-CBLB-5, COL18A1-AS2, lnc-RELL2-1) highly expressed in better prognosis iCCA. We further validated CDKN2B-AS1 (ANRIL) as a poor prognosis biomarker, not only in iCCA, but also in hepatocellular carcinoma, kidney renal clear cell carcinoma and uterine corpus endometrial carcinoma.

**Conclusions:** We report a prognosis lncRNA signature in iCCA and the clinical relevance of CDKN2B-AS1 (ANRIL) overexpression in several cancers.

© 2019 Editrice Gastroenterologica Italiana S.r.l. Published by Elsevier Ltd. All rights reserved.

### 1. Introduction

Q8 Cholangiocarcinomas (CCA) comprise several types of tumors arising from the malignant transformation of cholangiocytes lining different part of the biliary tree. Based on the anatomical location, intrahepatic (iCCA), perihilar (pCCA) and distal (dCCA) CCA are recognized [1,2]. Each of these CCA subtypes exhibits specific biological and pathological features, e.g. in term of clinical presentation, risk factors, prognosis and therapeutic strategies [2]. In the liver, iCCA represents the second most common type of malignant primary tumor after hepatocellular carcinoma (HCC), encompassing 10% to 15% of cases. However, an increase in iCCA incidence and mortality has been observed worldwide over the last decades. Today, surgical resection still remains the best curative treatment strategy of CCA, although it is associated with a high risk of tumor

recurrence [1]. For patients with unresectable or metastatic CCA, mostly as a result of a late diagnosis, systemic chemotherapy (usually a gemcitabine and cisplatin combination) is proposed as a palliative treatment [1]. Recently, adjuvant chemotherapy was demonstrated effective in resected CCA [3]. However, defining the optimal population that could benefit from adjuvant chemotherapy is particularly important. From a clinical point of view, the identification of innovative biomarkers for early diagnosis, prognosis and response to therapies, may improve the management and the survival of patients with iCCA. Although carbohydrate antigen 19-9 (CA19-9) and carcinoembryonic antigen (CEA) levels may be elevated in some patients, there is no specific serum biomarkers for the diagnosis of iCCA. Several prognostic tissue biomarkers have been proposed based on genomic analyses. Notably, by combining laser capture microdissection and unsupervised gene expression profiling, we previously established clinically relevant signatures specific of the tumor microenvironment in iCCA [4]. Thus, an increased expression of osteopontin (OPN) and lysyl oxidase like 2 (LOXL2) in the stroma was identified as a significant prognostic factor associated with a reduced survival of patients after tumor resection [4,5].

\* Corresponding author at: Inserm, UMR.S 1241, CHU Pontchaillou, 2 rue Henri Le Guilloux, Rennes F-35003, France.  
E-mail address: cedric.coulouarn@inserm.fr (C. Coulouarn).

More recently, we identified a novel long non-coding RNA (lncRNA) up-regulated by the transforming growth factor beta (TGF $\beta$ ) in human iCCA and associated with an inflammatory microenvironment, indicating that lncRNAs are also actively involved in iCCA carcinogenesis [6].

LncRNAs belong to an emerging class of regulatory RNAs that play critical roles in modulating a large variety of biological processes and cell signaling pathways. Accordingly, altered lncRNA expression has been reported in several cancers, including CCA [7]. Recent meta-analyses of The Cancer Genome Atlas (TCGA) database identified differentially expressed lncRNA in CCA (e.g. LINC00313, NEXN-AS1, COL18A1-AS1, HULC), the expression of some of them being significantly associated with overall survival (OS) of patients [8,9]. Mechanistically, co-expression network analysis of coding and non-coding RNA in resected CCA tumors identified lncRNA (e.g. APOC1P1, PVT1) possibly regulating inflammation and oxidative stress in malignant cholangiocytes [10,11]. Notably, pvt1 oncogene (PVT1) was shown to promote cell proliferation and migration by epigenetically silencing angiopoietin like 4 (ANGPTL4), a tumor suppressor gene candidate [12]. Cyclin dependent kinase inhibitor 1A (CDKN1A), another well-described tumor suppressor gene, was shown to be epigenetically silenced in CCA through the interaction of small nucleolar RNA host gene 1 (SNHG1) lncRNA with enhancer of zeste 2 (EZH2), the catalytic subunit of the polycomb repressive complex 2 (PRC2) [13]. Nuclear paraspeckle assembly transcript 1 (NEAT1) lncRNA may interact with EZH2 as well to repress the expression of E-cadherin (CDH1), thus promoting epithelial-to-mesenchymal transition (EMT) and metastasis [14]. Accordingly, an increased expression of SNHG1 and NEAT1 has been associated with aggressive tumorigenesis features in CCA [13,14]. NEAT1 has been also reported to contribute to gemcitabine sensitivity [15]. Conversely, lncRNA may positively affect the expression of oncogenic regulators, either directly or indirectly. Thus, epigenetically-induced lncRNA-1 (EPIC1) was reported to promote CCA cell growth and cancer progression by physically

interacting with MYC oncogene and possibly acting as a guide to direct MYC onto its target genes involved in cell cycle progression [16]. Interestingly, LINC01296 lncRNA was demonstrated to stabilize MYCN oncogene by sponging microRNA-5095, which naturally targets MYCN mRNA for degradation [17]. Urothelial cancer associated 1 (UCA1) lncRNA was reported to promote CCA formation and progression by activating a proliferative AKT/GSK-3 $\beta$ /CCND1 axis and by inducing EMT, migration and invasion [18]. Metastasis associated lung adenocarcinoma transcript 1 (MALAT1), a lncRNA induced in several cancers, promotes cell proliferation and invasion of CCA cells by activating the PI3K/AKT pathway as well [19]. While interesting mechanisms of lncRNA action have been elegantly described in CCA carcinogenesis, reports on their clinical relevance are scarce. The expression of few individual lncRNA (e.g. CRNDE, UCA1, TUG1) was reported to correlate with clinical progression (e.g. tumor grade, lymph node metastasis, TNM stage) and was identified as risk factors for an unfavorable overall survival (OS) in iCCA [16,18,20–23]. Circulating lncRNAs, including prostate cancer associated transcript 1 (PCAT1) and MALAT1, have been also reported in the plasma of patients with pCCA [24]. However, besides individual lncRNA, there is no exhaustive report on the clinical relevance of lncRNA expression as prognostic factors in iCCA so far [7,23]. Thus, this study was specifically designed to establish an unsupervised robust signature of lncRNA predictive of overall (OS) and/or disease-free (DFS) survival, by using pan-genomic microarrays and a cohort of clinically well-annotated iCCA.

## 2. Methods

### 2.1. Human iCCA samples

A cohort of 39 patients with iCCA was studied. Freshly frozen tumor samples were obtained through the French liver cancer biobanks network – INCa (BB-0033-00085). These patients underwent liver tumor resection for curative intent from January 2007 to July 2014. None of the patient underwent liver transplantation. Six patients underwent chemo- and/or radio-therapy prior surgery. For all cases, iCCA diagnosis was confirmed by a pathological examination. Tissue sections were evaluated after hematoxylin-eosin and Sirius Red staining (SI Fig. 1 in Supplementary material). Written informed consent was obtained from each patient included in the study. The study protocol conforms to the ethical guidelines of the 1975 Declaration of Helsinki (6th revision, 2008), as reflected in a priori approval by the local institution's human research committee and the institutional review board of Inserm (IRB00003888, IORG0003254). Clinical and pathological features of patients are reported in Table 1.

### 2.2. Gene expression profiling

Total RNA was extracted from tumor tissue sections and purified with a miRNAeasy kit (QIAGEN, Courtaboeuf, France). Genome-wide expression profiling was performed using the low-input QuickAmp labeling kit and human SurePrint G3 8 × 60 K pan-genomic microarrays (Agilent Technologies, Santa Clara, USA). Gene expression data were processed using Feature Extraction and GeneSpring softwares (Agilent Technologies), as previously described [6]. Clustering analysis was performed using Gene Cluster and TreeView softwares [25].

### 2.3. Q-RT-PCR

Quantitative-RT-PCR was performed by using a SYBR Green master mix (Applied Biosystems, Carlsbad, CA) as previously described [6]. A mixture of oligo-dT (250 ng) and random hexamers (100 ng) was used to prime the reverse transcription of

**Table 1**  
Clinical and pathological features of iCCA patients.

Clinical and pathological features	n = 39
Age (years, mean ± SD)	61 ± 14
Gender (male/female)	27/12
BMI	26 ± 3
Tobacco use	18 (46%)
Diabetes	7 (18%)
Etiology	
HBV or HCV infection	5 (13%)
Alcohol	3 (8%)
Hemochromatosis	1 (3%)
Primary biliary cirrhosis	1 (3%)
Histologically normal liver	3 (8%)
Association of factors	6 (15%)
Undetermined	20 (51%)
Metavir fibrosis score (F0/F1/F2/F3/F4/na)	7/6/6/4/6/10
Cirrhosis	6 (15%)
Steatosis	21 (54%)
Tumor size (mm, mean ± SD)	63 ± 27
Tumor ≥ 50 mm	27 (69%)
OMS differentiation grade	
Well-differentiated	15 (38%)
Moderately-differentiated	17 (44%)
Poorly-differentiated	7 (18%)
Satellite nodules > 1	19 (49%)
Tumor necrosis	16 (41%)
Microvascular tumor invasion	20 (51%)
Portal invasion	6 (15%)
Biliary tract invasion	10 (26%)
Perineural invasion	15 (38%)
Capsular invasion	8 (21%)
Lymph nodes invasion	11 (28%)
Extrahepatic tissue invasion	10 (26%)

Please cite this article in press as: Angenard G, et al. Expression of long non-coding RNA ANRIL predicts a poor prognosis in intrahepatic cholangiocarcinoma. Dig Liver Dis (2019), <https://doi.org/10.1016/j.dld.2019.03.019>

**Table 2**  
lncRNA signature predictive of overall (OS) and disease-free (DFS) survival.

Probe ID	Gene	Cytoband	OS		DFS	
			HR <sup>a</sup>	p-value <sup>b</sup>	HR <sup>a</sup>	p-Value <sup>b</sup>
<b>lncRNA up-regulated in poor prognosis iCCA</b>						
A.21.P0006229	lnc-CDK9-1	hs 9q34.11	3.83	0.007	3.65	0.03
A.21.P0012328	XLOC_12_009441	hs 22q11.1	1.99	0.018	2.01	0.01
A.19.P00322815	CDKN2B-AS1	hs 9p21.3	1.86	0.008	2.06	0.002
A.22.P00019478	HOXC13-AS	hs 12q13.13	1.83	0.047	1.75	0.048
A.21.P0014397	RALY-AS1	hs 20q11.22	24.36	0.002	ns	
A.22.P00018189	lnc-ZNF609-1	hs 15q22.31	3.39	0.036	ns	
A.22.P00001518	LOC101929064	hs 4q21.3	3.23	0.051	ns	
A.23.P431569	LOC100049716	hs 12p13.33	2.12	0.004	ns	
A.21.P0010648	XLOC_12_001086	hs 1q21.1	2.03	0.044	ns	
A.32.P850562	ZNF337-AS1	hs 20p11.1	1.88	0.022	ns	
A.21.P0004202	lnc-C5orf38-1	hs 5p15.33			3.13	0.009
A.21.P0009376	lnc-NLGN2-1	hs 17p13.1			2.82	0.005
<b>lncRNA down-regulated in poor prognosis iCCA</b>						
A.21.P0005160	lnc-CCHCR1-1	hs 6p21.33	0.72	0.001	0.71	0.005
A.24.P312325	lnc-AF131215.3.1	hs 8p23.1	0.65	0.005	0.56	0
A.21.P0003146	lnc-CBLB-5	hs 3q13.12	0.6	0.02	0.56	0.024
A.22.P00025222	COL18A1-AS2	hs 21q22.3	0.55	0.002	0.55	0.001
A.22.P00012968	lnc-RELL2-1	hs 5q31.3	0.39	0.003	0.38	0.001
A.21.P0005161	lnc-CCHCR1-1	hs 6p21.33	0.59	0.001	ns	
A.22.P00004717	lnc-CTDSP2-2	hs 15q21.1		ns	0.37	0.034
A.22.P00014082	HAND2-AS1	hs 4q34.1		ns	0.46	0.049
A.22.P00015084	lnc-SNURF-3	hs 15q11.2		ns	0.49	0.014
A.21.P0008621	lnc-EIF2AK4-2	hs 15q15.1		ns	0.64	0.032
A.22.P00010275	lnc-MTMR9-1	hs 8p23.1		ns	0.68	0.04
A.22.P00017999	lnc-ZNF132-1	hs 19q13.43		ns	0.71	0.046

<sup>a</sup> Hazard ratio.<sup>b</sup> p-Value, as determined by a log-rank test; ns: not significant.

149 1 µg total RNA (Superscript III RT, Invitrogen, Carlsbad, CA). Quantitative analysis of PCR data was conducted with the  $2^{-\Delta\Delta Ct}$  150 method using actin beta (ACTB) Ct values for normalization. 151 Melting analysis was conducted to validate the specificity of 152 PCR products. PCR analysis was performed using the following 153 primers: CDKN2B-AS1-Forward, 5'-TCCAGTGCAAGTATGGCTGT- 154 3'; CDKN2B-AS1-Reverse, 5'-TAGCAGAAAGCTGCAAAGGC-3'; 155 ACTB-Forward, 5'-GGACTTCGAGCAAGAGATGG-3'; ACTB-Reverse, 156 5'-AGCACTGTTGGCGTACAG-3'.

157 nодules were detected in 49% patients and lymph nodes invasion 158 in 28% patients.

### 3.2. A lncRNA signature predictive of OS and DFS

159 Gene expression profiling was performed on RNA extracted 160 from the 39 iCCA cases. In order to identify innovative prognostic 161 biomarkers, statistical analysis was restricted to the differential 162 expression of lncRNAs. By using an univariate Cox proportional 163 hazards model with Wald Statistic, 16 and 17 lncRNAs were 164 identified to be significantly ( $P < 0.05$ ) associated with OS and DFS, 165 respectively (Fig. 1A and Table 2). Among those, 9 were 166 predictive of both OS and DFS, including 4 up- and 5 down-regulated 167 lncRNA in poor prognosis iCCA (Fig. 1A and Table 2). CDKN2B-AS1 168 and COL18A1-AS2 are two examples of such prognostic lncRNAs. 169 Indeed, CDKN2B-AS1 median expression was able to segregate iCCA 170 tumors into two groups, where a high expression of CDKN2B-AS1 171 was significantly associated with a reduced OS ( $P = 0.008$ ) 172 and DFS ( $P = 0.002$ ). Conversely, highly COL18A1-AS2 expressing 173 iCCA tumors were significantly associated with a better prognosis 174 (Fig. 1B). In addition, clustering analysis of 39 iCCA tumors based 175 on the expression of the 9 lncRNA expression signature identified 176 two clusters: cluster A and cluster B (Fig. 1C). Validating this 177 prognostic lncRNA signature, patients included in clusters A and B 178 exhibited a significant difference in OS and DFS, as demonstrated 179 by Kaplan–Meier plot analysis and log-rank testing (Fig. 1D). Cluster 180 A was also associated with a significantly higher number of 181 poorly-differentiated iCCA (SI Table 1 in Supplementary material).

### 3.3. CDKN2B-AS1 is a poor prognosis biomarker in cancer

182 Quantitative RT-PCR was performed to validate the microarray 183 data. We focused on CDKN2B-AS1 that exhibited a high variability 184 among the samples and the more robust statistical significance 185 (Fig. 1C and Table 2). Thus, from our initial cohort of 39 iCCA, 186 two groups were defined based on the expression of CDKN2B-AS1, 187

### 2.4. Statistical analysis

188 Statistical analysis of microarray data was as previously 189 described [26]. Notably, lncRNAs significantly associated with 190 OS and/or DFS were identified using an univariate Cox proportional 191 hazards model with Wald Statistic [26,27]. Up- and down-regulated 192 lncRNA were determined by the ratio of their expression in poor 193 versus better prognosis iCCA. A meta-analysis of RNA-sequencing 194 data generated by The Cancer Genome Atlas (TCGA) was also 195 performed to determine the clinical relevance of CDKN2B-AS1/ANRIL 196 expression in independent datasets. The Kaplan–Meier method 197 was used to estimate OS and DFS, and group differences were 198 analyzed with the log-rank test [4,5,28].

## 3. Results

### 3.1. Patient characteristics

199 Thirty nine patients (27 men) who underwent liver resection 200 with curative intent for iCCA were included in the profiling study 201 (Table 1). The median age was  $61 \pm 14$  years. Similar to our 202 previous cohort [5], 69% patients had a tumor with a size  $>5$  cm. The 203 cohort included 15 (38%) well-differentiated, 17 (44%) moderately- 204 differentiated, and 7 (18%) poorly-differentiated tumors. Satellite 205

Please cite this article in press as: Angenard G, et al. Expression of long non-coding RNA ANRIL predicts a poor prognosis in intrahepatic cholangiocarcinoma. Dig Liver Dis (2019), <https://doi.org/10.1016/j.dld.2019.03.019>

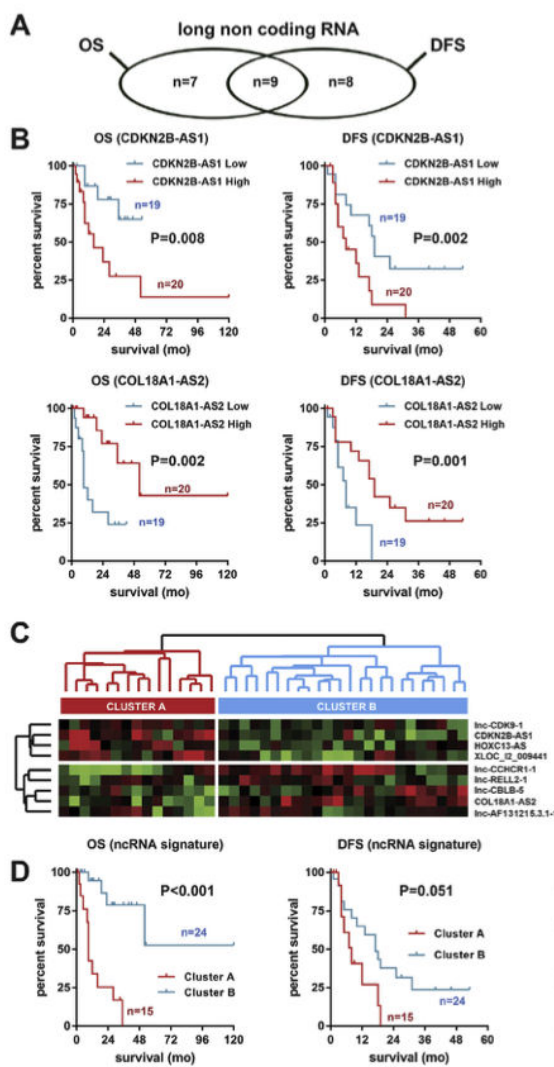


**Fig. 1.** Identification of a prognostic lncRNA signature in iCCA. Gene expression profiling of lncRNA was performed from 39 resected iCCA tumors. (A) Venn diagram analysis of lncRNA significantly ( $P < 0.05$ ) associated with overall (OS) and/or disease-free (DFS) survival. (B) Example of Kaplan–Meier plots for CDKN2B-AS1 and COL18A1-AS2 expression significantly associated with OS and DFS. (C) Clustering analysis of 39 iCCA samples based on the expression of the 9-lncRNA signature significantly associated with both OS and DFS. Two clusters, A and B, were identified. (D) Kaplan–Meier plots for iCCA samples from cluster A and cluster B.

including 15 highly expressing tumors and 15 tumors with low or no CDKN2B-AS1 expression (Fig. 2A). Validating our previous observation, a marked difference was observed in the OS of these two groups of patients (Fig. 2A). No significant association with other clinical and pathological variables was identified in our cohort of iCCA (SI Table 2 in Supplementary material). More interestingly, a high expression of CDKN2B-AS1 was shown to be significantly ( $P < 0.05$ ) associated with a reduced survival of patients with hepatocellular carcinoma, kidney renal clear cell carcinoma and uterine corpus endometrial carcinoma (Fig. 2B), identifying CDKN2B-AS1 as a poor prognosis biomarkers in several cancers.

#### 4. Discussion

CCA is a deadly cancer worldwide waiting for innovative biomarkers and therapeutic strategies to improve the survival of patients [1,2]. In iCCA, several clinical variables have been identified

as important prognostic factors after surgical resection for curative intent, including tumor size, pathological lymph node involvement and vascular invasion [1,29,30]. Omics approaches (e.g. genomics, proteomics, metabolomics) have been extensively used to screen for novel candidate serum, bile and tissue molecular biomarkers in iCCA [30]. As an example, by proteomic analysis, a high expression of SSP411 in the serum and/or the bile has been significantly associated with iCCA diagnosis [31]. Serum and bile CA 19-9 level has been also associated with lymph node metastasis and OS although the specificity and sensitivity was highly heterogeneous [30]. By focusing more specific molecular biomarkers in iCCA [30], we previously identified and validated specific mRNA and associated proteins, including OPN, LOXL2 and epithelial cell adhesion molecule (EPCAM), as independent prognostic tissue biomarkers associated with a reduced OS of patients with iCCA after tumor resection [4,5,28]. Here, we specifically focused on the expression of lncRNA and we identified a set of lncRNA predictive of OS ( $n = 16$ ) and/or DFS ( $n = 17$ ), among those 9 were predictive of both OS and DFS. Except for HAND2-AS1, HOXC13-AS, and CDKN2B-AS1, the identified lncRNA were poorly characterized. Our data indicated that HAND2-AS1 down-regulation in poor prognosis iCCA is predictive of DFS. Accordingly, HAND2-AS1 has been recently shown to inhibit cancer cell proliferation, migration, and invasion in esophageal squamous cell carcinoma and colorectal cancer by sponging oncogenic microRNA, including miR-21 [33,34]. HOXC13-AS (up-regulated in poor prognosis iCCA from our lncRNA signature) has been shown to positively affect cell proliferation and invasion in nasopharyngeal carcinoma by sponging miR-383-3p [35]. CDKN2B-AS1, also known as antisense non-coding RNA in the INK4 locus (ANRIL), was identified as a prognostic biomarker, not only in iCCA, but also in hepatocellular, kidney and uterine corpus carcinomas. Very promisingly, the low expressing group in iCCA showed a very high long term survival. In clinical context, one can question the need for adjuvant chemotherapy in a population with such high survival, potentially sparing toxicity for patients who do not require such therapy.

ANRIL is located at the CDKN2 A/B genomic locus on chromosome 9p21.3 in human [36]. Interestingly, this locus is associated with an increased risk of cancer and metabolic disease, including type 2 diabetes, obesity and cardiovascular diseases [37]. ANRIL expression and function have been extensively investigated in several cancers but not in iCCA [38]. Here, we demonstrated that ANRIL expression is associated with a dismal outcome. Although clinically relevant differences in the expression of ANRIL expression have been highlighted in iCCA tumor tissues in our study, it remains to be determined whether ANRIL is up-regulated in iCCA as compared to normal biliary epithelium, as it was previously reported in other cancers, including HCC [39]. Such an induction of ANRIL may suggest a key role in iCCA carcinogenesis. Indeed, gain and loss of function experiments in cancer cells demonstrated that ANRIL lncRNA favors cell proliferation and invasion. *In vivo*, ANRIL expression is associated with an increase of tumor size and growth, as well as invasive and metastatic phenotypes. Mechanistically, ANRIL was initially shown to promote cell proliferation and to inhibit apoptosis by epigenetically silencing the CDKN2 A/B genomic locus [40]. In non-small cell lung cancer ANRIL was reported to silence kruppel-like factor 2 (KLF2) and CDKN1 A/P21 expression as well [41]. In gastric cancer, the impact of ANRIL on proliferation and apoptosis was mediated by the epigenetic silencing of miR-99a and miR-449a, two miRNAs known to target mTOR and CDK6/E2F1 pathways

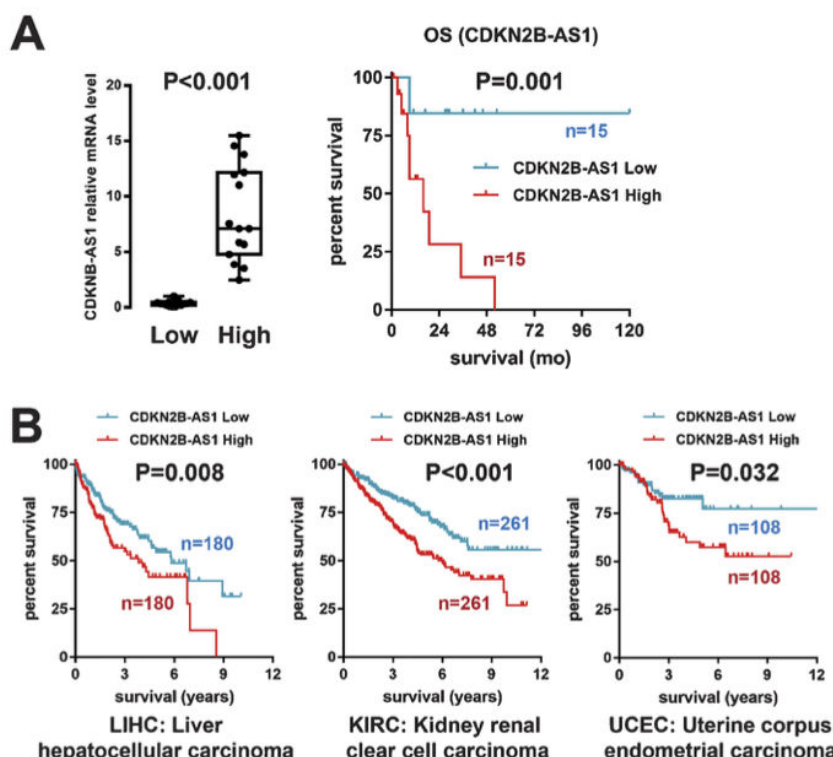


**Fig. 2.** CDKN2B-AS1 expression predicts a poor prognosis in several cancers. (A) Q-RT-PCR of CDKN2B-AS1 was performed in iCCA cases that were further ranked into low ( $n = 15$ ) and high ( $n = 15$ ) expressing tumors. Kaplan-Meier plots for iCCA classified into low vs. high CDKN2B-AS1 expressing tumors. (B) Kaplan-Meier plot analysis (OS) based on the expression of CDKN2B-AS1 in independent gene expression datasets from the TCGA consortium.

[42]. In ovarian [43] and bladder [44] cancers, ANRIL may induce BCL2 apoptosis regulator (BCL2) and repress CDKN2B/P15, BCL2 associated X, apoptosis regulator (BAX) and cleaved caspase-9, to promote cell cycle progression and inhibit apoptosis and senescence. In nasopharyngeal carcinoma, pro-tumorigenic features of ANRIL were associated with a glucose metabolism reprogramming and an induction of side-population stem-like cancer cells [45]. In thyroid cancer, ANRIL promotes tumor cell invasion and metastasis through TGF- $\beta$ /Smad signaling and EMT [46]. In HCC, sponging of liver enriched miR-122-5p by ANRIL induces cell proliferation, metastasis and invasion [47]. Interestingly, ANRIL was reported to contribute to paclitaxel resistance in lung cancer, partly through poly(ADP-ribose) polymerase (PARP) and BCL2 modulating mitochondrial pathway [48].

The clinical relevance of ANRIL expression has been evaluated in several types of cancers. Thus, a high ANRIL expression has been associated with TNM stage, advanced lymph node metastasis, tumor size, and was highlighted as an independent predictor of OS and/or DFS, particularly in nasopharyngeal [45], ovarian [43] or lung [41,49] cancers. Interestingly, it was recently reported that ANRIL was significantly up-regulated in lung cancer tissues and serum samples compared with normal controls, suggesting that ANRIL may serve as a relevant circulating lncRNA biomarker [50]. Given the significant association of ANRIL and prognosis factors, it would be interesting to evaluate its expression in body fluids, including serum, urine and/or bile. Another point of interest is to understand the mechanisms by which the expression of ANRIL is increased in poor prognosis tumors. External risk factors, including lifestyle, nutrition or environment, have been shown to influence the expression of lncRNA [51]. Thus, HOTAIR and MALAT1 have been the most studied lncRNA in the context of tobacco use in lung cancer [51]. However, in our analysis, no statistically significant

association was identified between the expression of ANRIL and lifestyle-associated factors (e.g. obesity, diabetes, tobacco, alcohol). Interestingly, ANRIL was shown to be transcriptionally induced by the cell cycle associated E2F1 transcription factor [42], notably in an ATM-dependent manner following DNA damage [52], suggesting a positive regulation in highly proliferative tumors. In addition, MYC oncogene was shown to positively regulate ANRIL expression in lung cancer [53]. Epigenetic regulation of ANRIL through promoter methylation has been also reported [54].

Altogether, these data suggest that ANRIL may represent not only a clinically relevant biomarker for cancer diagnosis, prognosis and response to treatment, but also an innovative therapeutic target due to the well described pro-tumorigenic features of this lncRNA.

#### Conflicts of interest

None declared.

#### Funding

This work was supported by Inserm, Université de Rennes 1, INCa, and ITMO Cancer AVIESAN (Alliance Nationale pour les Sciences de la Vie et de la Santé) dans le cadre du Plan cancer (Non-coding RNA in cancerology: fundamental to translational; [Grant C18007NS to CC]). CL is supported by a PhD fellowship from Université de Rennes 1.

#### Ethical statement

The study was approved by the institutional review board of Inserm (IRB00003888).

## Acknowledgements

The authors thank the core facilities of Université de Rennes 1, Biosit (US18, UMS 3480) and Biogenouest (CRB Santé BB-0033-00056, GEH and H2P2), and the French liver cancer biobanks network – Institut National du Cancer (INCa) BB-0033-00085, including Beaujon, Bordeaux, Mondor, Nantes, Paris-Sud and Rennes biobanks. CC and JE are members of the European Network for the Study of Cholangiocarcinoma (ENSCCA) and participate in the initiative COST Action EURO-CHOLANGIO-NET granted by the COST Association (CA18122).

## Appendix A. Supplementary data

Supplementary material related to this article can be found, in the online version, at doi:<https://doi.org/10.1016/j.dld.2019.03.019>.

## References

- Q9** [1] Banales JM, Cardinale V, Carpino G, et al. Expert consensus document: cholangiocarcinoma: current knowledge and future perspectives consensus statement from the European Network for the Study of Cholangiocarcinoma (ENS-CCA). *Nat Rev Gastroenterol Hepatol* 2016;13:261–80.
- [2] Rizvi S, Khan SA, Hallemeier CL, Kelley RK, Gores GJ. Cholangiocarcinoma - evolving concepts and therapeutic strategies. *Nat Rev Clin Oncol* 2018;15:95–111.
- [3] Primrose JNF, Fox R, Palmer DH, Prasad R, Mirza D, Anthoney DA. Adjuvant capecitabine for biliary tract cancer: the BILCAP randomized study. *J Clin Oncol* 2017;35:4006.
- [4] Sulpice L, Rayar M, Desille M, et al. Molecular profiling of stroma identifies osteopontin as an independent predictor of poor prognosis in intrahepatic cholangiocarcinoma. *Hepatology* 2013;58:1992–2000.
- [5] Bergeat D, Fautrel A, Turlin B, et al. Impact of stroma LOXL2 overexpression on the prognosis of intrahepatic cholangiocarcinoma. *J Surg Res* 2016;203:441–50.
- [6] Merdrignac A, Angenard G, Allain C, et al. A novel transforming growth factor beta-induced long noncoding RNA promotes an inflammatory microenvironment in human intrahepatic cholangiocarcinoma. *Hepatol Commun* 2018;2:254–69.
- [7] Wangyang Z, Daolin J, Yi X, et al. lncRNAs and Cholangiocarcinoma. *J Cancer* 2018;9:100–7.
- [8] Song W, Miao DL, Chen L. Comprehensive analysis of long noncoding RNA-associated competing endogenous RNA network in cholangiocarcinoma. *Biochem Biophys Res Commun* 2018;506:1004–12.
- Q11** [9] Wang X, Hu KB, Zhang YQ, Yang CJ, Yao HH. Comprehensive analysis of aberrantly expressed profiles of lncRNAs, miRNAs and mRNAs with associated ceRNA network in Cholangiocarcinoma. *Cancer Biomark* 2018.
- [10] Han BW, Ye H, Wei PP, et al. Global identification and characterization of lncRNAs that control inflammation in malignant cholangiocytes. *BMC Genomics* 2018;19:735.
- [11] Yang W, Li Y, Song X, Xu J, Xie J. Genome-wide analysis of long noncoding RNA and mRNA co-expression profile in intrahepatic cholangiocarcinoma tissue by RNA sequencing. *Oncotarget* 2017;8:26591–9.
- [12] Yu Y, Zhang M, Liu J, et al. Long non-coding RNA PVT1 promotes cell proliferation and migration by silencing ANGPTL4 expression in Cholangiocarcinoma. *Mol Ther Nucleic Acids* 2018;13:503–13.
- [13] Yu Y, Zhang M, Wang N, et al. Epigenetic silencing of tumor suppressor gene CDKN1A by oncogenic long non-coding RNA SNHG1 in cholangiocarcinoma. *Cell Death Dis* 2018;9:746.
- [14] Zhang C, Li JY, Tian FZ, et al. Long noncoding RNA NEAT1 promotes growth and metastasis of cholangiocarcinoma cells. *Oncol Res* 2018;26:879–88.
- [15] Parasramka M, Yan IK, Wang X, et al. BAP1 dependent expression of long non-coding RNA NEAT-1 contributes to sensitivity to gemcitabine in cholangiocarcinoma. *Mol Cancer* 2017;16:22.
- [16] Li Y, Cai Q, Li W, Feng Y, Yang L. Long non-coding RNA EPIC1 promotes cholangiocarcinoma cell growth. *Biochem Biophys Res Commun* 2018;504:654–9.
- [17] Zhang D, Li H, Xie J, et al. Long noncoding RNA LINC01296 promotes tumor growth and progression by sponging miR-5095 in human cholangiocarcinoma. *Int J Oncol* 2018;52:1777–86.
- [18] Xu Y, Yao Y, Leng K, et al. Long non-coding RNA UCA1 indicates an unfavorable prognosis and promotes tumorigenesis via regulating AKT/GSK-3beta signaling pathway in cholangiocarcinoma. *Oncotarget* 2017;8:96203–14.
- [19] Wang C, Mao ZP, Wang L, et al. Long non-coding RNA MALAT1 promotes cholangiocarcinoma cell proliferation and invasion by activating PI3K/Akt pathway. *Neoplasma* 2017;64:725–31.
- [20] Bai JG, Tang RF, Shang JF, Qi S, Yu CD, Sun C. Upregulation of long noncoding RNA CCAT2 indicates a poor prognosis and promotes proliferation and metastasis in intrahepatic cholangiocarcinoma. *Mol Med Rep* 2018;17:5328–35.
- [21] Xia XL, Xue D, Xiang TH, et al. Overexpression of long non-coding RNA CRNDE facilitates epithelial-mesenchymal transition and correlates with poor prognosis in intrahepatic cholangiocarcinoma. *Oncol Lett* 2018;15:4105–12.
- [22] Xu Y, Leng K, Li Z, et al. The prognostic potential and carcinogenesis of long non-coding RNA TUG1 in human cholangiocarcinoma. *Oncotarget* 2017;8:65823–35.
- [23] Zheng B, Jeong S, Zhu Y, Chen L, Xia Q, miRNA and lncRNA as biomarkers in cholangiocarcinoma(CCA). *Oncotarget* 2017;8:100819–30.
- [24] Shi J, Li X, Zhang F, et al. The Plasma LncRNA Acting as Fingerprint in Hilar Cholangiocarcinoma. *Cell Physiol Biochem* 2018;49:1694–702.
- [25] Allain C, Angenard G, Clement B, Coulouarn C. Integrative genomic analysis identifies the core transcriptional hallmarks of human hepatocellular carcinoma. *Cancer Res* 2016;76:6374–81.
- [26] Coulouarn C, Factor VM, Conner EA, Thorgerisson SS. Genomic modeling of tumor onset and progression in a mouse model of aggressive human liver cancer. *Carcinogenesis* 2011;32:1434–40.
- [27] Lee JS, Chu IS, Heo J, et al. Classification and prediction of survival in hepatocellular carcinoma by gene expression profiling. *Hepatology* 2004;40:667–76.
- [28] Sulpice L, Rayar M, Turlin B, et al. Epithelial cell adhesion molecule is a prognosis marker for intrahepatic cholangiocarcinoma. *J Surg Res* 2014;192:117–23.
- [29] Chan KM, Tsai CY, Yeh CN, et al. Characterization of intrahepatic cholangiocarcinoma after curative resection: outcome, prognostic factor, and recurrence. *BMC Gastroenterol* 2018;18:180.
- [30] Rahmehai-Azar AA, Weisbrod A, Dillhoff M, Schmidt C, Pawlik TM. Intrahepatic cholangiocarcinoma: molecular markers for diagnosis and prognosis. *Surg Oncol* 2017;26:125–37.
- [31] Shen J, Wang W, Wu J, et al. Comparative proteomic profiling of human bile reveals SSP411 as a novel biomarker of cholangiocarcinoma. *PLoS One* 2012;7:e47476.
- [32] Sulpice L, Desille M, Turlin B, et al. Gene expression profiling of the tumor microenvironment in human intrahepatic cholangiocarcinoma. *Genom Data* 2016;7:229–32.
- [33] Yan Y, Li S, Wang S, et al. Long noncoding RNA HAND2-AS1 inhibits cancer cell proliferation, migration, and invasion in esophagus squamous cell carcinoma by regulating microRNA-21. *J Cell Biochem* 2018.
- [34] Zhou J, Lin J, Zhang H, Zhu F, Xia R. lncRNA HAND2-AS1 sponging miR-1275 suppresses colorectal cancer progression by upregulating KLF14. *Biochem Biophys Res Commun* 2018;503:1848–53.
- [35] Gao C, Lu W, Lou W, Wang L, Xu Q. Long noncoding RNA HOXC13-AS positively affects cell proliferation and invasion in nasopharyngeal carcinoma via modulating miR-383-3p/HMGA2 axis. *J Cell Physiol* 2018.
- [36] Pasmant E, Laurendeau I, Heron D, Vidaud M, Vidaud D, Bieche I. Characterization of a germ-line deletion, including the entire INK4/ARF locus, in a melanoma-neural system tumor family: identification of ANRIL, an antisense noncoding RNA whose expression coclusters with ARF. *Cancer Res* 2007;67:3963–9.
- [37] Kong Y, Hsieh CH, Alonso LC. ANRIL: a lncRNA at the CDKN2A/B locus with roles in cancer and metabolic disease. *Front Endocrinol (Lausanne)* 2018;9:405.
- [38] Wang H, Liu Y, Zhong J, et al. Long noncoding RNA ANRIL as a novel biomarker of lymph node metastasis and prognosis in human cancer: a meta-analysis. *Oncotarget* 2018;9:14608–18.
- [39] Hua L, Wang CY, Yao KH, Chen JT, Zhang JJ, Ma WL. High expression of long non-coding RNA ANRIL is associated with poor prognosis in hepatocellular carcinoma. *Int J Clin Exp Pathol* 2015;8:3076–82.
- [40] Aguiló F, Zhou MM, Walsh MJ. Long noncoding RNA, polycomb, and the ghosts haunting INK4b-ARF-INK4a expression. *Cancer Res* 2011;71:5365–9.
- [41] Nie FQ, Sun M, Yang JS, et al. Long noncoding RNA ANRIL promotes non-small cell lung cancer cell proliferation and inhibits apoptosis by silencing KLF2 and P21 expression. *Mol Cancer Ther* 2015;14:268–77.
- [42] Zhang EB, Kong R, Yin DD, et al. Long noncoding RNA ANRIL indicates a poor prognosis of gastric cancer and promotes tumor growth by epigenetically silencing of miR-99a/miR-449a. *Oncotarget* 2014;5:2276–92.
- [43] Qiu JJ, Wang Y, Liu YL, Zhang Y, Ding JX, Hua KQ. The long non-coding RNA ANRIL promotes proliferation and cell cycle progression and inhibits apoptosis and senescence in epithelial ovarian cancer. *Oncotarget* 2016;7:32478–92.
- [44] Zhu H, Li X, Song Y, Zhang P, Xiao Y, Xing Y. Long non-coding RNA ANRIL is up-regulated in bladder cancer and regulates bladder cancer cell proliferation and apoptosis through the intrinsic pathway. *Biochem Biophys Res Commun* 2015;467:223–8.
- [45] Zou ZW, Ma C, Medoro L, et al. LncRNA ANRIL is up-regulated in nasopharyngeal carcinoma and promotes the cancer progression via increasing proliferation, reprogramming cell glucose metabolism and inducing side-population stem-like cancer cells. *Oncotarget* 2016;7:61741–54.
- [46] Zhao JJ, Hao S, Wang LL, et al. Long non-coding RNA ANRIL promotes the invasion and metastasis of thyroid cancer cells through TGF-beta/Smad signaling pathway. *Oncotarget* 2016;7:57903–18.
- [47] Ma J, Li T, Han X, Yuan H. Knockdown of LncRNA ANRIL suppresses cell proliferation, metastasis, and invasion via regulating miR-122-5p expression in hepatocellular carcinoma. *J Cancer Res Clin Oncol* 2018;144:205–14.
- [48] Xu R, Mao Y, Chen K, He W, Shi W, Han Y. The long noncoding RNA ANRIL acts as an oncogene and contributes to paclitaxel resistance of lung adenocarcinoma A549 cells. *Oncotarget* 2017;8:39177–84.
- [49] Lin L, Gu ZT, Chen WH, Cao KJ. Increased expression of the long non-coding RNA ANRIL promotes lung cancer cell metastasis and correlates with poor prognosis. *Diagn Pathol* 2015;10:14.

Please cite this article in press as: Angenard G, et al. Expression of long non-coding RNA ANRIL predicts a poor prognosis in intrahepatic cholangiocarcinoma. *Dig Liver Dis* (2019), <https://doi.org/10.1016/j.dld.2019.03.019>

- 508 [50] Xie Y, Zhang Y, Du L, et al. Circulating long noncoding RNA act as potential  
509 novel biomarkers for diagnosis and prognosis of non-small cell lung cancer.  
510 Mol Oncol 2018;12:648–58.
- 511 [51] Soares do Amaral N, Cruz EMN, et al. Noncoding RNA profiles in tobacco- and  
512 alcohol-associated diseases. Genes (Basel) 2016;8.
- 513 [52] Wan G, Mathur R, uthor>ZT Gu X, Chen WH, Cao KJ. Increased expression  
514 of the long non-coding RNA ANRIL promotes lung cancer cell metastasis and  
515 correlates with poor prognosis. Diagn Pathol 2015;10:14.
- 516 [50] Xie Y, Zhang Y, Du L, et al. Circulating long noncoding RNA act as potential  
517 novel biomarkers for diagnosis and prognosis of non-small cell lung cancer.  
Mol Oncol 2018;12:648–58.
- 518 [51] Soares do Amaral N, Cruz EMN, et al. Noncoding RNA profiles in tobacco- and  
519 alcohol-associated diseases. Genes (Basel) 2016;8.
- 520 [52] Wan G, Mathur R, Hu X, et al. Long non-coding RNA ANRIL (CDKN2B-AS) is  
521 induced by the ATM-E2F1 signaling pathway. Cell Signal 2013;25:1086–95.
- 522 [53] Lu Y, Zhou X, Xu L, Rong C, Shen C, Bian W. Long noncoding RNA ANRIL could  
523 be transactivated by c-Myc and promote tumor progression of non-small-cell  
524 lung cancer. Onco Targets Ther 2016;9:3077–84.
- 525 [54] Rodriguez C, Borgel J, Court F, Cathala G, Forne T, Piette J. CTCF is a DNA  
526 methylation-sensitive positive regulator of the INK/ARF locus. Biochem Biophys Res Commun 2010;392:129–34.

UNCORRECTED PROOF

Please cite this article in press as: Angenard G, et al. Expression of long non-coding RNA ANRIL predicts a poor prognosis in intrahepatic cholangiocarcinoma. Dig Liver Dis (2019), <https://doi.org/10.1016/j.dld.2019.03.019>

### *3. Article n°3*

Revue de la littérature en préparation

#### **«ARN longs non-codants et cholangiocarcinome »**

Cette revue de la littérature présente les ARNlnc identifiés dans le cholangiocarcinome selon leur rôle dans la cancérogénèse. Les ARNlnc identifiés jusqu'à présent sont tous surexprimés. Les mécanismes d'action de certains d'entre eux, e.g. NEAT1, par modulation épigénétique ont été mis en évidence. Des liens entre des ARNlnc et plusieurs voies de signalisation agissant sur la TEM et l'apoptose ont été décrits. Quelques variations génomiques d'ARNlnc ont été identifiées. Enfin, la pertinence clinique des ARNlnc comme biomarqueurs ou cibles thérapeutiques a été recherchée dans de nombreuses études.

Review

## **Long non-coding RNAs in cholangiocarcinoma**

Aude Merdrignac <sup>a</sup> and Cédric Coulouarn <sup>a</sup>

<sup>a</sup> Inserm, Univ Rennes, Inra, Institut NuMeCan (Nutrition Metabolisms and Cancer), UMR\_S 1241, CHU Rennes, Rennes, France

Correspondance to: Dr. Cédric Coulouarn, Inserm UMR\_S 1241, CHU Pontchaillou, 2 rue Henri Le Guilloux, F-35033 Rennes, France.

Phone +33 2 23 23 38 81 ; Fax +33 2 99 54 01 37

E-mail: cedric.coulouarn@inserm.fr

### **Acknowledgements**

Funding: This work was supported by Inserm, Université de Rennes 1, and ITMO Cancer AVIESAN (Alliance Nationale pour les Sciences de la Vie et de la Santé) dans le cadre du Plan cancer (Non-coding RNA in cancerology: fundamental to translational; [Grant C18007NS to CC]). CC is a member of the European Network for the Study of Cholangiocarcinoma (ENSCCA) and participates in the initiative COST Action EURO-CHOLANGIO-NET granted by the COST Association (CA18122).

## **Introduction**

Cholangiocarcinomas (CCA) are malignant tumors originating from the bile ducts and exhibiting cholangiocyte differentiation features. CCA are classified into three types according to the anatomical location: intrahepatic, perihilar and distal CCA. Intrahepatic CCA represent the second primary hepatic malignancy after hepatocellular carcinoma (HCC). CCA are aggressive and poor prognosis neoplasms with a median survival of 24 months after the initial diagnosis. Despite the recent identification of molecular alterations involved in CCA pathogenesis, there is no established molecular targeted therapy that significantly increases patient survival yet. Surgical resection remains the only potential curative treatment when feasible and performed at early stage of the disease <sup>1</sup>. Thus, a better understanding of molecular pathogenesis of CCA together with the identification of robust biomarkers and therapeutic targets is still necessary to improve the management of CCA.

Non coding RNAs (ncRNAs) belong to a heterogeneous class of RNA molecules. They account for the large majority of RNAs produced in human cells and tissues and are involved in numerous biological and pathological processes, including cancer onset and progression <sup>2</sup>. To date, ncRNAs are usually classified based on their size and structure and included microRNAs (miRNAs), long non coding RNAs (lncRNAs) and circular RNAs (circRNAs). miRNAs have been largely studied in CCA. For example, miR-21 is a well-known oncogenic miRNA overexpressed in CCA tumors and involved in the response to chemotherapy. miR-21 modulates gemcitabine-induced apoptosis by phosphatase and tensin homolog deleted on chromosome 10 (PTEN)-dependent activation of PI3K signaling <sup>3,4</sup>. Its overexpression in plasma makes it a potential circulating biomarker for CCA diagnosis and prognosis <sup>5</sup>. The first lncRNAs implicated in liver carcinogenesis were described in HCC (e.g. lncRNAs HULC, H19, MALAT1) and have been further studied in many others organs and pathologies <sup>6</sup>.

However, lncRNAs remain poorly studied in CCA. LncRNAs are defined by a size greater than 200 nucleotides and the lack of a functional open reading frame. They are transcribed

by RNA polymerase II and can be polyadenylated. Transcriptome analysis by deep sequencing and bioinformatics approaches have shown that the number of lncRNAs is greater than the one of protein coding mRNAs. Genomic location and organization of lncRNAs is complex and can be described according to their relationship to protein-coding genes: intergenic, sense, antisense, intronic and bidirectional<sup>7</sup>. Several lncRNAs have been functionally involved in pluripotency, differentiation, proliferation or cell survival although the function of most of the lncRNAs remains largely unknown. They show tissue specific expression and are tightly regulated at multiple levels, involving chromatin marks, independent promoters, regulation by transcription factors and splicing of multiple exons into a mature transcript. LncRNAs are located into the nucleus, the cytoplasm and could be also secreted, notably through extracellular vesicles (EVs). Based on their cellular location, lncRNA have been shown to modulate gene expression, notably by acting as chromatin remodeling factors or by interacting with transcription factors<sup>8</sup>. LncRNAs have been also reported to modulate post-transcriptional mRNA processing, protein function or localization and intercellular signaling through EVs<sup>9</sup>. In the cytoplasm, lncRNAs and circRNAs could interact directly with miRNA at post transcriptional level as competing endogenous RNA (ceRNA) (sponge for miRNAs)<sup>10,11</sup>.

This review presents lncRNAs identified in CCA according to their role in carcinogenesis.

### **LncRNAs and epigenetic modulation**

In the nucleus, lncRNAs could act at epigenetic level, mainly as scaffolding for chromatin or histone modifiers. Polycomb repressive complex 2 (PRC2) is a protein complex involved in methylating lysine 27 on histone H3 (H3K27). EZH2 is the catalytic subunit of PRC2. BAP1, as a chromatin modulator, can involve interactions with several methylation and deacetylase components and result in modulation of gene expression. LncRNA NEAT1, a lncRNA upregulated in CCA and a downstream-target of BAP1, is involved in responses to therapy as well as in maintenance of phenotypic characteristics such as the proliferative, migratory and invasive capabilities of CCA cells<sup>12</sup>. Exogenous silencing of NEAT1 expression using

siRNA in CCA cells reduced cell proliferation, migration, invasion and colony-forming abilities<sup>12</sup>. The effect of NEAT1 on modulating EZH2 expression further supports an effect of this lncRNA on tumor growth<sup>12</sup>. EZH2 recruitment by NEAT1 and subsequent involvement of the complex in the repression of E-cadherin promote CCA migration and invasion. Depletion of NEAT1 causes a reduction in EZH2 binding to the E-cadherin promoter and increases E-cadherin transcription. EZH2 suppresses gene expression through H3K27 trimethylation (H3K27me3). ChIP using an H3K27me3 antibody found decreased enrichment of H3K27me3 at the E-cadherin promoter. Taken together, these data suggest that EZH2 is recruited by NEAT1 to the promoter of E-cadherin and that together they repress E-cadherin expression<sup>13</sup>. NEAT1 can also regulate gene expression through its involvement in paraspeckle nuclear body formation<sup>14</sup>.

LncRNA SNHG1, upregulated in CCA, promotes CCA malignancy through a bond with EZH2, followed by repressing the expression of the CDKN1A. Knockdown of the SNHG1 lowered the binding of EZH2 as well as H3K27me3 levels at CDKN1A promoter, resulting in CDKN1A increased transcription and subsequent protein level, thus decreasing CCA growth through cell cycle inhibition<sup>15</sup>.

LncRNA SPRY4-IT1 might epigenetically repress underlying targets expression at transcriptional level. SPRY4-IT1, up regulated in CCA, exerts oncogenic properties partly dependent on repressing tumor suppressors KLF2 and LATS2 expression by scaffolding EZH2<sup>16</sup>. SPRY4-IT1 also functioned as a molecular sponge for miR-101-3p, antagonizing its ability to repress EZH2 protein translation<sup>16</sup>.

### **LncRNAs and deregulation of signaling pathways**

#### *Epithelial-mesenchymal transition, migration and invasion*

Several ncRNAs have been shown to play a key role in migration, invasion and metastatic process in CCA, notably by contributing to epithelial-mesenchymal transition (EMT). As

described above, lncRNA NEAT1 is one of the lncRNA involved in the repression of E-cadherin to promote CCA migration and invasion<sup>13</sup>. In vitro, the knockdown of numerous upregulated lncRNAs (e.g. HOTAIR, CRNDE, PANDAR, TUG1, CCAT1, CCAT2, SPRY4-IT1, UCA1) also reduced the expression of mesenchymal markers (Vimentin, N-cadherin), and increased the expression of epithelial marker E-cadherin, resulting in EMT reversion<sup>16-23</sup>. The oncogenic effects of lncRNAs through EMT are frequently mediated by acting as ceRNA (e.g. CCAT1, SPRY4-IT1, TUG1)<sup>16,21,24</sup>. As an example the oncogenic effects of CCAT1 in ICC cells are at least partly through inhibiting miR-152<sup>21</sup>. miR-152 inhibitor rescued the cell migration and invasion capability of ICC cells after CCAT1 knockdown. In CCAT1 silenced cells, miR-152 inhibitor increased the expression of N-cadherin and Vimentin, but reduced the expression of E-cadherin<sup>21</sup>.

Multiples lncRNAs have been identified as regulators or mediators of oncogenic pathways implicated in EMT. LncRNA MALAT1 has a key role in multiple human cancers and is upregulated in CCA. In hilar cholangiocarcinoma cells (HCCA), MALAT1 knockdown could significantly suppress proliferation, migration and invasion<sup>25</sup>. A positive correlation between MALAT1 expression and CXCR4 expression has been demonstrated in HCCA tissues. Acting as a ceRNA, MALAT1 regulates negatively miR-204 expression in HCCA cells. MALAT1 exerts its promotive functions in HCCA cell proliferation, migration and invasion by miR-204-dependent CXCR4 regulation<sup>25</sup>.

In 2016, Wang et al. analyzed 5 RNAseq datasets in order to identify lncRNA implicated in inflammation and oxidative stress in CCA. H19 and HULC were up-regulated after both short and long-term oxidative stress, implying their pivotal roles in inflammation promotion and CCA pathogenesis. H19 and HULC regulate cell migration and invasion by increasing pivotal inflammation cytokine IL-6 and chemokine receptor CXCR4 through sponging let-7a/let-7b and miR-372/miR-373, respectively<sup>26</sup>. Xu et al. confirmed in 2017 that H19 promotes cell migration and invasion. Knockdown of H19 decreased proliferation, increased apoptosis and reversed EMT in CCA cells<sup>27</sup>.

Transforming Growth Factor beta (TGF $\beta$ ) pathway is tightly implicated in EMT. TLINC is a lncRNA induced by TGF $\beta$  and upregulated in human intrahepatic CCA. Its long isoform is associated with a migratory phenotype in CCA cells and promotes an inflammatory microenvironment through upregulation of IL8 both in vitro and in resected human intrahepatic CCA<sup>28</sup>.

LncRNA PCAT1 is upregulated in extrahepatic cholangiocarcinoma and regulates its progression via the Wnt/ $\beta$ -catenin signaling pathway<sup>29</sup>. Downregulation of PCAT1 following transfection with silencing RNA reduced ECC cell growth, migration and invasion. PCAT1 acts as a ceRNA against miR-122. WNT1 mRNA levels were significantly reduced upon miR-122 mimic transfection, whereas transfection of a miR-122 inhibitor increased WNT1 mRNA level. In ECC cells, PCAT1 depletion dramatically decreased  $\beta$ -catenin levels, and increased GSK3 $\beta$  levels. In ECC cells co-transfected with miR-122 inhibitor and PCAT1 siRNA, protein level of  $\beta$ -catenin was restored and colony formation increased. PCAT1 regulates Wnt/ $\beta$ -catenin-signaling pathway and cell growth via miR-122<sup>29</sup>.

#### *Apoptosis and survival*

The majority of lncRNAs promote cell proliferation and downregulate cell apoptosis in CCA. Thus, knockdown of several upregulated lncRNAs, including HOTAIR, PANDAR, CCAT2, PCAT1 and TP73-AS1, increases the expression of caspase-3 and caspase-9<sup>17,19,22,30</sup>. LncRNAs PANDAR and TUG1 also restrained the expression of Bcl-2 and increased the expression of Bax in CCA cells<sup>19,20</sup>. However, the exact mechanisms are not described.

LncRNA UCA1, upregulated in CCA, affects EMT but also cell apoptosis and cell cycle in vitro in CCA cells through the activation of AKT/GSK-3 $\beta$ /CCND1 signaling pathway<sup>23</sup>. PI3K/AKT pathway is also activated by MALAT1 and SOX2-OT to promote cholangiocarcinoma cell proliferation and invasion<sup>31-33</sup>.

MAP kinase pathway has a critical role in regulating cell apoptosis and proliferation. LncRNA AFAP1-AS1 is upregulated in CCA. AFAP1-AS1 silencing resulted in a significant decrease in cell migration and invasion, cell proliferation and colony formation with downregulation of MMP2 and MMP9. Thus, AFAP1-AS1 silencing resulted in suppression of proliferation by arresting cell cycle via decreases of the protein levels of Cyclin D1 and c-Myc<sup>34,35</sup>. Both tumor volume and tumor weight were significantly decreased in mice xenografted with CCA cells with knocked down AFAP1-AS1. Tumors had also weaker Ki67 and PCNA expression. The tumor metastatic effects of AFAP1-AS1 may be mediated by the altered AFAP1 protein levels<sup>35</sup>.

LncRNAs could also alter gene expression by modulating transcription factors. Li et al. demonstrated by RNA immunoprecipitation that lncRNA EPIC1, upregulated in CCA, directly targets the transcription factor MYC in CCA cells. MYC is a key transcription factor regulating the expression of a wide range of genes involved in cell growth, proliferation and survival. Accordingly, MYC targets, including Cyclin A/D and CDK9, were downregulated in cells transfected with EPIC1 siRNA. MYC knockout also suppresses CCA cell growth, colony formation and apoptosis<sup>36</sup>.

LINC01296 was demonstrated to sponge miR-5095, which targets MYCN mRNA (MYCN proto-oncogene bHLH transcription factor) in human CCA. By inhibition of miR-5095, LINC01296 overexpression upregulated the expression of MYCN and promoted cell viability, migration and invasion in CCA cells<sup>37</sup>.

### **LncRNAs and genetic instability**

Genomic variations and/or alterations such as single nucleotide polymorphisms (SNPs), mutations and gene fusions referring to coding regions are common events in human carcinogenesis. LncRNAs which are less conserved across species are even more susceptible to genomic variations. Fujimoto et al. provided in 2016 a comprehensive whole-genome mutational analysis of 300 liver tumors from Japanese patients including CCA,

combined CCA-HCC and a majority of HCC<sup>38</sup>. The analysis revealed NEAT1 and MALAT1 to be prominently mutated among the non-coding genes in liver tumors. The IncRNAsNP is a database of SNPs in lncRNAs in human and mouse<sup>39</sup>. HULC and MALAT1 SNPs were found implicated in HCC carcinogenesis<sup>40</sup>. However, no lncRNA SNPs were reported so far in CCA carcinogenesis.

### Clinical relevance of lncRNA expression

#### *LncRNAs as biomarkers*

Multiple studies focused on evaluating miRNA abundance in tissues, serum and bile as diagnostic biomarkers in CCA<sup>41</sup>. Some of them were also identified as promising prognostic biomarkers in serum<sup>42,43</sup>. To date, all the variations reported in the expression of lncRNAs in CCA tissues are an overexpression compared to the adjacent non tumoral tissues. Thus, most of the lncRNAs are overexpressed in CCA cells and tissues and were identified as regulators of carcinogenesis processes (e.g. epigenetic deregulation, EMT, apoptosis). This overexpression is also frequently associated with a poor prognosis (H19, SOX2OT, CRNDE, UCA1, HOTAIR, GAPLINC)<sup>17,18,23,27,33,44</sup> and poor histologic features (CCAT1, AFAP1-AS1, PANDAR, TUG1, SPRY4-IT1, TP73-AS1, LINC01296, CPS1-IT1)<sup>16,20,21,24,30,34,35,37,45,46,47</sup>. Some lncRNAs are not yet relevant for prognosis and just potential diagnostic biomarker (e.g. NEAT1, SNHG1, PCAT1, EPIC1, TLINC, MALAT)<sup>13,15,29,36</sup>. However, ideal biomarkers are those obtained with non-invasive tests from body fluids, such as serum. In a recent meta-analysis, lncRNAs were found to be of high diagnostic value for HCC and their expression could potentially be used as auxiliary biomarkers in confirming HCC diagnosis (e.g. UCA1, MALAT1, SPRY4-IT1)<sup>48</sup>. A recent study found circulating PCAT1, MALAT1 and CPS1-IT1 significantly increased in plasma samples of HCCA patients<sup>49</sup>.

### *LncRNAs as therapeutic targets*

The capability of lncRNAs to regulate gene expression makes them potential targets for therapeutic research. However, actual drugs are unable to directly target lncRNAs. Promising strategies are in development including siRNA mediated silencing and lncRNA knockdown by antisense oligonucleotides to target oncogenic lncRNAs<sup>8</sup>. The ability of lncRNAs to sponge miRNAs could be also exploited to sequester oncogenic miRNAs. This mechanism has been used experimentally with an artificial lncRNA to overcome sorafenib resistance in HCC cells<sup>50</sup>. In CCA, few lncRNAs were found to influence current therapeutics. NEAT1 is a downstream target of BAP1, a frequently mutated chromatin modulator, and contributes to sensitivity to gemcitabine in CCA cells<sup>12</sup>. Inhibition of NEAT1 restored cells response to gemcitabine and could be a potential sensitizer.

### *New players in the field: circRNAs*

In our work, we highlighted circular isoforms of TLINC, a TGFβ induced lncRNA, in CCA tissues<sup>28</sup>. CircRNAs are particular ncRNAs mostly greater than 200 nucleotides characterized by covalently closed loop structures with neither 5' to 3' polarity nor polyadenylated tail<sup>51</sup>. This structure is formed by a back-splicing that ligates a downstream splice donor site reversely with an upstream splice acceptor site<sup>52</sup>. This circular structure renders circRNA particularly resistant to the action of RNases. Thus, circRNAs may represent interesting stable biomarkers in tissues or circulating in EVs such as exosomes detectable in serum<sup>56</sup>.

Some circRNA were already identified as potential molecular biomarker in CCA e.g. CircRNA Cdr1as and Hsa\_circ\_0001649<sup>53,54</sup>. Hsa\_circ\_0001649 is aberrantly downregulated in CCA tissues and cells, and its downregulation is associated with tumor size and differentiation grade in CCA<sup>54</sup>. Overexpressed circRNA Cdr1as may serve as a potential molecular biomarker to predict the aggressive tumor progression and worse prognosis for CCA patients

<sup>53</sup>. Circ2174, an intergenic circular RNA, can act as a sponge to regulate the expression of miR149 <sup>55</sup>.

## **Conclusion**

CCA are aggressive neoplasms resulting from a complex multifactorial carcinogenesis process. LncRNAs are implicated in a large variety of functions in cancer development. Their potential interactions with DNA, RNA and protein result in regulation at epigenetic, transcriptional and post-transcriptional levels. They act as regulators of key processes in cancer, including EMT, apoptosis, and proliferation. Thus, lncRNAs represent a promising class of biomarkers for diagnosis and prognosis of CCA, as well as interesting therapeutic targets.

**Table: List of lncRNAs induced in ICC**

LncRNA name	Mechanisms of action	Biological functions	Related pathways Targets	Biomarker	References	
NEAT1	epigenetic, mutation	proliferation, migration, invasion, EMT, resistance to therapeutic	EZH2, E-cadherin	diagnostic	12,13,14	
SNHG1	epigenetic, ceRNA	proliferation, invasion, cell cycle	TLR4/NF-kB EZH2, CDKN1A, miR-140	diagnostic	15	
SPRY4-IT1	epigenetic, ceRNA	proliferation, migration, invasion, EMT, apoptosis	EZH2, KLF2, LATS2, miR-101-3p	diagnostic	16	
HOTAIR		migration, invasion, EMT, apoptosis		diagnostic, prognostic	17	
CRNDE		proliferation, migration, invasion, EMT		diagnostic, prognostic	18	
PANDAR		proliferation, migration, invasion, EMT, apoptosis		diagnostic, prognostic	19,46	
TUG1	ceRNA	proliferation, migration, invasion, EMT, apoptosis	miR-145,Sirt3, GDH	diagnostic, prognostic	20,24	
CCAT1	ceRNA	migration, invasion, EMT	miR-152	diagnostic, prognostic	21,45	
CCAT2		migration, invasion, EMT, apoptosis		diagnostic	22	
UCA1		proliferation, migration, invasion, EMT, apoptosis, cell cycle	AKT/GSK-3béta/CCND1	diagnostic, prognostic	23	
MALAT1	mutation, ceRNA	proliferation, migration, invasion	CXCR4, PI3K/AKT	miR-204	diagnostic	25,31
H19	ceRNA	proliferation, migration, invasion,EMT, apoptosis	CXCR4/IL6	let-7a, miR-372	diagnostic, prognostic	26,27
HULC	ceRNA	migration, invasion	CXCR4/IL6	let-7b, miR-373	diagnostic	26,4
TLINC/CASC15		migration	TGFβ		diagnostic	28
PCAT1	ceRNA	proliferation, migration, invasion, apoptosis	Wnt/béta-catenin	miR-122	diagnostic	29
TP73-AS1		migration, invasion, EMT, apoptosis			diagnostic	30
SOX2-OT		proliferation, invasion	PI3K/AKT		diagnostic, prognostic	32,33
AFAP1-AS1		proliferation, migration, invasion, cell cyle	MAPK		diagnostic, prognostic	34,35
EPIC1	transcription factor	proliferation, apoptosis	MYC, cyclin A/D, CDK9	diagnostic	36	
LINC01296	ceRNA	migration, invasion	MYC, miR-5095	diagnostic, prognostic	37	
GAPLINC		proliferation, migration, invasion			diagnostic, prognostic	44
CPS1-IT1		proliferation, apoptosis			diagnostic, prognostic	47

Blanks: unknown

## References

1. Rizvi S, Gores GJ. Pathogenesis, Diagnosis, and Management of Cholangiocarcinoma. *Gastroenterology* 2013; 145: 1215–1229.
2. Esteller M. Non-coding RNAs in human disease. *Nat Rev Genet* 2011; 12: 861–874.
3. Selaru FM, Olaru AV, Kan T, et al. MicroRNA-21 is overexpressed in human cholangiocarcinoma and regulates programmed cell death 4 and tissue inhibitor of metalloproteinase 3. *Hepatol Baltim Md* 2009; 49: 1595.
4. Meng F, Henson R, Lang M, et al. Involvement of Human Micro-RNA in Growth and Response to Chemotherapy in Human Cholangiocarcinoma Cell Lines. *Gastroenterology* 2006; 130: 2113–2129.
5. Correa-Gallego C, Maddalo D, Doussot A, et al. Circulating Plasma Levels of MicroRNA-21 and MicroRNA-221 Are Potential Diagnostic Markers for Primary Intrahepatic Cholangiocarcinoma. *PLoS ONE*; 11. Epub ahead of print 29 September 2016. DOI: 10.1371/journal.pone.0163699.
6. Takahashi K, Yan I, Haga H, et al. Long non-coding RNA in liver diseases. *Hepatology* 2014.
7. He Y, Meng X-M, Huang C, et al. Long noncoding RNAs: Novel insights into hepatocellular carcinoma. *Cancer Lett* 2014; 344: 20–27.
8. Klingenberg M, Matsuda A, Diederichs S, et al. Non-coding RNA in hepatocellular carcinoma: Mechanisms, biomarkers and therapeutic targets. *J Hepatol* 2017; 67: 603–618.
9. Wang M, Zhou L, Yu F, et al. The functional roles of exosomal long non-coding RNAs in cancer. *Cell Mol Life Sci*. Epub ahead of print 25 January 2019. DOI: 10.1007/s00018-019-03018-3.
10. Salmena L, Poliseno L, Tay Y, et al. A ceRNA hypothesis: the Rosetta stone of a hidden RNA language? *Cell* 2011; 146: 353–358.
11. Kristensen LS, Hansen TB, Venø MT, et al. Circular RNAs in cancer: opportunities and challenges in the field. *Oncogene* 2018; 37: 555–565.
12. Parasramka M, Yan IK, Wang X, et al. BAP1 dependent expression of long non-coding RNA NEAT-1 contributes to sensitivity to gemcitabine in cholangiocarcinoma. *Mol Cancer* 2017; 16: 22.
13. Zhang C, Li J-Y, Tian F-Z, et al. Long Noncoding RNA NEAT1 Promotes Growth and Metastasis of Cholangiocarcinoma Cells. Epub ahead of print 2018. DOI: info:doi/10.3727/096504017X15024935181289.
14. Clemson CM, Hutchinson JN, Sara SA, et al. An Architectural Role for a Nuclear Noncoding RNA: NEAT1 RNA Is Essential for the Structure of Paraspeckles. *Mol Cell* 2009; 33: 717–726.
15. Yu Y, Zhang M, Wang N, et al. Epigenetic silencing of tumor suppressor gene CDKN1A by oncogenic long non-coding RNA SNHG1 in cholangiocarcinoma. *Cell Death Dis*; 9. Epub ahead of print 3 July 2018. DOI: 10.1038/s41419-018-0768-6.
16. Xu Y, Yao Y, Jiang X, et al. SP1-induced upregulation of lncRNA SPRY4-IT1 exerts oncogenic properties by scaffolding EZH2/LSD1/DNMT1 and sponging miR-101-3p in cholangiocarcinoma. *J Exp Clin Cancer Res CR*; 37. Epub ahead of print 11 April 2018. DOI: 10.1186/s13046-018-0747-x.

17. Qin W, Kang P, Xu Y, et al. Long non-coding RNA HOTAIR promotes tumorigenesis and forecasts a poor prognosis in cholangiocarcinoma. *Sci Rep*; 8. Epub ahead of print 15 August 2018. DOI: 10.1038/s41598-018-29737-4.
18. Xia X-L, Xue D, Xiang T-H, et al. Overexpression of long non-coding RNA CRNDE facilitates epithelial-mesenchymal transition and correlates with poor prognosis in intrahepatic cholangiocarcinoma. *Oncol Lett* 2018; 15: 4105–4112.
19. Xu Y, Jiang X, Cui Y. Upregulated long noncoding RNA PANDAR predicts an unfavorable prognosis and promotes tumorigenesis in cholangiocarcinoma. *OncoTargets Ther* 2017; 10: 2873–2883.
20. Xu Y, Leng K, Li Z, et al. The prognostic potential and carcinogenesis of long non-coding RNA TUG1 in human cholangiocarcinoma. *Oncotarget* 2017; 8: 65823–65835.
21. Zhang S, Xiao J, Chai Y, et al. LncRNA-CCAT1 Promotes Migration, Invasion, and EMT in Intrahepatic Cholangiocarcinoma Through Suppressing miR-152. *Dig Dis Sci* 2017; 62: 3050–3058.
22. Xu Y, Yao Y, Qin W, et al. Long non-coding RNA CCAT2 promotes cholangiocarcinoma cells migration and invasion by induction of epithelial-to-mesenchymal transition. *Biomed Pharmacother* 2018; 99: 121–127.
23. Xu Y, Yao Y, Leng K, et al. Long non-coding RNA UCA1 indicates an unfavorable prognosis and promotes tumorigenesis via regulating AKT/GSK-3 $\beta$  signaling pathway in cholangiocarcinoma. *Oncotarget* 2017; 8: 96203–96214.
24. Zeng B, Ye H, Chen J, et al. LncRNA TUG1 sponges miR-145 to promote cancer progression and regulate glutamine metabolism via Sirt3/GDH axis. *Oncotarget* 2017; 8: 113650–113661.
25. Tan X, Huang Z, Li X. Long Non-Coding RNA MALAT1 Interacts With miR-204 to Modulate Human Hilar Cholangiocarcinoma Proliferation, Migration, and Invasion by Targeting CXCR4. *J Cell Biochem*.
26. Wang W-T, Ye H, Wei P-P, et al. LncRNAs H19 and HULC, activated by oxidative stress, promote cell migration and invasion in cholangiocarcinoma through a ceRNA manner. *J Hematol Oncol Hematol Oncol* 2016; 9: 117.
27. Xu Y, Wang Z, Jiang X, et al. Overexpression of long noncoding RNA H19 indicates a poor prognosis for cholangiocarcinoma and promotes cell migration and invasion by affecting epithelial-mesenchymal transition. *Biomed Pharmacother* 2017; 92: 17–23.
28. Merdrignac A, Angenard G, Allain C, et al. A novel transforming growth factor beta-induced long noncoding RNA promotes an inflammatory microenvironment in human intrahepatic cholangiocarcinoma. *Hepatol Commun* 2018; 2: 254–269.
29. Zhang F, Wan M, Xu Y, et al. Long noncoding RNA PCAT1 regulates extrahepatic cholangiocarcinoma progression via the Wnt/ $\beta$ -catenin-signaling pathway. *Biomed Pharmacother* 2017; 94: 55–62.
30. Yao Y, Sun Y, Jiang Y, et al. Enhanced expression of lncRNA TP73-AS1 predicts adverse phenotypes for cholangiocarcinoma and exerts oncogenic properties in vitro and in vivo. *Biomed Pharmacother* 2018; 106: 260–266.
31. Wang C, Mao ZP, Wang L, et al. Long non-coding RNA MALAT1 promotes cholangiocarcinoma cell proliferation and invasion by activating PI3K/Akt pathway. *Neoplasma* 2017; 64: 725–731.

32. Wei C-X, Wong H, Xu F, et al. IRF4-induced upregulation of lncRNA SOX2-OT promotes cell proliferation and metastasis in cholangiocarcinoma by regulating SOX2 and PI3K/AKT signaling. *Eur Rev Med Pharmacol Sci* 2018; 22: 8169–8178.
33. Li Z, Li J, Ji D, et al. Overexpressed long noncoding RNA Sox2ot predicts poor prognosis for cholangiocarcinoma and promotes cell proliferation and invasion. *Gene* 2018; 645: 131–136.
34. Lu X, Zhou C, Li R, et al. Long Noncoding RNA AFAP1-AS1 Promoted Tumor Growth and Invasion in Cholangiocarcinoma. *Cell Physiol Biochem* 2017; 42: 222–230.
35. Shi X, Zhang H, Wang M, et al. LncRNA AFAP1-AS1 promotes growth and metastasis of cholangiocarcinoma cells. *Oncotarget* 2017; 8: 58394–58404.
36. Li Y, Cai Q, Li W, et al. Long non-coding RNA EPIC1 promotes cholangiocarcinoma cell growth. *Biochem Biophys Res Commun*. Epub ahead of print 8 September 2018. DOI: 10.1016/j.bbrc.2018.08.174.
37. Zhang D, Li H, Xie J, et al. Long noncoding RNA LINC01296 promotes tumor growth and progression by sponging miR-5095 in human cholangiocarcinoma. *Int J Oncol* 2018; 52: 1777–1786.
38. Fujimoto A, Furuta M, Totoki Y, et al. Whole-genome mutational landscape and characterization of noncoding and structural mutations in liver cancer. *Nat Genet* 2016; 48: 500–509.
39. Gong J, Liu W, Zhang J, et al. lncRNAsNP: a database of SNPs in lncRNAs and their potential functions in human and mouse. *Nucleic Acids Res* 2015; 43: D181–D186.
40. Liu Y, Pan S, Liu L, et al. A Genetic Variant in Long Non-Coding RNA HULC Contributes to Risk of HBV-Related Hepatocellular Carcinoma in a Chinese Population. *PLoS ONE* 2012; 7: e35145.
41. Zhou J, Liu Z, Yang S, et al. Identification of microRNAs as biomarkers for cholangiocarcinoma detection: A diagnostic meta-analysis. *Clin Res Hepatol Gastroenterol* 2017; 41: 156–162.
42. Wang L-J, Zhang K-L, Zhang N, et al. Serum miR-26a as a diagnostic and prognostic biomarker in cholangiocarcinoma. *Oncotarget* 2015; 6: 18631–18640.
43. Zheng B, Jeong S, Zhu Y, et al. miRNA and lncRNA as biomarkers in cholangiocarcinoma(CCA). *Oncotarget* 2017; 8: 100819–100830.
44. Wang X-P, Song J, Liu G-T, et al. Upregulation of gastric adenocarcinoma predictive long intergenic non-coding RNA promotes progression and predicts poor prognosis in perihilar cholangiocarcinoma. *Oncol Lett* 2018; 16: 3964–3972.
45. Jiang X-M, Li Z-L, Li J-L, et al. LncRNA CCAT1 as the unfavorable prognostic biomarker for cholangiocarcinoma. *Eur Rev Med Pharmacol Sci* 2017; 21: 1242–1247.
46. Xu Y, Jiang X, Cui Y. Upregulated long noncoding RNA PANDAR predicts an unfavorable prognosis and promotes tumorigenesis in cholangiocarcinoma. *OncoTargets and Therapy*. Epub ahead of print 6 June 2017. DOI: 10.2147/OTT.S137044.
47. Ma S-L, Li A-J, Hu Z-Y, et al. Co-expression of the carbamoyl-phosphate synthase 1 gene and its long non-coding RNA correlates with poor prognosis of patients with intrahepatic cholangiocarcinoma. *Mol Med Rep* 2015; 12: 7915–7926.
48. Zheng C, Hao H, Chen L, et al. Long noncoding RNAs as novel serum biomarkers for the diagnosis of hepatocellular carcinoma: a systematic review and meta-analysis. *Clin Transl Oncol* 2017; 19: 961–968.

49. Shi J, Li X, Zhang F, et al. The Plasma LncRNA Acting as Fingerprint in Hilar Cholangiocarcinoma. *Cell Physiol Biochem* 2018; 49: 1694–1702.
50. Tang S, Tan G, Jiang X, et al. An artificial lncRNA targeting multiple miRNAs overcomes sorafenib resistance in hepatocellular carcinoma cells. *Oncotarget* 2016; 7: 73257–73269.
51. Pan X, Xiong K. PredcircRNA: computational classification of circular RNA from other long non-coding RNA using hybrid features. *Mol Biosyst* 2015; 11: 2219–2226.
52. Chen L-L, Yang L. Regulation of circRNA biogenesis. *RNA Biol* 2015; 12: 381–388.
53. Jiang X-M, Li Z-L, Li J-L, et al. A novel prognostic biomarker for cholangiocarcinoma: circRNA Cdr1as. *Eur Rev Med Pharmacol Sci* 2018; 22: 365–371.
54. Xu Y, Yao Y, Zhong X, et al. Downregulated circular RNA hsa\_circ\_0001649 regulates proliferation, migration and invasion in cholangiocarcinoma cells. *Biochem Biophys Res Commun* 2018; 496: 455–461.
55. Moirangthem A, Wang X, Yan IK, et al. Network analyses-based identification of circular ribonucleic acid-related pathways in intrahepatic cholangiocarcinoma: Tumor Biol. Epub ahead of print 31 August 2018. DOI: 10.1177/1010428318795761.

#### 4. Communications

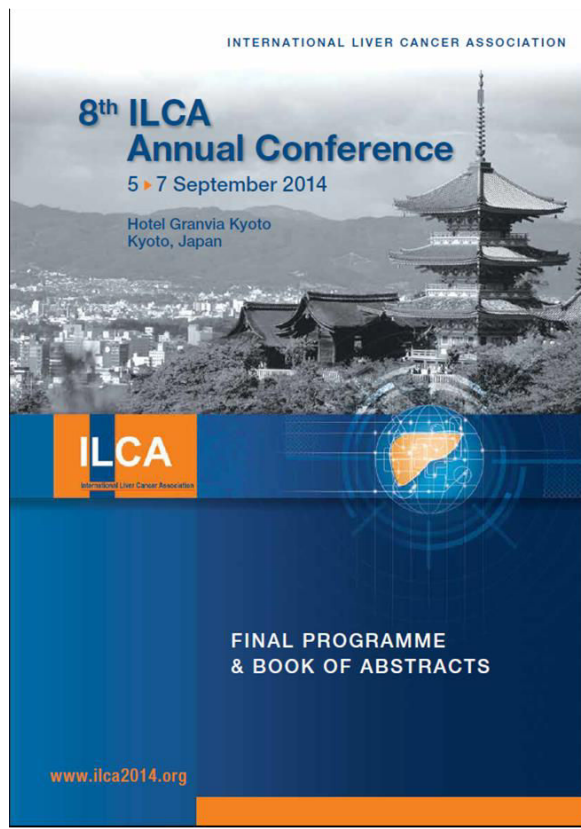
e-Poster au 8<sup>ème</sup> congrès annuel de l'International Liver Cancer Association (ILCA) en septembre 2014 à Kyoto, Japon

P-017

#### FUNCTIONAL CHARACTERIZATION OF T-LINC-1, A TGF-BETA-REGULATED LONG NON CODING RNA IN HUMAN INTRAHEPATIC CHOLANGIOPAPILLARY CARCINOMA

A. Merdignac <sup>1</sup>, G. Angenard <sup>1</sup>, D. Bergeat <sup>1</sup>, A. Fautrel <sup>1</sup>, B. Turlin <sup>1</sup>, P. Loyer <sup>1</sup>, L. Sulcipe <sup>1</sup>, C. Couloouarn <sup>1,2</sup>

<sup>1</sup>UMR991, Inserm, Rennes, France

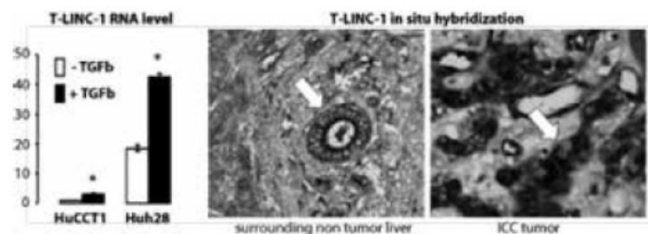


**Introduction:** Intrahepatic cholangiocarcinoma (ICC) is the second most common type of primary cancer in the liver after hepatocellular carcinoma (HCC). ICC is an aggressive malignancy with a poor prognosis and limited therapeutic options. The molecular mechanisms contributing to ICC pathogenesis are not well understood. Recently, we demonstrated that the overexpression of TGF-beta in the stroma of ICC was significantly correlated with a poor prognosis, suggesting that TGF-beta contributed to ICC progression. These results prompted us to investigate the role of the TGF-beta and associated target genes, including long non coding RNA, in ICC.

**Methods:** In vitro experiments were conducted in HuCCT1 and Huh28 ICC cell lines stimulated by TGF-beta. Gene expression profiling was done using Agilent pangenomic microarrays. The expression of relevant target genes was validated at the RNA and protein levels by RT-PCR and Western blot, respectively. Cellular localization of long non coding RNA was determined by *in situ* hybridization in human ICC. Functional analysis (e.g. proliferation and migration assays) was done following gain and loss of function experiments using expression plasmids and siRNA.

**Results:** TGF-beta associated gene signatures were established in HuCCT1 and Huh28 cell lines. The deregulation of known and new TGF-beta target genes was validated by RT-PCR, including T-LINC-1, a long non coding RNA strongly up-regulated by TGF-beta. In vitro, T-LINC-1 was found induced by TGF-beta not only in ICC cells but also in HCC cells and hepatic stellate cells. *In vivo*, gene profiling of microdissected ICC demonstrated that T-LINC-1 was up-regulated both in tumor cholangiocytes and in stromal cells. Cell fractionation and *in situ* hybridization demonstrated that T-LINC-1 was predominantly localized in the cytoplasm and suggested a role in the control of translation, as it was reported for other long non coding RNA (e.g. microRNA precursors or sponges). Interestingly, the predicted secondary structure of T-LINC-1 highlighted a hairpin-like sequence that may serve as a precursor for a microRNA known to target the cell cycle regulator P21. Preliminary results obtained following gain and loss of function demonstrated that T-LINC-1 greatly impacted the expression of P21.

#### Image:



**Conclusion:** The study identified the first TGF-beta regulated long non coding RNA which may control the cytostatic effects of TGF-beta in ICC. Thus, deregulation of T-LINC-1 may participate in the oncogenic switch of TGF-beta in cancer cells.

**Disclosure of Interest:** None Declared

Communication orale aux 75<sup>ème</sup> journées scientifiques de l'Association Française pour l'Etude du Foie (AEFEF) en septembre 2014 à Paris



### **Identification et caractérisation fonctionnelle de T-linc1, un ARN non codant de longue taille induit par le TGF-béta dans le cholangiocarcinome intrahépatique**

Merdrignac A. (1, 2) ; Angenard G. (2) ; Bergeat D. (1) ; Fautrel A. (2) ; Turlin B. (3) ; Loyer P. (2) ; Sulpice L. (1) ; Clément B. (2) ; Coulouam C. (2) (1) Service de chirurgie hépatobiliaire et digestive, C.H.U. Pontchaillou, Rennes ; (2) UMR 991, Inserm, Rennes ; (3) Service d'anatomie et cytologie pathologiques, C.H.U. Pontchaillou, Rennes

#### **Introduction**

Le cholangiocarcinome intrahépatique (CCI), seconde tumeur primitive hépatique après le carcinome hépatocellulaire (CHC), est caractérisé par un mauvais pronostic, des options thérapeutiques limitées et une mauvaise connaissance des mécanismes de癌érogenèse. Récemment, nous avons démontré qu'une surexpression de TGF-béta dans le stroma du CCI est corrélée à un mauvais pronostic (i.e. survie globale réduite). Dans ce contexte, l'objectif de notre travail est d'étudier le rôle de la voie TGF-béta et de ses gènes cibles dans la癌érogenèse du CCI.

#### **Matériaux et Méthodes**

Une analyse transcriptomique a été réalisée sur les lignées cellulaires HuCCT1 et Huh28 stimulées par le TGF-béta. L'expression des gènes cibles a été validée par RT-PCR et leur localisation cellulaire a été déterminée par hybridation *in situ* sur des coupes de CCI. L'analyse fonctionnelle a été réalisée après modulation de l'expression des gènes cibles par transfection de plasmides et de petits ARN interférents.

#### **Résultats**

Les signatures d'expression génique associées au TGF-béta ont été établies dans les lignées HuCCT1 et Huh28. La dérégulation de plusieurs gènes cibles (e.g. SMAD7, SNAI1) a été validée par RT-PCR, dont T-linc1, un ARN non codant de longue taille dont la fonction était complètement inconnue. *In vitro*, T-linc1 est induit par le TGF-béta dans les lignées de CCI mais également dans les lignées de CHC et les cellules étoilées hépatiques. *In vivo*, l'étude de CCI réséqués montre que T-linc1 est surexprimé dans les cholangiocytes tumoraux et le stroma. L'hybridation *in situ* révèle une prédominance de T-linc1 dans le cytoplasme, suggérant un rôle dans le contrôle de la traduction. De façon intéressante, la structure secondaire prédictive de T-linc1 met en évidence une séquence qui pourrait servir de précurseur à un microARN connu pour cibler le régulateur du cycle cellulaire P21. Les résultats obtenus après gain et perte de fonction montrent que la modulation de T-linc1 influence l'expression de P21.

#### **Conclusion**

Notre étude est la première à identifier un ARN non codant de longue taille dont l'expression est contrôlée par le TGF-béta et qui pourrait contrôler ses effets cytostatiques dans le CCI. Plus largement, la dérégulation de T-linc1 pourrait participer à orienter la voie du TGF-béta vers son versant oncogénique au cours de la progression tumorale.

Présentation à l'Académie Nationale de Chirurgie en 2015 suite à l'obtention du Prix parcours cancérologie 2014 du Master 2 Sciences Chirurgicales



« Identification et caractérisation de T-LINC 1, un ARN non codant de longue taille régulé par le TGF $\beta$  dans le cholangiocarcinome intrahépatique »

Le cholangiocarcinome intrahépatique (CCI) est caractérisé par un mauvais pronostic, des options thérapeutiques limitées et une mauvaise connaissance des mécanismes impliqués dans sa cancérogenèse. Il a été démontré récemment qu'une surexpression de TGF $\beta$  dans le stroma du CCI est corrélée à un mauvais pronostic, suggérant une implication de la voie TGF $\beta$  dans la progression du CCI.

L'objectif de notre travail était d'étudier le rôle de la voie TGF $\beta$  et de ses gènes cibles, dont les longs ARN non codants, dans la cancérogenèse du CCI.

Les signatures d'expression génique associées au TGF $\beta$  ont été établies dans des lignées cellulaires de CCI (HuCCT1 et Huh28). La dérégulation de plusieurs gènes cibles de la voie TGF $\beta$  a été validée par RT-PCR, dont T-LINC1, un long ARN non codant dont la fonction était complètement inconnue. *In vitro*, T-LINC1 est induit par le TGF $\beta$  dans les lignées de CCI. Il a été localisé dans le cytoplasme, mais également dans des corps nucléaires particuliers évocateurs de *paraspeckles*. L'analyse transcriptomique après modulation de T-LINC1 a montré que T-LINC1 pourrait être un régulateur de NEAT1 dans la réponse immunitaire médiée par l'IL8 en agissant au niveau des *paraspeckles*. *In vivo*, l'étude du profil d'expression de CCI humains a montré que T-LINC1 est surexprimé dans les cholangioocytes tumoraux.

##### 5. Publications de travaux cliniques

Gaignard E, Bergeat D, Courtin-Tanguy L, Rayar M, **Merdrignac A**, Robin F, Boudjema K, Beloeil H, Meunier B, Sulpice L. Is systematic nasogastric decompression after pancreaticoduodenectomy really necessary? Langenbecks Arch Surg. 2018 Aug;403(5):573-580.

Borel F, Ouassis M, **Merdrignac A**, Venara A, De Franco V, Sulpice L, Hamy A, Regenet N. Pancreatico-jejunostomy decreases post-operative pancreatic fistula incidence and severity after central pancreatectomy. ANZ J Surg. 2018 Jan;88(1-2):77-81.

**Merdrignac A**, Jeddou H, Houssel-Debry P, Flecher E, Rayar M, Boudjema K. Venous stent in liver transplant candidates: dodging the top tip traps. Liver Transplantation 2017 Jul;23(7):972-975.

Bergeat D, Rayar M, Mouchel Y, **Merdrignac A**, Meunier B, Lièvre A, Boudjema K, Sulpice L. Preoperative bevacizumab and surgery for colorectal liver metastases: a propensity score analysis. Langenbecks Arch Surg 2017;402:57-67.

**Merdrignac A**, Bergeat D, Rayar M, Harnoy Y, Turner K, Courtin-Tanguy L, Boudjema K, Meunier B, Sulpice L. Frey procedure combined with biliary diversion in chronic pancreatitis. Surgery 2016;160:1264-70.

**Merdrignac A**, Bergeat D, Levi Sandri GB, Agus M, Boudjema K, Sulpice L, Meunier B. Hepatic artery reinforcement after post pancreatectomy haemorrhage caused by pancreatitis. Gland Surg 2016;5:427-30.

Courtin-Tanguy L, **Merdrignac A**, Meunier B, Sulpice L. A weird polyp, 8 years after the Whipple procedure. Surgery 2016; in press.

Bergeat D, Fautrel A, Turlin B, **Merdrignac A**, Rayar M, Boudjema K, Coulouarn C, Sulpice L. Impact of stroma LOXL2 overexpression on the prognosis of intrahepatic cholangiocarcinoma. J Surg Res 2016;203:441-50.

Bergeat D, Rayar M, Beuzit L, Levi Sandri GB, Dagher J, **Merdrignac A**, Tanguy L, Boudjema K, Sulpice L, Meunier B. An unusual case of adrenocortical carcinoma with liver metastasis that occurred at 23 years after surgery. Hepatobiliary Surg Nutr 2016;5:265-8.

**Merdrignac A**, Proisy M, Fremond B, Habonimana E, Nardi N, Arnaud AP.

An Unusual Intussusception. J Pediatr 2016;175:240.

Courtin-Tanguy L, Rayar M, Bergeat D, **Merdrignac A**, Harnoy Y, Boudjema K, Meunier B, Sulpice L. The true prognosis of resected distal cholangiocarcinoma. J Surg Oncol 2016;113:575-80.

Bergeat D, Sulpice L, Rayar M, Edeline J, **Merdrignac A**, Meunier B, Boucher E, Boudjema K. Extended liver resections for intrahepatic cholangiocarcinoma: friend or foe? Surgery 2015;157:656-65.

Robert PE, Leux C, Ouaissi M, Miguet M, Paye F, **Merdrignac A**, Delpero JR, Schwarz L, Carrere N, Muscari F, Gayet B, Dussart D, Hamy A, Regenet N. Predictors of long-term survival following resection for ampullary carcinoma: a large retrospective French multicentric study. Pancreas 2014;43:692-7.

**Merdrignac A**, Sulpice L, Rayar M, Rohou T, Quehen E, Zamreek A, Boudjema K, Meunier B. Pancreatic head cancer in patients with chronic pancreatitis.

Hepatobiliary Pancreat Dis Int 2014;13:192-7.

#### **IV. Discussion**

Le CCI est une tumeur peu fréquente dont la cancérogénèse est complexe. Son diagnostic tardif amène peu de patients vers une résection chirurgicale. La quantité de matériel tumoral disponible permettant d'étudier ses altérations moléculaires est donc limitée. Cependant, de multiples variations génomiques et dérégulations de voies de signalisation ont pu être décrites. Ces données sont indispensables au développement de nouvelles thérapies ciblées. Le peu d'efficacité des thérapies ciblant VEGFR, EGFR, PDGFR ou BRAF encourage à orienter la recherche vers d'autres voies<sup>26</sup>.

##### *1. Signature TGFβ dans le CCI*

Le profil d'expression génique précédemment réalisé dans l'équipe avait montré une surexpression du TGFβ dans le stroma tumoral de CCI humains réséqués corrélée à un mauvais pronostic<sup>18</sup>. Une surexpression de TGFβ avait également déjà été montrée dans une signature spécifique du stroma du CCI<sup>24</sup>. Cependant, il n'existe pas de signature transcriptomique spécifique de l'impact du TGFβ sur les cellules de CCI. La validation de notre signature est montrée par la présence de gènes cibles connus de la voie TGFβ. L'analyse par enrichissement d'ensemble de gènes (GSEA) conforte sa spécificité avec l'association à des signatures liées au TGFβ, aux protéines SMAD2/3 et à la TEM.

Nous avons validé une activation endogène de la voie TGFβ dans la lignée cellulaire Huh28 concordant avec son phénotype mésenchymateux. Peu de lignées cellulaires de CCI existent (moins de 100 : d'origine humaine ou murine) en comparaison par exemple au CHC (plus de 200) (source Cellosaurus, <https://web.expasy.org/cellosaurus/>). Cette lignée pourrait permettre de tester des inhibiteurs de la voie TGFβ (i.e. efficacité et marqueurs de réponse).

De nouveaux gènes cibles du TGFβ codants et non-codants ont été identifiés. Les deux gènes KRT 14 et 17 codants pour des kératines de type I, protéines constituant les filaments intermédiaires du cytosquelette des cellules épithéliales, font partie des nouveaux gènes codants induits par le TGFβ dans notre signature. KRT14 et 17 sont exprimés dans les cancers épidermoïdes dont les cancers oraux<sup>112,113</sup>. KRT17 est également exprimé dans le

cholangiocarcinome, et les cancers du sein et de l'estomac où il est un marqueur pronostique<sup>114-116</sup>. Dans le cancer oral, la vimentine, qui est exprimée au cours de la TEM, régule la différentiation tumorale. Les niveaux d'expression de la vimentine et de la KRT14 sont corrélés et un niveau d'expression élevé vimentine-KRT14 est corrélé au pronostic<sup>113</sup>.

La présence de KRT14 et 17 augmentés dans d'autres cancers valide notre signature.

## 2. ARNlnc et CCI

Parmi les gènes non-codants, trois ARNlnc intergéniques sont présents dans notre signature TGFβ : LINC00340, LINC00312 et LINC00313. Ceux sont les premiers ARNlnc régulés par le TGFβ identifiés dans le CCA. LINC00312 est surexprimé dans plusieurs cancers, notamment pulmonaire où il agit comme régulateur du TGFβ via sa liaison au facteur de transcription YBX1<sup>117</sup>. Dans les cancers de la thyroïde et de la vessie, LINC00312 agit par l'intermédiaire du microARN miR-197-3p<sup>118,119</sup>. LINC00313, qui a été moins étudié, est également surexprimé dans les cancers du poumon et papillaires de la thyroïde<sup>120,121</sup>. Il a été récemment associé à un mauvais pronostic du CCI dans une analyse de réseaux d'ARNlnc agissant comme éponge à miARN à partir de la base TCGA<sup>87</sup>.

Notre travail s'est intéressé particulièrement à LINC00340 devant la présence de 2 sondes de microarrays surexprimées par le TGFβ. LINC00340 ou CASC15 (cancer susceptibility candidate 15) est un ARNlnc intergénique situé sur le chromosome 6p22. L'étude de CASC15 est rendue complexe par ses nombreuses isoformes. CASC15 comprend 12 exons et au moins 8 isoformes sont prédictes actuellement (source [www.ensembl.org](http://www.ensembl.org)). Un ARNlnc anti-sens NBAT1/CASC14 est également décrit sur le locus.

Dans le mélanome, Lessard et al ont mis en évidence plusieurs isoformes<sup>122</sup>. L'expression globale des différentes isoformes de CASC15 était corrélée à la progression et prédictive de la récidive et de la survie. L'inhibition globale de CASC15 était associée à un *switch* phénotypique entre prolifération et invasion évocateur de la TEM, mais une régulation par le TGFβ n'avait pas été montrée. CASC15 aurait un rôle pro-oncogénique dans le mélanome en agissant au niveau épigénétique sur EZH2<sup>123</sup>.

Deux isoformes ont été particulièrement étudiées dans le neuroblastome par Russell et al.<sup>124</sup>. L'isoforme courte CASC15-S a été identifiée comme isoforme fonctionnelle associée à un effet suppresseur de tumeur. La faible expression de CASC15-S est corrélée à un phénotype de neuroblastome agressif. Son inhibition augmente la prolifération et la migration cellulaire, alors que l'inhibition de l'isoforme longue n'a pas d'impact sur la viabilité cellulaire. Le rôle suppresseur de tumeur de CASC15 dans le neuroblastome a depuis été confirmé dans des études plus récentes pour les 2 isoformes et 3 *single nucleotide polymorphisms* (SNP)<sup>125,126</sup>. CASC15 et CASC14 agissent de façon synergique pour contrôler la progression du neuroblastome<sup>125</sup>.

Au vu de ces études contradictoires, il semble que CASC15 ait plusieurs fonctions dépendantes des organes et du stade tumoral. Au cours de nos travaux, nous avons renommé CASC15 par TLINC pour *TGFβ induced long intergenic non coding RNA*. Nous nous sommes intéressés aux deux isoformes courte et longue déjà connues dans le neuroblastome. L'isoforme courte a été mise en évidence dans la lignée HuH28 associée à un phénotype mésenchymateux et donc une action plutôt « tardive » du TGFβ. L'isoforme longue a été mise en évidence dans la lignée HuCCT1 associée à un phénotype épithelial et donc une action plutôt « précoce » du TGFβ. Ces résultats suggèrent des fonctions différentes de TLINC par le biais de plusieurs isoformes selon le contexte cellulaire en réponse à l'activation de la voie TGFβ.

L'étude fonctionnelle a montré une tendance à l'augmentation de la migration cellulaire après surexpression de TLINC. L'analyse transcriptomique a montré une surexpression de nombreux gènes impliqués dans la réponse inflammatoire, dont IL8, après surexpression de TLINC dans la lignée HUCCT1. Ces résultats ont été confirmés par la GSEA. La surexpression d'IL8 dans le groupe de tumeurs présentant une expression forte de TLINC confirme ce rôle dans la réponse inflammatoire. Ces résultats permettent d'émettre l'hypothèse d'un rôle de TLINC dans le remodelage d'un microenvironnement inflammatoire impliqué dans la cancérogénèse.

La présence de TLINC dans les cholangiocytes tumoraux et dans le stroma tumoral confirme un rôle à différents niveaux transcriptionnel et post-transcriptionnel. L'analyse transcriptomique de la lignée HuCCT1 après surexpression de TLINC a notamment montré l'ARNlnc NEAT1 parmi les gènes surexprimés. NEAT1 est essentiel à la formation de structures nucléaires particulières, les *paraspeckles*<sup>127</sup>. NEAT1 régule l'expression d'IL8 au cours de la réponse immunitaire aux virus en se liant à un répresseur d'IL8 dans le noyau<sup>128</sup>. Ces résultats supposent que TLINC pourrait réguler l'expression d'IL8 en se liant à NEAT1 dans le noyau où il aurait également une action au niveau épigénétique. NEAT1 est déjà connu pour être co-régulé avec MALAT1, un autre ARNlnc dans des cellules d'adénocarcinome du sein humain<sup>129</sup>. NEAT1 et MALAT1 sont tous les 2 surexprimés dans le cholangiocarcinome humain et représentent les ARNlnc les plus mutés dans les tumeurs hépatiques<sup>130</sup>. De multiples mécanismes d'action pour un même ARNlnc ont déjà été montrés pour plusieurs ARNlnc dans le CCI. Par exemple, SPRY4-IT1 a un rôle dans la régulation épigénétique mais agit également dans le cytoplasme comme éponge pour miR-101-3p<sup>131</sup>.

CASC15 a été identifié dans plusieurs autres cancers mais sans étude des différentes isoformes. Dans le cancer gastrique, l'expression de CASC15 est corrélée à un mauvais pronostic. In vitro, la surexpression de CASC15 induit la TEM. CASC15 agit à plusieurs niveaux, dans le noyau en diminuant l'expression de CDKN1A par une régulation épigénétique au niveau de EZH2, et dans le cytoplasme comme éponge à miR-33a-5p<sup>132</sup>. Dans le CHC, CASC15 a un rôle pro-oncogénique lié à la TEM. Son expression est corrélée à un mauvais pronostic<sup>133</sup>. CASC15 est également surexprimé dans le cancer du côlon. Il régule la progression tumorale par l'intermédiaire de miR-4310 et la voie Wnt/β caténine<sup>134</sup>. Ce lien avec la TEM dans plusieurs cancers renforcent nos résultats montrant la régulation de CASC15 par le TGFβ.

L'identification croissante de nouveaux ARN non-codants montre que la régulation de l'expression des gènes est plus complexe que celle imaginée auparavant. De multiples réseaux moléculaires comprenant des ARNlnc, des miARN et des ARNcirc interviennent

dans la régulation des voies de signalisation. Ceci complique la compréhension des mécanismes de cancérogénèse mais ouvre également de nouvelles possibilités thérapeutiques.

Perspectives : L'étude de LINC00312 et LINC00313, les deux ARNlnc régulés par le TGF $\beta$  dans notre signature, vont être étudiés dans l'équipe. Des travaux préliminaires ont clairement permis de valider l'induction de LINC00312 et LINC00313 par le TGF $\beta$  (voie canonique SMAD dépendante) (figure 20).

#### Expression de LINC00312 et LINC00313 après inhibition de SMAD3 et SMAD4 +/-TGF $\beta$ dans les cellules HUCCT1

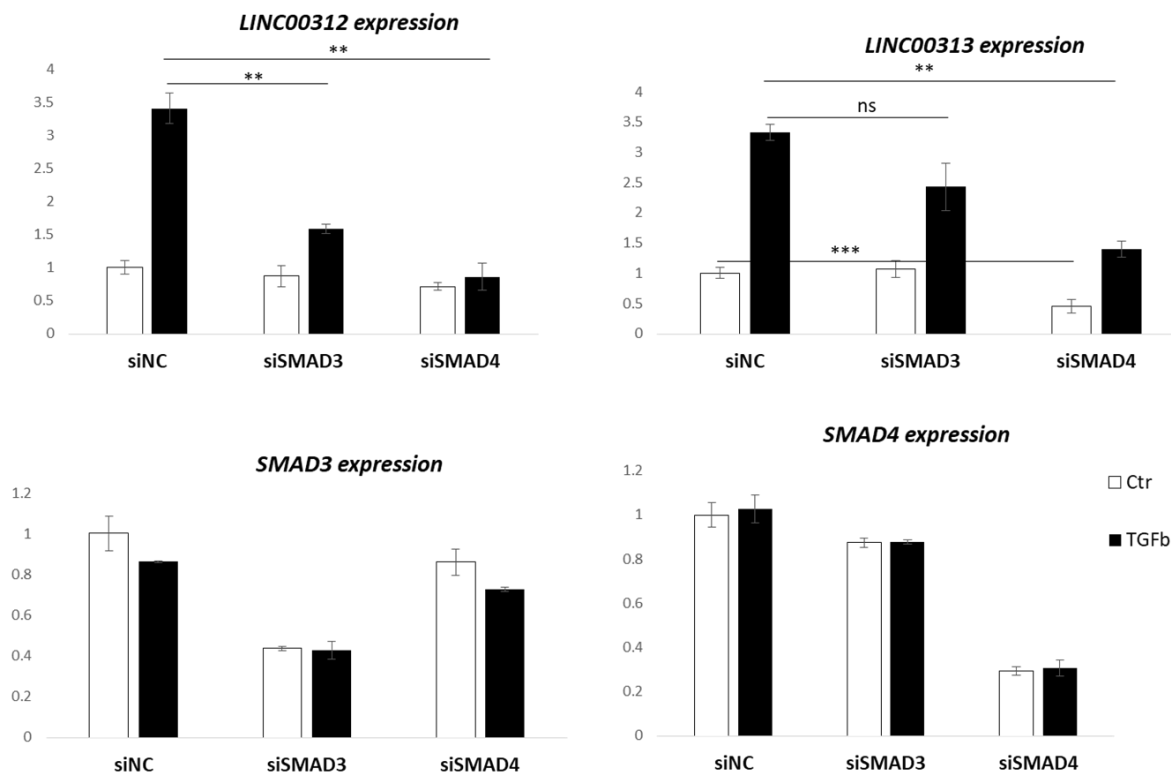


Figure 20 : Niveaux d'expression de LINC00312 et LINC00313 par qPCR après inhibition de SMAD3 et SMAD4 par siRNA, sans et avec stimulation par le TGF $\beta$ 1 (1ng/ml) pendant 16 heures dans les cellules HUCCT1.

Le panel du haut montre une induction de l'expression de LINC00312 et LINC00313 par le TGF $\beta$ . L'expression de LINC00312 est significativement moins importante après inhibition de SMAD3 et SMAD4 et donc dépendante de la voie canonique. L'expression de LINC00313 est significativement moins importante après inhibition de SMAD3 sans et avec stimulation par le TGF $\beta$  et donc également dépendante de la voie canonique.

Le panel du bas montre les contrôles de l'inhibition significative de SMAD3 et SMAD4 par leurs siRNA respectifs.

### *3. ARN non codants biomarqueurs*

Nos résultats ont montré que TLINC/CASC15 est un potentiel biomarqueur diagnostique dans les tissus de CCI humains. Les 2 isoformes de TLINC/CASC15 étaient surexprimées dans le tissu tumoral par rapport au tissu adjacent non tumoral. Cependant, l'expression des 2 isoformes était corrélée et ne montrait pas de corrélation au pronostic. La plupart des études publiées sur CASC15 ne prennent pas en compte les différentes isoformes. Cependant, la surexpression globale de CASC15 a été constatée *in vivo* dans le tissu tumoral de plusieurs cancers. Dans la majorité des cancers, cette expression a été associée à un caractère pro oncogénique et un mauvais pronostic. Dans le neuroblastome en revanche, son expression a été associée à un effet suppresseur de tumeur. CASC15 représente donc un potentiel biomarqueur diagnostique et pronostique dans les tissus tumoraux.

Dans le but d'identifier une signature d'ARNlnc prédictive de la survie, nous avons comparé les profils d'expression génique de tumeurs d'une cohorte de patients. Parmi les 9 ARNlnc significativement associés à la survie sans récidive et globale, 5 étaient surexprimés dans les CCI de bon pronostic et 4 étaient surexprimés dans les CCI de mauvais pronostic dont l'ARNlnc ANRIL. Nous avons focalisé notre analyse sur ANRIL (ou CDKN2B-AS1) car il a déjà été identifié comme biomarqueur pronostique dans d'autres cancers (CHC, cancer du rein et de l'utérus). Cependant, le biomarqueur idéal est non invasif et donc détectable dans le sang, les urines ou la salive. Des miARN détectables dans le sérum ou la bile ont déjà été bien étudiés dans le CCI soit individuellement ou en panel<sup>85,135,136</sup>. En revanche, peu d'études se sont intéressées à la détection d'ARNlnc dans le sérum, le plasma ou la bile. Le dosage dans le plasma d'ARNlnc connus pour être dérégulés dans le cholangiocarcinome hilaire a montré que les ARNlnc Prostate Cancer Associated Transcript 1 (PCAT1), MALAT1 et CPS1 Intronic Transcript 1 (CPS1-IT1) étaient de potentiels biomarqueurs diagnostiques sérieux<sup>137</sup>. Il n'existe actuellement pas de donnée sur la recherche d'ARNlnc dans le plasma ou le sérum dans le CCI.

Des ARNlnc intacts ont pu être détectés dans des exosomes extraits de la bile de patients présentant un cholangiocarcinome<sup>138</sup>. Comme dans le plasma, une caractéristique des exosomes présents dans la bile est leur stabilité due à leur protection par une double couche lipidique. Dans l'étude de Ge et al., la combinaison de 2 ARNlnc (ENST00000588480.1 et ENST00000517758.1) a été validée pour sa capacité diagnostique meilleure que le CA 19-9. La faible expression des 2 ARNlnc était corrélée à un meilleur pronostic<sup>138</sup>.

Les ARNcirc sont une autre forme d'ARN non-codants abondants avec des propriétés de stabilité et de spécificité d'organe intéressantes en tant que biomarqueur<sup>73,139</sup>. Comme les ARNlnc, les ARNcirc peuvent être excrétés dans des exosomes et constituer des biomarqueurs d'autant plus stables. Le développement d'outils de bioinformatique et de séquençage ARN ont permis de prédire de nombreux ARNcirc. Une isoforme circulaire d'ANRIL associée au risque d'athérosclérose, a été identifiée dans des lignées cellulaires de cancer<sup>140</sup>. Hsa\_circ\_0001649 et circRNA Cdr1as ont été associés à la progression du CCI<sup>141,142</sup>. En 2013, Salzman et al. avait prédit au moins une isoforme circulaire de CASC15 dérivée de l'exon 7 dans la lignée cellulaire HeLa<sup>143</sup>. Au moins 3 ARNcirc liés à CASC15 ont aussi été mises en évidence dans le carcinome basocellulaire<sup>144</sup>. A l'aide d'amorces spécifiques (convergentes et divergentes) et de traitements à la RNase R (dégradation spécifique des ARN linéaires), nous avons ainsi confirmé l'existence de plusieurs isoformes circulaires prédites de TLINC dans les lignées cellulaires de CCI traitées avec le TGFβ et les tissus de CCI. L'analyse par PCR des tissus de CCI de notre cohorte a montré que l'amplification des isoformes circulaires n'était pas identique dans toutes les tumeurs. La variabilité entre les tumeurs pourrait permettre d'utiliser ces ARNcirc comme biomarqueurs pronostiques.

Perspectives : Nos travaux n'ont pas permis d'identifier un ensemble exhaustif d'ARNcirc, ni d'évaluer précisément leur expression mais seulement de détecter l'existence de certains d'entre eux dans le CCI. Pour les identifier à large échelle, un profil d'expression des ARNcirc dans les lignées de CCI avec et sans TGFβ a récemment été réalisé dans l'équipe.

La combinaison au profil d'expression de microARN va permettre d'identifier les ARNcirc potentiels éponges à microARN (figure 21). Des résultats préliminaires ont déjà été obtenus.

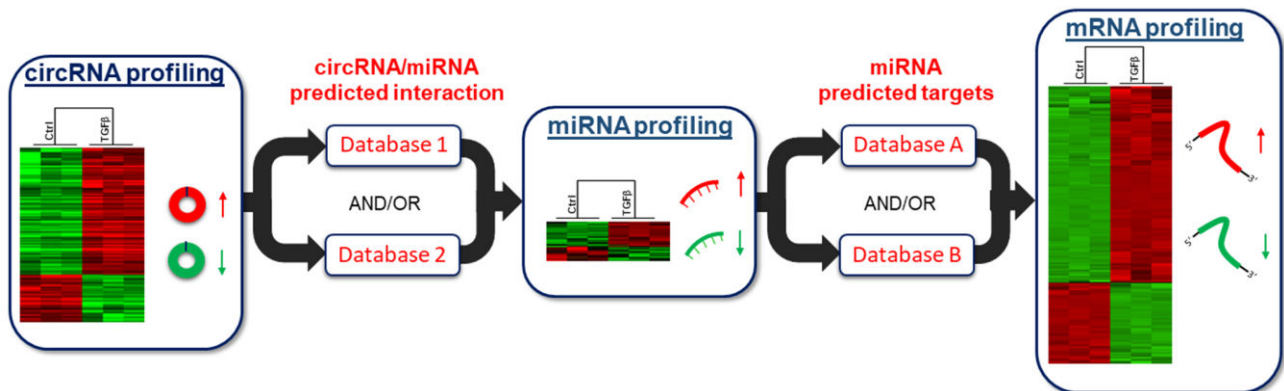


Figure 21 : Schéma du déroulement de l'analyse intégrée du profil d'expression des ARNcirc régulés par le TGF $\beta$ , puis du profil d'expression des microARN prédis interagissant avec ces ARNcirc et du profil d'expression de leurs ARNm cibles prédis.

#### 4. Applications thérapeutiques

##### I. Voie TGF $\beta$

La voie TGF $\beta$  est une cible déjà étudiée pour de nouvelles thérapies en cancérologie hépatique. L'action pharmacologique peut se situer au niveau du ligand avec des oligonucléotides antisens, de l'interaction entre ligand et récepteur avec des anticorps monoclonaux ou du signal intracellulaire avec des inhibiteurs des récepteurs kinase<sup>145</sup>. Le galunisertib est un des inhibiteurs du TGFBR1. Il a permis de diminuer la prolifération cellulaire sur des coupes de tumeurs fraîches de CHC en potentialisant les effets du sorafenib<sup>146</sup>. L'utilisation du galunisertib sur des cultures primaires de CCI a eu pour effet une diminution de la migration cellulaire<sup>147</sup>. Nous l'avons utilisé dans nos travaux en raison de son usage déjà possible en pratique clinique chez l'homme. Des essais cliniques sont recensés pour des patients porteurs de CHC, cancer pancréatique, cancer colorectal, mais pas encore dans le CCI. Le M7824 est un anticorps monoclonal conçu pour bloquer les voies de signalisation couramment utilisées par les cellules cancéreuses pour contrer le système immunitaire. Il agit contre la protéine programmed death-ligand 1 (PD-L1) liée au domaine

extracellulaire du récepteur TGF $\beta$  2. Un essai de phase II utilisant cet anticorps en monothérapie chez des patients avec des cholangiocarcinomes localement avancés en échec de chimiothérapie aux sels de platine doit démarrer cette année (ClinicalTrials.gov NCT03833661).

Le TGF $\beta$  est impliqué dans la TEM qui est impliquée dans de nombreux mécanismes de résistance aux traitements. La TEM a été identifiée *in vitro* comme un mécanisme de résistance à la gemcitabine et au cisplatine utilisés en combinaison dans le traitement du CCI<sup>148</sup>. Une diminution de la sensibilité au 5-fluorouracile liée aux caractéristiques mésenchymateuses qui accompagnent la TEM induite par le TGF $\beta$  dans la lignée de CCI TFK-1 a également été observée<sup>149</sup>. L'acquisition de propriétés de cellules souches cancéreuses induites par la TEM dans le CCI est un des effets qui contribue à la résistance aux chimiothérapies<sup>20</sup>. Des thérapies ciblant de TGF $\beta$  pourraient donc être utilisées en combinaison de chimiothérapie systémique pour améliorer leur efficacité.

Cependant, le TGF $\beta$  a des propriétés suppressives de tumeur à un stade tumoral précoce mais des effets tumorigéniques à un stade avancé. Mu et al. ont montré que le TGF $\beta$  épithélial n'induisait pas la fibrose et protégerait du développement du cholangiocarcinome<sup>71</sup>. Les thérapies ciblant le TGF $\beta$  trop tôt dans le développement tumoral pourraient donc être délétères. Le moment d'utilisation de ces thérapies doit donc être bien évalué<sup>49</sup>. La sélection des patients potentiels répondeurs est nécessaire. Les ARN non codants induits par le TGF $\beta$  pourraient être des biomarqueurs prédictifs de réponse aux thérapies ciblant le TGF $\beta$ .

Perspectives : L'effet du galunisertib sur tumeurs fraîches de CCI va être étudié dans l'équipe. Un modèle d'étude *in ovo* permettant d'implanter des tumeurs fraîches au niveau de la membrane chorio-amniotique d'œufs de poule est en cours de mise au point.

## *II. ARN non codants*

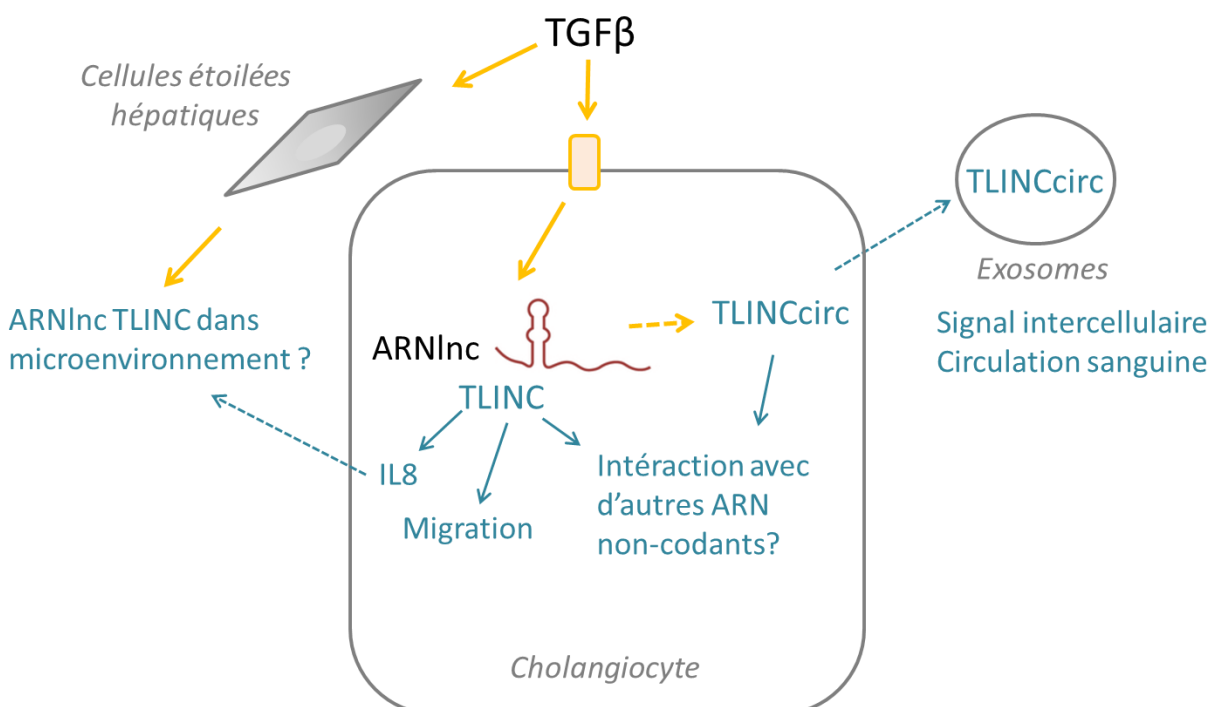
Les ARN non codants sont de potentielles cibles thérapeutiques du CCI en inhibant ou en renforçant leur action. Le microARN miR-195 placé dans des vésicules extracellulaires délivrées aux cellules de CCI chez le rat a permis une diminution de la taille tumorale et une prolongation de la survie<sup>150</sup>.

Il a été montré que CASC15/TLINC participe à la résistance au traitement du cancer du côlon<sup>151</sup>. CASC15 est surexprimé dans les tissus et les cellules de cancer colique résistants à l'oxaliplatine. Les patients avec un haut niveau d'expression de CASC15 ont un mauvais pronostic. CASC15 agit comme éponge au microARN miR-145 pour lever la répression de l'expression d'ATP Binding Cassette Subfamily C Member 1 . La diminution de CASC 15 resensibilise les cellules à l'oxaliplatine et représente donc une potentielle cible thérapeutique dans les cancers du côlon résistants à l'oxaliplatine.

Les ARNlnc peuvent également représenter des outils thérapeutiques. Un ARNlnc artificiel a été créé pour cibler plusieurs miARN surexprimés dans les cellules de CHC résistantes au sorafenib. Après infection des cellules par l'ARNlnc artificiel, une diminution de la prolifération et une augmentation de l'apoptose renforçant les effets du Sorafenib ont été observées<sup>152</sup>.

## V. Conclusion

La voie TGF $\beta$  est une des voies de signalisation impliquées dans la cancérogénèse du CCI. Nos travaux ont permis d'identifier de nouveaux gènes cibles de la voie TGF $\beta$  *in vitro* et de déterminer la pertinence clinique de leur dérégulation *in vivo* dans le CCI. Parmi ces nouveaux gènes, plusieurs ARNlnc ont été mis en évidence dont TLINC/CASC15 qui exerce un rôle dans le remodelage d'un microenvironnement inflammatoire impliqué dans la cancérogénèse du CCI. La surexpression de TLINC a également une tendance à augmenter la migration cellulaire. Les ARNlnc sont de potentiels biomarqueurs diagnostiques et/ou pronostiques du CCI tel que l'ARNlnc ANRIL. Les ARNcirc, une autre catégorie d'ARN non-codants, pourraient être aussi des biomarqueurs du CCI intéressants car très stables et détectables de façon non invasive dans le sérum. Enfin, les ARN non-codants pourraient constituer de potentielles cibles thérapeutiques en tant que médiateurs de la voie TGF $\beta$ . Les interactions complexes entre les différents ARN non-codants constituent encore un large domaine de recherche pour de nouvelles thérapies.



## VI. Références

1. Hamilton SR, Aaltonen LA. *Pathology and Genetics of Tumours of the Digestive System*, <http://publications.iarc.fr/Book-And-Report-Series/Who-Iarc-Classification-Of-Tumours/Pathology-And-Genetics-Of-Tumours-Of-The-Digestive-System-2000>.
2. Blechacz B, Komuta M, Roskams T, et al. Clinical diagnosis and staging of cholangiocarcinoma. *Nat Rev Gastroenterol Hepatol* 2011; 8: 512–522.
3. Shaib Y, El-Serag HB. The Epidemiology of Cholangiocarcinoma. *Semin Liver Dis* 2004; 24: 115–125.
4. Bragazzi MC, Cardinale V, Carpino G, et al. Cholangiocarcinoma: Epidemiology and risk factors. *Transl Gastrointest Cancer* 2011; 1: 21-32–32.
5. Banales JM, Cardinale V, Carpino G, et al. Expert consensus document: Cholangiocarcinoma: current knowledge and future perspectives consensus statement from the European Network for the Study of Cholangiocarcinoma (ENS-CCA). *Nat Rev Gastroenterol Hepatol* 2016; 13: 261–280.
6. Doussot A, Lim C, Gómez-Gavara C, et al. Multicentre study of the impact of morbidity on long-term survival following hepatectomy for intrahepatic cholangiocarcinoma. *BJS* 2016; 103: 1887–1894.
7. Razumilava N, Gores GJ. Classification, Diagnosis, and Management of Cholangiocarcinoma. *Clin Gastroenterol Hepatol* 2013; 11: 13-21.e1.
8. Palmer WC, Patel T. Are common factors involved in the pathogenesis of primary liver cancers? A meta-analysis of risk factors for intrahepatic cholangiocarcinoma. *J Hepatol* 2012; 57: 69–76.
9. Shaib YH, Davila JA, McGlynn K, et al. Rising incidence of intrahepatic cholangiocarcinoma in the United States: a true increase? *J Hepatol* 2004; 40: 472–477.
10. Khan SA, Emadossadaty S, Ladep NG, et al. Rising trends in cholangiocarcinoma: Is the ICD classification system misleading us? *J Hepatol* 2012; 56: 848–854.
11. Welzel TM, Graubard BI, Zeuzem S, et al. Metabolic syndrome increases the risk of primary liver cancer in the United States: a population-based case-control study. *Hepatol Baltim Md* 2011; 54: 463–471.
12. Yamasaki S. Intrahepatic cholangiocarcinoma: macroscopic type and stage classification. *J Hepatobiliary Pancreat Surg* 2003; 10: 288–291.
13. Mavros MN, Economopoulos KP, Alexiou VG, et al. Treatment and prognosis for patients with intrahepatic cholangiocarcinoma: Systematic review and meta-analysis. *JAMA Surg* 2014; 149: 565–574.
14. Maeda T, Kajiyama K, Adachi E, et al. The expression of cytokeratins 7, 19, and 20 in primary and metastatic carcinomas of the liver. *Mod Pathol Off J U S Can Acad Pathol Inc* 1996; 9: 901–909.

15. Rullier A, Bail BL, Fawaz R, et al. Cytokeratin 7 and 20 Expression in Cholangiocarcinomas Varies Along the Biliary Tract But Still Differs From That in Colorectal Carcinoma Metastasis. *Am J Surg Pathol* 2000; 24: 870–876.
16. Sirica AE, Gores GJ. Desmoplastic Stroma and Cholangiocarcinoma: Clinical Implications and Therapeutic Targeting. *Hepatol Baltim Md* 2014; 59: 2397–2402.
17. Sirica AE. The role of cancer-associated myofibroblasts in intrahepatic cholangiocarcinoma. *Nat Rev Gastroenterol Hepatol* 2012; 9: 44–54.
18. Sulpice L, Rayar M, Desille M, et al. Molecular profiling of stroma identifies osteopontin as an independent predictor of poor prognosis in intrahepatic cholangiocarcinoma. *Hepatol Baltim Md* 2013; 58: 1992–2000.
19. Fabregat I, Caballero-Díaz D. Transforming Growth Factor- $\beta$ -Induced Cell Plasticity in Liver Fibrosis and Hepatocarcinogenesis. *Front Oncol*; 8. Epub ahead of print 10 September 2018. DOI: 10.3389/fonc.2018.00357.
20. Cardinale V, Renzi A, Carpino G, et al. Profiles of Cancer Stem Cell Subpopulations in Cholangiocarcinomas. *Am J Pathol* 2015; 185: 1724–1739.
21. Fan B, Malato Y, Calvisi DF, et al. Cholangiocarcinomas can originate from hepatocytes in mice. *J Clin Invest* 2012; 122: 2911–2915.
22. Sekiya S, Suzuki A. Intrahepatic cholangiocarcinoma can arise from Notch-mediated conversion of hepatocytes. *J Clin Invest* 2012; 122: 3914–3918.
23. Moeini A, Sia D, Bardeesy N, et al. Molecular Pathogenesis and Targeted Therapies for Intrahepatic Cholangiocarcinoma. *Am Assoc Cancer Res* 2016; 22: 291–300.
24. Andersen JB, Spee B, Blechacz BR, et al. Genomic and Genetic Characterization of Cholangiocarcinoma Identifies Therapeutic Targets for Tyrosine Kinase Inhibitors. *Gastroenterology* 2012; 142: 1021-1031.e15.
25. Arai Y, Totoki Y, Hosoda F, et al. Fibroblast growth factor receptor 2 tyrosine kinase fusions define a unique molecular subtype of cholangiocarcinoma. *Hepatology* 2014; 59: 1427–1434.
26. Sia D, Tovar V, Moeini A, et al. Intrahepatic cholangiocarcinoma: pathogenesis and rationale for molecular therapies. *Oncogene* 2013; 32: 4861–4870.
27. Sia D, Hoshida Y, Villanueva A, et al. Integrative Molecular Analysis of Intrahepatic Cholangiocarcinoma Reveals 2 Classes That Have Different Outcomes. *Gastroenterology* 2013; 144: 829–840.
28. Patel AH, Harnois DM, Klee GG, et al. The utility of CA 19-9 in the diagnoses of cholangiocarcinoma in patients without primary sclerosing cholangitis. *Am J Gastroenterol* 2000; 95: 204–207.
29. Tamandl D, Herberger B, Gruenberger B, et al. Influence of Hepatic Resection Margin on Recurrence and Survival in Intrahepatic Cholangiocarcinoma. *Ann Surg Oncol* 2008; 15: 2787–2794.
30. Uenishi T, Yamazaki O, Tanaka H, et al. Serum Cytokeratin 19 Fragment (CYFRA21-1) as a Prognostic Factor in Intrahepatic Cholangiocarcinoma. *Ann Surg Oncol* 2008; 15: 583–589.

31. Loosen SH, Roderburg C, Kauertz KL, et al. Elevated levels of circulating osteopontin are associated with a poor survival after resection of cholangiocarcinoma. *J Hepatol* 2017; 67: 749–757.
32. Sulpice L, Rayar M, Turlin B, et al. Epithelial cell adhesion molecule is a prognosis marker for intrahepatic cholangiocarcinoma. *J Surg Res.* DOI: 10.1016/j.jss.2014.05.017.
33. Bergeat D, Fautrel A, Turlin B, et al. Impact of stroma LOXL2 overexpression on the prognosis of intrahepatic cholangiocarcinoma. *J Surg Res* 2016; 203: 441–450.
34. Arbelaitz A, Azkargorta M, Krawczyk M, et al. Serum extracellular vesicles contain protein biomarkers for primary sclerosing cholangitis and cholangiocarcinoma. *Hepatology* 2017; 66: 1125–1143.
35. Valls C, Gumà A, Puig I, et al. Intrahepatic peripheral cholangiocarcinoma: CT evaluation. *Abdom Imaging* 2000; 25: 490–496.
36. Sulpice L, Rayar M, Boucher E, et al. Treatment of recurrent intrahepatic cholangiocarcinoma. *Br J Surg* 2012; 99: 1711–1717.
37. Bridgewater J, Galle PR, Khan SA, et al. Guidelines for the diagnosis and management of intrahepatic cholangiocarcinoma. *J Hepatol* 2014; 60: 1268–1289.
38. Goldaracena N, Gorgen A, Sapisochin G. Current status of liver transplantation for cholangiocarcinoma. *Liver Transpl* 2018; 24: 294–303.
39. Valle J, Wasan H, Palmer DH, et al. Cisplatin plus Gemcitabine versus Gemcitabine for Biliary Tract Cancer. *N Engl J Med* 2010; 362: 1273–1281.
40. Shroff RT, Kennedy EB, Bachini M, et al. Adjuvant Therapy for Resected Biliary Tract Cancer: ASCO Clinical Practice Guideline. *J Clin Oncol* 2019; JCO.18.02178.
41. Edeline J, Benabdellghani M, Bertaut A, et al. Gemcitabine and Oxaliplatin Chemotherapy or Surveillance in Resected Biliary Tract Cancer (PRODIGE 12-ACCORD 18-UNICANCER GI): A Randomized Phase III Study. *J Clin Oncol* 2019; 37: 658–667.
42. Edeline J, Du FL, Rayar M, et al. Glass Microspheres 90Y Selective Internal Radiation Therapy and Chemotherapy as First-Line Treatment of Intrahepatic Cholangiocarcinoma. *Clin Nucl Med* 2015; 40: 851–855.
43. Chun YS, Javle M. Systemic and Adjuvant Therapies for Intrahepatic Cholangiocarcinoma. *Cancer Control J Moffitt Cancer Cent*; 24. Epub ahead of print 7 September 2017. DOI: 10.1177/1073274817729241.
44. Sirica AE, Gores GJ, Groopman JD, et al. Intrahepatic Cholangiocarcinoma: Continuing Challenges and Translational Advances. *Hepatology*; 0. DOI: 10.1002/hep.30289.
45. Larkin J, Chiarioti-Silenti V, Gonzalez R, et al. Combined Nivolumab and Ipilimumab or Monotherapy in Previously Untreated Melanoma. *N Engl J Med* 2015; 373: 23–34.
46. Massagué J. TGF $\beta$  signalling in context. *Nat Rev Mol Cell Biol* 2012; 13: 616–630.
47. Massagué J, Gomis RR. The logic of TGF $\beta$  signaling. *FEBS Lett* 2006; 580: 2811–2820.

48. Akhurst RJ, Hata A. Targeting the TGF $\beta$  signalling pathway in disease. *Nat Rev Drug Discov* 2012; 11: 790–811.
49. Principe DR, Doll JA, Bauer J, et al. TGF- $\beta$ : Duality of Function Between Tumor Prevention and Carcinogenesis. *JNCI J Natl Cancer Inst*; 106. Epub ahead of print 6 February 2014. DOI: 10.1093/jnci/djt369.
50. Luo L, Li N, Lv N, et al. SMAD7: a timer of tumor progression targeting TGF- $\beta$  signaling. *Tumor Biol* 2014; 1–7.
51. Massagué J. TGF $\beta$  in Cancer. *Cell* 2008; 134: 215–230.
52. De Wever O, Pauwels P, De Craene B, et al. Molecular and pathological signatures of epithelial–mesenchymal transitions at the cancer invasion front. *Histochem Cell Biol* 2008; 130: 481–494.
53. Vaquero J, Guedj N, Clapérón A, et al. Epithelial-mesenchymal transition in cholangiocarcinoma: From clinical evidence to regulatory networks. *J Hepatol* 2017; 66: 424–441.
54. Dongre A, Weinberg RA. New insights into the mechanisms of epithelial–mesenchymal transition and implications for cancer. *Nat Rev Mol Cell Biol* 2019; 20: 69.
55. You H, Ding W, Rountree CB. Epigenetic Regulation of Cancer Stem Cell Marker CD133 by Transforming Growth Factor- $\beta$ . *Hepatol Baltim Md* 2010; 51: 1635–1644.
56. Ding W, Mouzaki M, You H, et al. CD133+ Liver Cancer Stem Cells from Methionine Adenosyl Transferase 1A-Deficient Mice Demonstrate Resistance to Transforming Growth Factor (TGF)- $\beta$ -Induced Apoptosis. *Hepatol Baltim Md* 2009; 49: 1277–1286.
57. Xiong B, Gong L-L, Zhang F, et al. TGF- $\beta$ 1 expression and angiogenesis in colorectal cancer tissue. *World J Gastroenterol* 2002; 8: 496–498.
58. Goumans M-J, Lebrin F, Valdimarsdottir G. Controlling the Angiogenic Switch: A Balance between Two Distinct TGF- $\beta$  Receptor Signaling Pathways. *Trends Cardiovasc Med* 2003; 13: 301–307.
59. Padua D, Zhang XH-F, Wang Q, et al. TGF $\beta$  primes breast tumors for lung metastasis seeding through angiopoietin-like 4. *Cell* 2008; 133: 66–77.
60. Bertran E, Crosas-Molist E, Sancho P, et al. Overactivation of the TGF- $\beta$  pathway confers a mesenchymal-like phenotype and CXCR4-dependent migratory properties to liver tumor cells. *Hepatology* 2013; 58: 2032–2044.
61. Sato Y, Harada K, Itatsu K, et al. Epithelial-Mesenchymal Transition Induced by Transforming Growth Factor- $\beta$ 1/Snail Activation Aggravates Invasive Growth of Cholangiocarcinoma. *Am J Pathol* 2010; 177: 141–152.
62. Oishi N, Kumar MR, Roessler S, et al. Transcriptomic profiling reveals hepatic stem-like gene signatures and interplay of miR-200c and epithelial-mesenchymal transition in intrahepatic cholangiocarcinoma. *Hepatology* 2012; 56: 1792–1803.
63. Manzanares MÁ, Usui A, Campbell DJ, et al. Transforming Growth Factors  $\alpha$  and  $\beta$  Are Essential for Modeling Cholangiocarcinoma Desmoplasia and Progression in a Three-Dimensional Organotypic Culture Model. *Am J Pathol* 2017; 187: 1068–1092.

64. Shimizu T, Yokomuro S, Mizuguchi Y, et al. Effect of transforming growth factor- $\beta$ 1 on human intrahepatic cholangiocarcinoma cell growth. *World J Gastroenterol WJG* 2006; 12: 6316–6324.
65. Huang C-K, Aihara A, Iwagami Y, et al. Expression of transforming growth factor  $\beta$ 1 promotes cholangiocarcinoma development and progression. *Cancer Lett* 2016; 380: 153–162.
66. Zen Y, Harada K, Sasaki M, et al. Intrahepatic cholangiocarcinoma escapes from growth inhibitory effect of transforming growth factor- $\beta$ 1 by overexpression of cyclin D1. *Lab Invest* 2005; 85: 572–581.
67. Benckert C, Jonas S, Cramer T, et al. Transforming Growth Factor  $\beta$ 1 Stimulates Vascular Endothelial Growth Factor Gene Transcription in Human Cholangiocellular Carcinoma Cells. *Cancer Res* 2003; 63: 1083–1092.
68. Chen Y, Ma L, He Q, et al. TGF- $\beta$ 1 expression is associated with invasion and metastasis of intrahepatic cholangiocarcinoma. *Biol Res*; 48. Epub ahead of print December 2015. DOI: 10.1186/s40659-015-0016-9.
69. Zou S, Li J, Zhou H, et al. Mutational landscape of intrahepatic cholangiocarcinoma. *Nat Commun* 2014; 5: 5696.
70. Kim Y-H, Hong E-K, Kong S-Y, et al. Two classes of intrahepatic cholangiocarcinoma defined by relative abundance of mutations and copy number alterations. *Oncotarget* 2016; 7: 23825–23836.
71. Mu X, Pradere J-P, Affò S, et al. Epithelial Transforming Growth Factor- $\beta$  Signaling Does Not Contribute to Liver Fibrosis but Protects Mice From Cholangiocarcinoma. *Gastroenterology*. DOI: 10.1053/j.gastro.2015.11.039.
72. Iyer MK, Niknafs YS, Malik R, et al. The Landscape of Long Noncoding RNAs in the Human Transcriptome. *Nat Genet* 2015; 47: 199–208.
73. Memczak S, Jens M, Elefsinioti A, et al. Circular RNAs are a large class of animal RNAs with regulatory potency. *Nature* 2013; 495: 333–338.
74. Derrien T, Johnson R, Bussotti G, et al. The GENCODE v7 catalog of human long noncoding RNAs: Analysis of their gene structure, evolution, and expression. *Genome Res* 2012; 22: 1775–1789.
75. Wong C-M, Tsang FH-C, Ng IO-L. Non-coding RNAs in hepatocellular carcinoma: molecular functions and pathological implications. *Nat Rev Gastroenterol Hepatol* 2018; 15: 137–151.
76. He Y, Meng X-M, Huang C, et al. Long noncoding RNAs: Novel insights into hepatocellular carcinoma. *Cancer Lett* 2014; 344: 20–27.
77. Batista PJ, Chang HY. Long noncoding RNAs: Cellular address codes in development and disease. *Cell* 2013; 152: 1298–1307.
78. Wang KC, Yang YW, Liu B, et al. Long noncoding RNA programs active chromatin domain to coordinate homeotic gene activation. *Nature* 2011; 472: 120–124.
79. Tsai M-C, Manor O, Wan Y, et al. Long Noncoding RNA as Modular Scaffold of Histone Modification Complexes. *Science* 2010; 329: 689–693.

80. Hung T, Wang Y, Lin MF, et al. Extensive and coordinated transcription of noncoding RNAs within cell-cycle promoters. *Nat Genet* 2011; 43: 621–629.
81. Sotillo E, Thomas-Tikhonenko A. The long reach of noncoding RNAs. *Nat Genet* 2011; 43: 616–617.
82. Matouk IJ, DeGroot N, Mezan S, et al. The H19 non-coding RNA is essential for human tumor growth. *PLoS One* 2007; 2: e845.
83. Keniry A, Oxley D, Monnier P, et al. The H19 lncRNA is a developmental reservoir of miR-675 that suppresses growth and Igf1r. *Nat Cell Biol* 2012; 14: 659–665.
84. Gao L, Ren W, Zhang L, et al. PTENp1, a natural sponge of miR-21, mediates PTEN expression to inhibit the proliferation of oral squamous cell carcinoma. *Mol Carcinog* 2017; 56: 1322–1334.
85. Wangyang Z, Daolin J, yi X, et al. NcRNAs and Cholangiocarcinoma. *J Cancer* 2018; 9: 100–107.
86. Wang J, Xie H, Ling Q, et al. Coding-noncoding gene expression in intrahepatic cholangiocarcinoma. *Transl Res* 2016; 168: 107–121.
87. Song W, Miao D, Chen L. Comprehensive analysis of long noncoding RNA-associated competing endogenous RNA network in cholangiocarcinoma. *Biochem Biophys Res Commun* 2018; 506: 1004–1012.
88. Wang X, Hu KB, Zhang YQ, et al. Comprehensive analysis of aberrantly expressed profiles of lncRNAs, miRNAs and mRNAs with associated ceRNA network in cholangiocarcinoma. *Cancer Biomark* 2018; 23: 549–559.
89. Yang W, Li Y, Song X, et al. Genome-wide analysis of long noncoding RNA and mRNA co-expression profile in intrahepatic cholangiocarcinoma tissue by RNA sequencing. *Oncotarget* 2017; 8: 26591–26599.
90. Yu Y, Zhang M, Wang N, et al. Epigenetic silencing of tumor suppressor gene CDKN1A by oncogenic long non-coding RNA SNHG1 in cholangiocarcinoma. *Cell Death Dis*; 9. Epub ahead of print 3 July 2018. DOI: 10.1038/s41419-018-0768-6.
91. Zhang C, Li J-Y, Tian F-Z, et al. Long Noncoding RNA NEAT1 Promotes Growth and Metastasis of Cholangiocarcinoma Cells. *Oncol Res* 2018; 26: 879–888.
92. Li Y, Cai Q, Li W, et al. Long non-coding RNA EPIC1 promotes cholangiocarcinoma cell growth. *Biochem Biophys Res Commun*. Epub ahead of print 8 September 2018. DOI: 10.1016/j.bbrc.2018.08.174.
93. Wang C, Mao ZP, Wang L, et al. Long non-coding RNA MALAT1 promotes cholangiocarcinoma cell proliferation and invasion by activating PI3K/Akt pathway. *Neoplasma* 2017; 64: 725–731.
94. Xia X-L, Xue D, Xiang T-H, et al. Overexpression of long non-coding RNA CRNDE facilitates epithelial-mesenchymal transition and correlates with poor prognosis in intrahepatic cholangiocarcinoma. *Oncol Lett* 2018; 15: 4105–4112.
95. Zeng B, Ye H, Chen J, et al. LncRNA TUG1 sponges miR-145 to promote cancer progression and regulate glutamine metabolism via Sirt3/GDH axis. *Oncotarget* 2017; 8: 113650–113661.

96. Xu Y, Leng K, Li Z, et al. The prognostic potential and carcinogenesis of long non-coding RNA TUG1 in human cholangiocarcinoma. *Oncotarget* 2017; 8: 65823–65835.
97. Beltran M, Puig I, Peña C, et al. A natural antisense transcript regulates Zeb2/Sip1 gene expression during Snail1-induced epithelial–mesenchymal transition. *Genes Dev* 2008; 22: 756–769.
98. Yuan J, Yang F, Wang F, et al. A Long Noncoding RNA Activated by TGF- $\beta$  Promotes the Invasion-Metastasis Cascade in Hepatocellular Carcinoma. *Cancer Cell* 2014; 25: 666–681.
99. Fan Y-H, Ji C, Xu B, et al. Long noncoding RNA activated by TGF- $\beta$  in human cancers: A meta-analysis. *Clin Chim Acta* 2017; 468: 10–16.
100. Zhang J, Han C, Ungerleider N, et al. A Transforming Growth Factor- $\beta$  and H19 Signaling Axis in Tumor-Initiating Hepatocytes That Regulates Hepatic Carcinogenesis. *Hepatology*; 0. Epub ahead of print 16 July 2018. DOI: 10.1002/hep.30153.
101. Takahashi K, Yan IK, Kogure T, et al. Extracellular vesicle-mediated transfer of long non-coding RNA ROR modulates chemosensitivity in human hepatocellular cancer. *FEBS Open Bio* 2014; 4: 458–467.
102. Mondal T, Subhash S, Vaid R, et al. MEG3 long noncoding RNA regulates the TGF- $\beta$  pathway genes through formation of RNA–DNA triplex structures. *Nat Commun*; 6. Epub ahead of print 24 July 2015. DOI: 10.1038/ncomms8743.
103. He Y, Wu Y-T, Huang C, et al. Inhibitory effects of long noncoding RNA MEG3 on hepatic stellate cells activation and liver fibrogenesis. *Biochim Biophys Acta* 2014; 1842: 2204–2215.
104. Braconi C, Kogure T, Valeri N, et al. microRNA-29 can regulate expression of the long non-coding RNA gene MEG3 in hepatocellular cancer. *Oncogene* 2011; 30: 4750–4756.
105. Tang J, Zhuo H, Zhang X, et al. A novel biomarker Linc00974 interacting with KRT19 promotes proliferation and metastasis in hepatocellular carcinoma. *Cell Death Dis* 2014; 5: e1549.
106. Takahashi Y, Sawada G, Kurashige J, et al. Amplification of PVT-1 is involved in poor prognosis via apoptosis inhibition in colorectal cancers. *Br J Cancer* 2014; 110: 164–171.
107. Wang F, Yuan J-H, Wang S-B, et al. Oncofetal long noncoding RNA PVT1 promotes proliferation and stem cell-like property of hepatocellular carcinoma cells by stabilizing NOP2. *Hepatology* 2014; 60: 1278–1290.
108. Zhao J-J, Hao S, Wang L-L, et al. Long non-coding RNA ANRIL promotes the invasion and metastasis of thyroid cancer cells through TGF- $\beta$ /Smad signaling pathway. *Oncotarget* 2016; 7: 57903–57918.
109. Chen D, Zhang Z, Mao C, et al. ANRIL inhibits p15INK4b through the TGF $\beta$ 1 signaling pathway in human esophageal squamous cell carcinoma. *Cell Immunol* 2014; 289: 91–96.
110. Congrains A, Kamide K, Ohishi M, et al. ANRIL: Molecular Mechanisms and Implications in Human Health. *Int J Mol Sci* 2013; 14: 1278–1292.

111. Ma J, Li T, Han X, et al. Knockdown of LncRNA ANRIL suppresses cell proliferation, metastasis, and invasion via regulating miR-122-5p expression in hepatocellular carcinoma. *J Cancer Res Clin Oncol* 2018; 144: 205–214.
112. Moll R, Divo M, Langbein L. The human keratins: biology and pathology. *Histochem Cell Biol* 2008; 129: 705–733.
113. Dmello C, Sawant S, Alam H, et al. Vimentin regulates differentiation switch via modulation of keratin 14 levels and their expression together correlates with poor prognosis in oral cancer patients. *PLoS ONE*; 12. Epub ahead of print 22 February 2017. DOI: 10.1371/journal.pone.0172559.
114. Merkin RD, Vanner EA, Romeiser JL, et al. Keratin 17 is overexpressed and predicts poor survival in estrogen receptor-negative/human epidermal growth factor receptor-2-negative breast cancer. *Hum Pathol* 2017; 62: 23–32.
115. Ide M, Kato T, Ogata K, et al. Keratin 17 Expression Correlates with Tumor Progression and Poor Prognosis in Gastric Adenocarcinoma. *Ann Surg Oncol* 2012; 19: 3506–3514.
116. Chu PG, Schwarz RE, Lau SK, et al. Immunohistochemical staining in the diagnosis of pancreatobiliary and ampulla of Vater adenocarcinoma: application of CDX2, CK17, MUC1, and MUC2. *Am J Surg Pathol* 2005; 29: 359–367.
117. Peng Z, Wang J, Shan B, et al. The long noncoding RNA LINC00312 induces lung adenocarcinoma migration and vasculogenic mimicry through directly binding YBX1. *Mol Cancer*; 17. Epub ahead of print 23 November 2018. DOI: 10.1186/s12943-018-0920-z.
118. Liu K, Huang W, Yan D-Q, et al. Overexpression of long intergenic noncoding RNA LINC00312 inhibits the invasion and migration of thyroid cancer cells by down-regulating microRNA-197-3p. *Biosci Rep*; 37. Epub ahead of print 20 July 2017. DOI: 10.1042/BSR20170109.
119. Wang Y-Y, Wu Z-Y, Wang G-C, et al. LINC00312 inhibits the migration and invasion of bladder cancer cells by targeting miR-197-3p. *Tumor Biol* 2016; 37: 14553–14563.
120. Li M, Qiu M, Xu Y, et al. Differentially expressed protein-coding genes and long noncoding RNA in early-stage lung cancer. *Tumor Biol* 2015; 36: 9969–9978.
121. Wu WJ, Yin H, Hu JJ, et al. Long noncoding RNA LINC00313 modulates papillary thyroid cancer tumorigenesis via sponging miR-4429. *Neoplasma* 2018; 65: 933–942.
122. Lessard L, Liu M, Marzese DM, et al. The CASC15 long intergenic non-coding RNA locus is involved in melanoma progression and phenotype-switching. *J Invest Dermatol* 2015; 135: 2464–2474.
123. Yin Y, Zhao B, Li D, et al. Long non-coding RNA CASC15 promotes melanoma progression by epigenetically regulating PDCD4. *Cell Biosci*; 8. Epub ahead of print 13 July 2018. DOI: 10.1186/s13578-018-0240-4.
124. Russell MR, Penikis A, Oldridge DA, et al. CASC15-S is a tumor suppressor lncRNA at the 6p22 neuroblastoma susceptibility locus. *Cancer Res* 2015; 75: 3155–3166.
125. Mondal T, Juvvuna PK, Kirkeby A, et al. Sense-Antisense lncRNA Pair Encoded by Locus 6p22.3 Determines Neuroblastoma Susceptibility via the USP36-CHD7-SOX9 Regulatory Axis. *Cancer Cell* 2018; 33: 417-434.e7.

126. Zhang J, Zhuo Z-J, Wang J, et al. CASC15 gene polymorphisms reduce neuroblastoma risk in Chinese children. *Oncotarget* 2017; 8: 91343–91349.
127. Clemson CM, Hutchinson JN, Sara SA, et al. An Architectural Role for a Nuclear Noncoding RNA: NEAT1 RNA Is Essential for the Structure of Paraspeckles. *Mol Cell* 2009; 33: 717–726.
128. Imamura K, Imamachi N, Akizuki G, et al. Long Noncoding RNA NEAT1-Dependent SFPQ Relocation from Promoter Region to Paraspeckle Mediates IL8 Expression upon Immune Stimuli. *Mol Cell* 2014; 53: 393–406.
129. West JA, Davis CP, Sunwoo H, et al. The Long Noncoding RNAs NEAT1 and MALAT1 Bind Active Chromatin Sites. *Mol Cell* 2014; 55: 791–802.
130. Fujimoto A, Furuta M, Totoki Y, et al. Whole-genome mutational landscape and characterization of noncoding and structural mutations in liver cancer. *Nat Genet* 2016; 48: 500–509.
131. Xu Y, Yao Y, Jiang X, et al. SP1-induced upregulation of lncRNA SPRY4-IT1 exerts oncogenic properties by scaffolding EZH2/LSD1/DNMT1 and sponging miR-101-3p in cholangiocarcinoma. *J Exp Clin Cancer Res CR*; 37. Epub ahead of print 11 April 2018. DOI: 10.1186/s13046-018-0747-x.
132. Wu Q, Xiang S, Ma J, et al. Long non-coding RNA CASC15 regulates gastric cancer cell proliferation, migration and epithelial mesenchymal transition by targeting CDKN1A and ZEB1. *Mol Oncol* 2018; 12: 799–813.
133. He T, Zhang L, Kong Y, et al. Long non-coding RNA CASC15 is upregulated in hepatocellular carcinoma and facilitates hepatocarcinogenesis. *Int J Oncol* 2017; 51: 1722–1730.
134. Jing N, Huang T, Guo H, et al. LncRNA CASC15 promotes colon cancer cell proliferation and metastasis by regulating the miR-4310/LGR5/Wnt/β-catenin signaling pathway. *Mol Med Rep* 2018; 18: 2269–2276.
135. Zheng B, Jeong S, Zhu Y, et al. miRNA and lncRNA as biomarkers in cholangiocarcinoma(CCA). *Oncotarget* 2017; 8: 100819–100830.
136. Li L, Masica D, Ishida M, et al. Human bile contains MicroRNA-laden extracellular vesicles that can be used for cholangiocarcinoma diagnosis. *Hepatology* 2014; 60: 896–907.
137. Shi J, Li X, Zhang F, et al. The Plasma LncRNA Acting as Fingerprint in Hilar Cholangiocarcinoma. *Cell Physiol Biochem* 2018; 49: 1694–1702.
138. Ge X, Wang Y, Nie J, et al. The diagnostic/prognostic potential and molecular functions of long non-coding RNAs in the exosomes derived from the bile of human cholangiocarcinoma. *Oncotarget* 2017; 8: 69995–70005.
139. Han Y-N, Xia S-Q, Zhang Y-Y, et al. Circular RNAs: A novel type of biomarker and genetic tools in cancer. *Oncotarget*; 8. Epub ahead of print 8 September 2017. DOI: 10.18632/oncotarget.18350.
140. Burd CE, Jeck WR, Liu Y, et al. Expression of Linear and Novel Circular Forms of an INK4/ARF-Associated Non-Coding RNA Correlates with Atherosclerosis Risk. *PLoS Genet*; 6. Epub ahead of print 2 December 2010. DOI: 10.1371/journal.pgen.1001233.

141. Xu Y, Yao Y, Zhong X, et al. Downregulated circular RNA hsa\_circ\_0001649 regulates proliferation, migration and invasion in cholangiocarcinoma cells. *Biochem Biophys Res Commun* 2018; 496: 455–461.
142. Jiang X-M, Li Z-L, Li J-L, et al. A novel prognostic biomarker for cholangiocarcinoma: circRNA Cdr1as. *Eur Rev Med Pharmacol Sci* 2018; 22: 365–371.
143. Salzman J, Chen RE, Olsen MN, et al. Cell-Type Specific Features of Circular RNA Expression. *PLoS Genet* 2013; 9: e1003777.
144. Sand M, Bechara FG, Sand D, et al. Long-noncoding RNAs in basal cell carcinoma. *Tumor Biol* 2016; 37: 10595–10608.
145. Zhang S, Sun W-Y, Wu J-J, et al. TGF- $\beta$  signaling pathway as a pharmacological target in liver diseases. *Pharmacol Res* 2014; 85: 15–22.
146. Serova M, Tijeras-Raballand A, Santos CD, et al. Effects of TGF- $\beta$  signalling inhibition with galunisertib (LY2157299) in hepatocellular carcinoma models and in ex vivo whole tumor tissue samples from patients. *Oncotarget* 2015; 6: 21614–21627.
147. Lustri AM, Di Matteo S, Fraveto A, et al. TGF- $\beta$  signaling is an effective target to impair survival and induce apoptosis of human cholangiocarcinoma cells: A study on human primary cell cultures. *PLoS ONE*; 12. Epub ahead of print 5 September 2017. DOI: 10.1371/journal.pone.0183932.
148. Yamada D, Kobayashi S, Wada H, et al. Role of crosstalk between interleukin-6 and transforming growth factor- $\beta$  1 in epithelial–mesenchymal transition and chemoresistance in biliary tract cancer. *Eur J Cancer* 2013; 49: 1725–1740.
149. Shuang Z-Y, Wu W-C, Xu J, et al. Transforming growth factor- $\beta$ 1-induced epithelial–mesenchymal transition generates ALDH-positive cells with stem cell properties in cholangiocarcinoma. *Cancer Lett* 2014; 354: 320–328.
150. Li L, Piontek K, Ishida M, et al. Extracellular vesicles carry microRNA-195 to intrahepatic cholangiocarcinoma and improve survival in a rat model. *Hepatology* 2017; 65: 501–514.
151. Gao R, Fang C, Xu J, et al. LncRNA CACS15 contributes to oxaliplatin resistance in colorectal cancer by positively regulating ABCC1 through sponging miR-145. *Arch Biochem Biophys* 2019; 663: 183–191.
152. Tang S, Tan G, Jiang X, et al. An artificial lncRNA targeting multiple miRNAs overcomes sorafenib resistance in hepatocellular carcinoma cells. *Oncotarget* 2016; 7: 73257–73269.

**Titre :** Etude de la voie TGF $\beta$  dans le cholangiocarcinome intrahépatique

**Mots clés :** cholangiocarcinome, voie de signalisation TGF $\beta$ , ARN non-codant

**Résumé :** Le cholangiocarcinome intra hépatique (CCI) est une tumeur hépatique primitive développée aux dépens des canaux biliaires. Son pronostic est mauvais avec les traitements actuels qui augmentent peu la survie des patients. Sa cancérogénèse est complexe impliquant de nombreuses voies de signalisation dont la voie TGF $\beta$ . L'hypothèse du projet est l'implication des ARN longs non-codants (ARNlnc) comme médiateurs de la voie TGF $\beta$  dans le développement du CCI.

Les objectifs de notre travail étaient d'identifier des ARNlnc régulés par le TGF $\beta$  et potentiels biomarqueurs diagnostiques ou pronostiques.

Nous avons identifié une signature transcriptomique spécifique du TGF $\beta$  après stimulation de lignées cellulaires de CCI. Parmi les nouveaux gènes cibles, plusieurs ARNlnc ont été identifiés dont *CASC15* renommé *TLINC* pour *TGF $\beta$ -induced long intergenic non-coding RNA*.

TLINC aurait un rôle dans le remodelage du microenvironnement impliqué dans la cancérogénèse du CCI notamment par la régulation de l'IL8. Ce rôle pourrait s'exercer par l'interaction avec d'autres ARNlnc déjà identifiés dans le CCI e.g. NEAT1. TLINC est surexprimé dans les tumeurs humaines de CCI et pourrait constituer un biomarqueur diagnostique. Des isoformes circulaires de TLINC mises en évidence dans les tumeurs pourraient être détectables dans le sérum et constituer des biomarqueurs non invasifs.

L'analyse transcriptomique d'une cohorte de patients divisée en 2 sous-groupes de pronostic différent a identifié une signature d'ARNlnc prédictive de la survie. L'ARNlnc ANRIL, déjà connu dans d'autres cancers, est un des ARNlnc qui pourrait constituer un biomarqueur pronostique.

**Title :** TGF $\beta$  signaling pathway in intrahepatic cholangiocarcinoma

**Keywords :** cholangiocarcinoma, TGF $\beta$  pathway, non-coding RNA

**Abstract:** Intrahepatic cholangiocarcinoma (ICC) is a primary liver tumor developed from bile ducts. ICC prognosis is poor with current treatments that slightly increase patient survival. ICC carcinogenesis is complex and involves multiple signaling pathways including TGF $\beta$  pathway. Our hypothesis relies on the involvement of long non-coding RNA (lncRNA) as mediators of TGF $\beta$  pathway in the development of ICC.

The aim of the study was to identify and to characterize TGF $\beta$  regulated lncRNA as ICC potential diagnostic or prognostic biomarkers.

We identified a specific transcriptomic signature after stimulation of ICC cell lines with TGF $\beta$ . Among the novel TGF $\beta$  target genes, several lncRNAs were identified including *CASC15* renamed *TLINC* standing for *TGF $\beta$ -induced long intergenic non-coding RNA*.

TLINC may play a role in the remodeling of an inflammatory microenvironment involved in ICC carcinogenesis, including the regulation of IL8. This role could be exerted by the interaction with other lncRNAs already identified in the ICC e.g. NEAT1. TLINC is overexpressed in human ICC tumors and may represent a relevant diagnostic biomarker. Circular isoforms of TLINC found in tumors may be detectable in serum and be noninvasive biomarkers.

Transcriptomic analysis of tumors from a cohort of patients divided into 2 prognostic groups identified a lncRNAs signature predictive for survival. LncRNA ANRIL, already known to be upregulated in other cancers, is one of the lncRNAs that could be a prognostic biomarker in ICC.